REAL-TIME MONITORING OF A MULTIPLE RETROGRESSIVE LANDSLIDE

A Thesis Submitted to the

College of Graduate Studies and Research

in Partial Fulfillment of the Requirements for the

Degree of Master of Science

in the Department of Civil and Geological Engineering

University of Saskatchewan

Saskatoon, Canada

By

Chad Dennis Salewich

PERMISSION TO USE

In presenting this thesis in partial fulfillment of the requirements for a Postgraduate degree from the University of Saskatchewan, I agree that the Libraries of this University may make it freely available for inspection. I further agree that permission for copying of this thesis/dissertation in any manner, in whole or in part, for scholarly purposes may be granted by Dr. J. Sharma or Dr. S.L. Barbour who supervised my thesis work or, in their absence, by the Head of the Department or the Dean of the College in which my thesis work was done. It is understood that any copying or publication or use of this thesis or parts thereof for financial gain shall not be allowed without my written permission. It is also understood that due recognition shall be given to me and to the University of Saskatchewan in any scholarly use which may be made of any material in my thesis.

Requests for permission to copy or to make other uses of materials in this thesis/dissertation in whole or part should be addressed to:

Head, Department of Civil & Geological Engineering

University of Saskatchewan,

Saskatoon, Saskatchewan, S7N 5A9, Canada

OR

Dean, College of Graduate Studies and Research

University of Saskatchewan,

Saskatoon, Saskatchewan, S7N 5A2, Canada

ABSTRACT

In this thesis the data collected from the field monitoring of slope inclinometers, in-place inclinometers (IPIs) and vibrating wire piezometers (VWPs) installed in a multiple retrogressive landslide are evaluated and re-interpreted. The goal of this research was to evaluate the IPIs in particular, as part of a real-time slope stability monitoring system.

The real-time monitoring system was installed by the Saskatchewan Ministry of Highways and Infrastructure (SMHI) to monitor a multiple retrogressive landslide affecting Highway No. 302 near Prince Albert, Saskatchewan. The instrumentation was connected to an automatic data collection and communication system so that data was available remotely via the ARGUS monitoring website. The instrumentation system was implemented after manual displacement monitoring confirmed high rates of movement. The automated landslide monitoring system utilized IPIs and VWPs. The instruments were installed next to Highway No. 302 at the crest of the slope and next to the North Saskatchewan River at the toe of the slope. Data was collected between September 18, 2005 and July 2, 2006. The near real-time data provided from the instrumentation was pore-water pressure, river level, and lateral slope displacement at an hourly interval.

Site investigation and slope inclinometer monitoring confirmed a major slip surface located in the glaciolacustrine clay deposit just above the clay/till contact. Slope inclinometer monitoring showed that the toe of the slope was moving at greater rates and magnitudes than the crest of slope. This observation of movement was consistent in the literature regarding other multiple retrogressive landslides using manual methods of monitoring.

The installation of the automated monitoring system allowed instrument data to be collected at hourly intervals. Consistent periodic reading intervals captured data from the IPIs that showed the crest of the slope was moving more quickly than the toe. This was a significant observation that may not have been captured with manual readings with a traversing slope inclinometer probe. Observations were also made by correlating displacement data from IPIs at the toe of the slope with river level. It was shown that movement began after a rise and fall in river level. This

suggests that displacement of the landslide was triggered by river bank erosion due to higher seasonal flows or alternately a rapid drawdown mechanism.

On October 13, 2005, 25 days after installation of the IPIs, a major disturbance in the readings at both the crest and toe of the slope occurred. After this disturbance the crest was moving at greater rates than the toe. The initial disturbance was attributed to a settling of the head assembly of the IPIs triggered by global failure of the slope. Additional disturbances were noted in the IPIs at the toe of the slope and attributed to the casing contacting the IPIs. A geometric analysis was developed to verify that the unexpected movement could have been caused by the casing contacting the IPIs. The geometric analysis included observation of the shear induced deformation profile of the slope inclinometer casing, IPIs diameter, IPIs length and the annular space between the casing and the IPIs. The geometric analysis verified that the IPIs at the toe of the slope were likely affected by the IPIs coming into contact with the casing. Casing contact could affect the IPIs orientation and depth position, resulting in unexpected data.

An additional set of IPIs data from a landslide near Aylesbury, Saskatchewan was used to compare to the IPIs data from Highway No. 302. Data comparison showed that there were erratic readings from the IPIs at the Highway No. 302 site while the IPIs at the Aylesbury site generally remained stable and consistent. This data also confirmed that the IPIs at Highway No. 302 were affected by casing contact.

The near real-time monitoring system was an excellent risk management tool for SMHI. Due to the rate and magnitude of movement the instrumentation was destroyed sooner than expected. The data set produced allowed for evaluation of the landslide and performance of the IPIs. In conjunction with the river data the IPIs helped identify potential failure mechanisms. Additional work is required to ensure that the data from IPIs can be used to evaluate landslide kinematics. In particular ensuring that the IPIs are not used beyond their capability and providing realistic data.

ACKNOWLEDGEMENT

I would like to thank the Saskatchewan Ministry of Highways and Infrastructure (SMHI) and NSERC (Discovery Grant) on behalf of my supervising professors for financial support.

Thank you to my primary supervisor Dr. Jitendra Sharma and co-supervisor Dr. Lee Barbour for the opportunity to pursue graduate studies and their support throughout. It has been a long road, and I appreciate your guidance throughout the journey.

To the committee members, thank you. Allen Kelly and Jorge Antunes for your time in setting up this research and providing support, Dr. Chris Hawkes for your input and advice when and Dr. James Kells for chairing the committee.

I would like to thank Lyle, Garret and Ryan from the SMHI drilling crew. This project was the first of many opportunities to get to work with and learn from a great bunch.

I got to know many people through my journey in graduate studies. In particular Adam Meier who shared many coffees and conversations, Pat Schmidt and all other 3C54 office students. I also need to thank Dr. Manoj Singh for the continuous encouragement and support he provided during my studies.

Of course I need to thank my family, especially my parents whom supported me through **ALL** my years of schooling and continue to be there whenever called upon. Thanks also to my in-laws, for their encouragement, support, and review.

Finally, thank you to my wife Mary! You were with me through it all. Having you to come home to made life so much easier. Thank you for all your love, encouragement and support. I never would have finished without you. I love you very much and continue to look forward to our future together!

TABLE OF CONTENTS

LIST OF TABLES

LIST OF FIGURES

Chapter 1 Introduction

1.1 Landslides in Saskatchewan

Landslides occur throughout the province of Saskatchewan. Although Saskatchewan is described as a 'flat' province the existing river valleys are prone to landslides (Christiansen and Sauer 1984). Deglaciation provided fast flowing water resulting in glacial melt-water spillways, glacial lakes, and deep river valleys such as the North and South Saskatchewan River valleys (Christiansen 1979).

Formation of the river valleys exposed weak layers of soil and formed steep slopes. This combination provided ideal conditions for landslides to develop, many of which are still prevalent today (Christiansen and Sauer 1984).

Typically, landslides in the Saskatchewan River valleys propagate from the toe of the slope, to the crest of the slope and are made up of multiple landslide blocks. A landslide naming methodology was developed by Cruden and Varnes (1996) to describe a landslide type and movement. Using this system the Highway No. 302 landslide would be described as a retrogressive multiple landslide. In the Saskatchewan literature these have been termed as multiple retrogressive landslides.

The movement of landslides may be rapid and catastrophic, extremely slow, or dormant. Multiple retrogressive landslides in the North and South Saskatchewan River valleys range from dormant to slow moving, and the landslides typically experience a few millimetres of movement per year. Initiation and rates of movement are dependent on soil conditions such as soil type, pore-water pressure, geometry, erosion, etc.

The purpose of landslide monitoring is to protect infrastructure and public safety while providing observations (e.g., data) which can be interpreted to improve our understanding of landslide kinematics and mechanisms. Some examples of geotechnical monitoring for Saskatchewan landslides are highlighted in Haug et al. (1977), Yoshida and Krahn (1985), Kelly et al. (1995), and Pauls et al. (1999).

Systems used to monitor landslides have traditionally relied on instrumentation requiring manual measurements of horizontal displacement, pore-water pressures, and river level. Manual data collection often results in large time gaps between measurements and limits the ability for monitoring systems to be used for early warning of slope failure. Linearization of readings between readings can result in an oversimplified version of findings. Irregular and unsystematic collection of data can have serious implications on the integrity of infrastructure as it relates to public safety. It is evident that to reduce risk and increase our understanding of landslide kinematics and mechanisms a more frequent monitoring system may be required.

Dunnicliff (1993) describes instruments that can be used as a part of an Automatic Data Acquisition Systems (ADAS) to collect data at user defined intervals. These systems can be implemented where continuous monitoring would be justified based on the level of risk, uncertainty, or accessibility.

The Saskatchewan Ministry of Highways and Infrastructure (SMHI) developed a risk management system used to evaluate landslides in the province (Kelly et al. 2004). These evaluations identify the level of risk to infrastructure and public safety associated with the landslide hazard. If the level of risk is evaluated as urgent, an increased level of monitoring is recommended that would require monitoring intervals to be increased. In order to achieve this, an upgrade from manual data collection to an automated real-time monitoring system may be required.

1.2 Background

The Highway No. 302 landslide is located approximately 5 km west of the city of Prince Albert, Saskatchewan, Canada (Figure 1.1). The highway runs nearly parallel to the North Saskatchewan River and is set back approximately 250 m from the south river bank.

Several measurements with slope inclinometers were used to define the location (depth) and rate of movement of the landslide. The instruments were located near the highway (crest of the failing slope) and riverbank (toe of the failing slope). The landslide was founded on a weak lacustrine clay soil layer at depths between 40 and 45 m. Movement was severely damaging the highway infrastructure.

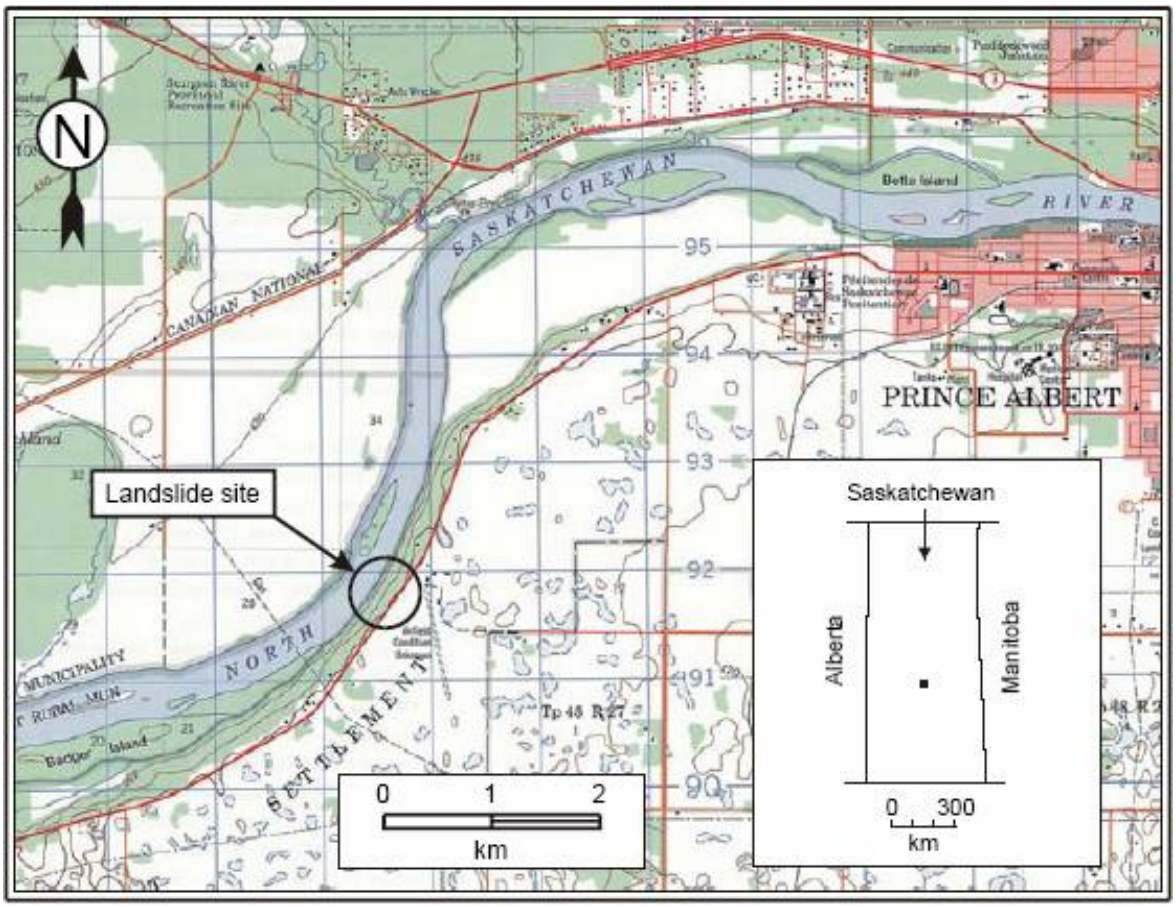

Figure 1.1: Location of landslide site (from Kelly et al. 2005a, National Topographic System Map Sheet 73/H).

The Highway No. 302 landslide was monitored with slope inclinometers for three years (2002-2005) at the slope crest and one and a half years (2004-2005) at the slope to toe. During this time four slope inclinometer casings were destroyed due to excessive movement (two slope inclinometer casings at the crest of the slope and two at the toe). Evaluation of this landslide indicated that an increased level of monitoring was required and a real-time monitoring system was recommended (Kelly et al., 2005a).

Electronic instrumentation that was used for the real-time monitoring system was electrolytic in-place inclinometers (IPIs) to measure displacement across the shear zone and vibrating wire piezometers (VWP) to measure pore-water pressure across the shear zone. A vented VWP was also installed in the river bed to monitor river level.

Installed in the late summer and early fall of 2005, the instrumentation had the ability to record, communicate, process, and store data. Automatic alarm messages could also be sent to personnel in the form of portable document files (pdf) if pre-set measurement values were breached. As a result of unprecedented movement rates during the spring and summer of 2006 the real-time instrumentation was destroyed (see Appendix A for a pictorial of the failure).

IPIs were an integral part of the real-time monitoring system at this study site. This monitoring system is of particular interest since it is a relatively untested monitoring technology for SMHI. Although the system functioned well during its 6 to 10 month lifespan, unexpected data was recorded. IPIs displacement data showed movement in multiple directions (negative, upslope and positive, down slope). This movement implied by the data collected could not be explained based on our current understanding of landslide processes. In order to use this data to describe slope kinematics and mechanisms potential causes for the unexpected IPIs results required examination.

1.3 Research Objectives

The broad objective of this research is to evaluate the monitoring data from in-place inclinometers at the Highway No. 302 landslide site and in particular, to evaluate the use of IPIs

as part of a real-time slope stability monitoring system. In order to meet the overall objective, the following three specific objectives have been identified:

1. Develop a synthesis of the underlying theory, operation, capabilities, and limitations of the IPIs to monitor landslide deformation and kinematics.

2. Evaluate and quantify the performance of the IPIs installed in the Highway No. 302 landslide.

3. Interpret the monitoring results from the Highway No. 302 IPIs, along with other real-time monitoring and site information, and develop a conceptual model for the potential slide mechanisms at this site.

1.4 Project Scope

A detailed study will not be completed on all available techniques used to monitor deformation and pore-water water pressure. A review of other case studies will be confined mainly to multiple retrogressive landslides and sites with similar geotechnical monitoring systems. This study will not include numerical modelling and quantitative analysis of landslide mechanisms.

1.5 Organization of the Thesis

This thesis is organised into six chapters.

- Chapter 1 (this chapter) describes landslides in Saskatchewan, project background, research objectives and scope.

- Chapter 2 includes a literature review. The literature review describes multiple retrogressive landslides, the general area geology and hydrogeology, geotechnical instrumentation, relevant case studies and information with regards to theory, operation, capabilities and limitations of the slope inclinometer and IPIs.

- Chapter 3 presents a site investigation summary which includes a description of the type of instrumentation and installation technique.

- Chapter 4 presents the data that was gathered from the slope inclinometer, IPIs, and VWP. This includes both the manual acquisition of data and data provided by the real-time monitoring system.

- Chapter 5 evaluates the IPIs performance and quantifies the results based on a geometric analysis of the IPIs system. Additionally the data is used to discuss landslide kinematics, mechanism and provide general interpretation of the data set.

- Chapter 6 provides the conclusions discerned from the study as well as suggestions for further research.

Chapter 2 Literature Review

The objective of this literature review is to provide background information of the landslide area, type, case histories and instrumentation use. Discussion with regard to monitoring will focus on the use of slope inclinometers and in-place inclinometers (IPIs).

2.1 Multiple Retrogressive Landslides

Landslides are a result of all or some of the following: geology, geomorphology, hydrogeology, climatic conditions and human activities. Depending on the situation, a variety of landslide types and processes are plausible.

Cruden and Varnes (1996) present terminology used to describe landslides in meaningful and unified terms. Landslide terminology was created to identify a variety of landslide types and processes in a consistent manner. The description or name of a landslide can include items such as material (i.e., rock or earth), movement rate (activity level), distribution and style. Two important components include the distribution and style of the landslide failure. For example, "Retrogressive multiple" indicates a "retrogressive" distribution and "multiple" indicates the landslide being comprised of more than one failure block.

Cruden and Varnes (1996) also classify how the movement is distributed throughout the displaced mass, or the kinematics of a landslide and movement features. Movement features include a fall, topple, slide, spread and flow (Figure 2.1). Note that both the slide and spread movement types appear to be have a retrogressive distribution and multiple blocks.

Landslides are a product of many conditions such as geology, geomorphology, and hydrogeology. Weiczorek (1996) states, that a single mechanism or trigger must occur to either decrease shear resistance or increase mobilizing stresses for landslides to move. Some examples

include intense rainfall, volcanic eruption, earthquake and water level change (i.e. river erosion, rapid drawdown and pore-water pressure).

Christiansen and Sauer (1984) studied landslides extensively in the Saskatchewan Rivers plain. They found that multiple retrogressive landslides are the most common type of landslide in the study region. Characteristics of these landslides include:

- They occur where extraglacial and glacial spillways have eroded in the Upper Cretaceous, over-consolidated (OC) marine clay shale or normally consolidated (NC) glacial lake deposits.

- The shear zones are found in OC bedrock clay shale in the upper part of the Lea Park formation and in NC glaciolacustrine clay deposits, typically near stratigraphic contacts (i.e. glaciolacustine clay and till interfaces).

- Each landslide block fails where it intersects the weak layer of material which is typically relatively horizontal;

- They have moved, or continue to move a few millimetres per year, and have reached residual strength with angles of friction in the range of 5° to 9°, which allow them to be easily reactivated if dormant.

- They usually occur on the outside bend of river meanders and are controlled in part by river erosion of the toe as well as regional and local groundwater regimes.

Specific studies of these types of landslides support the above conclusions. These studies include those conducted by Haug et al. (1977), Christiansen (1983), Sauer (1983), Yoshida and Krahn (1985), Clifton et al. (1986), Eckel et al. (1987), Misfeldt et al. (1991), Kelly et al. (1995), and Pauls et al. (1999).

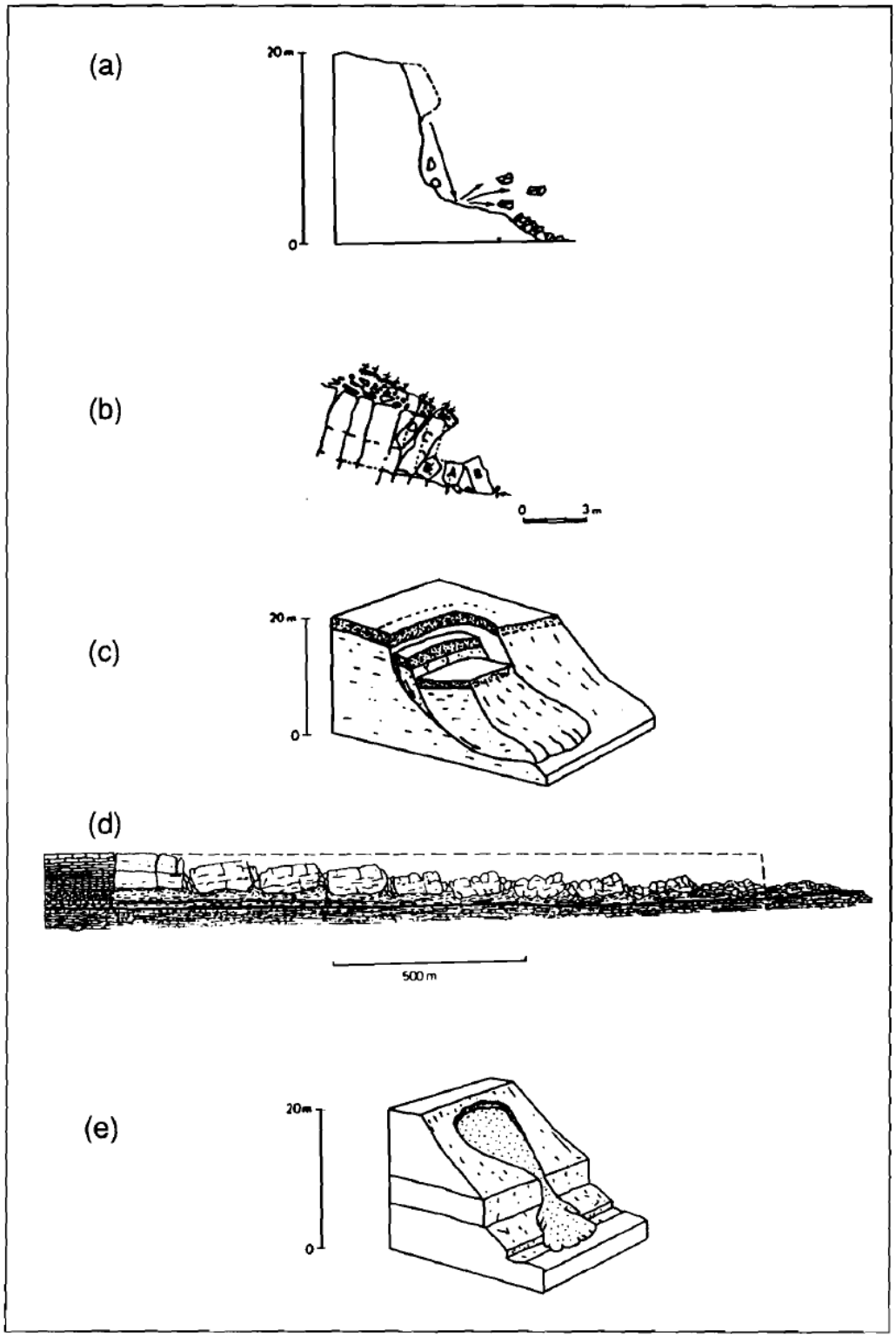

Figure 2.1: Type of movement including (a) fall (b) topple (c) slide (d) spread and (e) flow (from Cruden and Varnes 1996).

2.1.1 Kinematics and Mechanism

Kinematics of a landslide is described as how movement is distributed through a displaced soil mass (Cruden and Varnes 1996). Mechanism was described as the one trigger that causes the landslide to move (Wieczorek 1996).

Thomson and Hayley (1975) studied a multiple retrogressive landslide in the Peace River Valley in Alberta. The landslide slip surface was located in clay shale. They observed that the landslide typically moved more at the toe than at the crest of the landslide, but also realized that there must be a relationship between the movements of the multiple blocks. The mechanism responsible for the slow landslide failure was the gradual erosion at the toe of the slope by the river.

Haug et al. (1977) also showed that river erosion was affecting the stability of the Beaver Creek landslide near Saskatoon, Saskatchewan. The slip surface of this landslide was located in glaciolacustrine clay deposits. This multiple retrogressive landslide was also shown to be moving from the toe to the crest. It was stated that the rate of movement between the blocks likely varies based on the stability of an individual block at any given time.

Thomson and Tweedie (1978) witnessed a landslide that progressed from crest to toe. A new 2.3 m scarp was formed and the landslide appeared to consist of highly fractured material and an old graben feature. This suggested that the slope may have previously moved from the toe to the crest. The mechanism for movement was hypothesized as a springtime rise in pore-water pressure since the slide mass was already disturbed and jointed so that water had easy ingress into the slope. Once movement was initiated at the crest of the slope it was delayed reaching the toe of the slope as movement was absorbed in the landslide mass through the closing of joints and fissures. The presence of joints, fissures, and an old graben feature indicate this area had previous active landslide movement. It was suggested that the crest movement was absorbed by the landslide mass since no observable bulge near the river was observed.

Yoshida and Krahn (1985) reanalysed the Beaver Creek landslide. They showed that the multiple retrogressive landslides can be analysed as a single landslide mass rather than individual blocks, but did state that the study of the relationship between individual landslide blocks is important.

Stauffer et al. (1990) described the extension of a land mass and resulting topography due to a retrogressive landslide (Figure 2.2). The landslide topography depends on the amount of movement from crest to toe. Figure 2.2b highlights a scenario where all landslide blocks extend equally and the surface is composed of horst and graben features at approximately the same level. Figure 2.2c shows a scenario where 30% extension occurs at the toe reducing to 10% at the crest of the slope.

Misfeldt et al. (1991) examined the influence of groundwater dynamics on slope stability for a dormant landslide. Two slip surfaces were determined to exist. The slip surfaces were located in the clay shale. It was observed that the groundwater regime is affected during landslide failure. Movement of the landslide deforms the structure of the soil mass. Distortion of the geologic structure changes the permeability of the soils and affects the pore-water pressure regime. Additionally, river erosion, and the geometry at the toe of the slope was shown as a factor in slope stability.

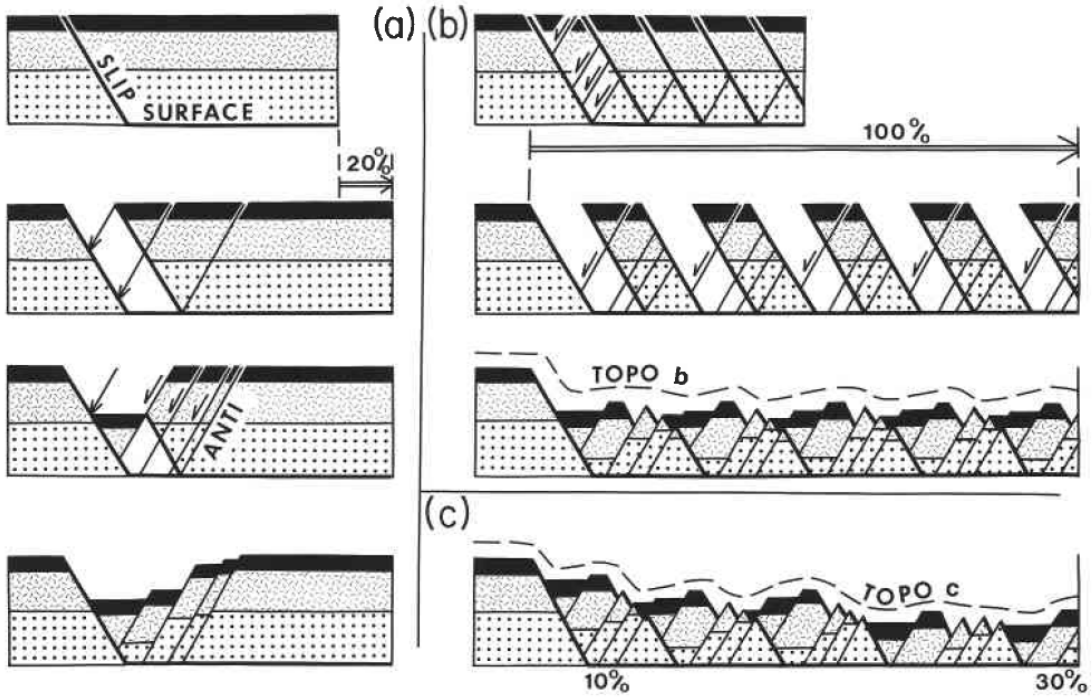

Figure 2.2: Development of multiple retrogressive landslide topography (from Stauffer et al. 1990).

Kelly et al. (1995) studied the stability of a multiple retrogressive landslide with two active failure planes located in clay shale. It was shown that the stability of the landslide was controlled by the groundwater regime. Increases in pore-water pressures in the Empress group would reduce stability and trigger movement of the landslide.

Pauls et al. (1999) explored a rapid drawdown mechanism for the Carrot river landslide near Nipawin, Saskatchewan. The mechanism was evaluated due to a flood event that was expected to cause slope movement. The landslide slip surface was located in glaciolacustrine clay.

Kelly et al. 2005b analysed the Frenchman River Valley landslide near Shaunovan, Saskatchewan. This landslide was affecting Highway No. 37 of the Saskatchewan Highway network and appeared to be retrogressive in nature with multiple landslide blocks. Due to construction in the vicinity of the landslide mass it was observed that movement was triggered from the top of the landslide from fill placement. The resulting placement of fill showed that failure of these landslides was triggered from the crest where movement at the crest was greater than that at the toe.

In general these studies confirm the kinematics of a multiple retrogressive landslides where observed movement was suggested to extend from the toe to the crest. Landslide movement was triggered by changes to slope geometry (river erosion at the slope toe), and groundwater regime. Additionally, it was shown that disturbed landslide masses may move greater at the crest under certain conditions.

2.2 Geologic Setting

The Prince Albert area is defined by map sheet 73H of the National Topographic System (NTS). Separation of regions using the NTS map system was a convenient way to present the geology and groundwater resources of different areas of Saskatchewan (Millard 1990).

2.2.1 Geology and Geomorphology

Christiansen (1968a, 1968b, 1992) classified the materials between the bedrock (Cretaceous) and surface (Quaternary) deposits. The Quaternary deposits were separated into a specific epoch and

group. Figure 2.3 shows the stratigraphic chart for the Prince Albert area as developed by Christiansen and Sauer (1993).

Till materials were classified based on differences in carbonate content, separation of zones identified by weathered material and separation of zones by intertill stratified drift. The tills have also been differentiated by studying mechanical properties such as pre-consolidation pressures (McDonald and Sauer 1970; Sauer 1974; Sauer and Christiansen 1991).

<table>
<tr><th>PERIOD</th><th>EPOCH</th><th>GROUP</th><th colspan="2">STRATIGRAPHIC UNIT</th></tr>
<tr><td rowspan="5">QUATERNARY</td><td rowspan="2">HOLOCENE</td><td rowspan="3">SASKATOON</td><td></td><td>sand and silt</td></tr>
<tr><td></td><td>silt and clay</td></tr>
<tr><td rowspan="3">PLEISTOCENE</td><td>BATTLEFORD FORMATION</td><td></td></tr>
<tr><td>FLORAL FORMATION</td><td rowspan="2">silt and gravel</td></tr>
<tr><td>SUTHERLAND</td><td></td></tr>
<tr><td>TERTIARY</td><td>PLIOCENE</td><td>EMPRESS</td><td></td><td></td></tr>
<tr><td rowspan="3">CRETACEOUS</td><td rowspan="2">LATE CRETACEOUS</td><td>LEA PARK AND UPPER COLORADO GROUP</td><td></td><td></td></tr>
<tr><td>LOWER COLORADO GROUP</td><td colspan="2" rowspan="2"></td></tr>
<tr><td>EARLY CRETACEOUS</td><td>MANVILLE/SWAN RIVER FORMATION</td></tr>
</table>

Figure 2.3: Stratigraphic chart for the Prince Albert Area (after Christiansen and Sauer 1993).

2.2.1.1 Cretaceous Geology and Geomorphology

The base of the lower Cretaceous succession consists of the Mannville Group, which is sometimes referred to as the Swan River Formation in Saskatchewan. The Mannville Group was deposited following a period during which older strata were uplifted, exposed and eroded (Hayes et al. 1994). The eroded sediments in-filled areas and covered an area ranging from the Rocky Mountains in western Canada to the Great Plains area towards the east. The thickness of this wedge-shaped stratigraphic unit ranges from 700 m near the Rocky Mountain foothills to as little as 40 m in parts of the Great Plains area.

Millard (1990) describes the Mannville Group in the Prince Albert area as uniform units composed of fine-to-coarse grained quartz-rich sand, with silt and clay layers. In the Prince Albert area this unit has recorded thicknesses of 100 to 215 m. The base of the unit is encountered at shallower depths in the north eastern portion of the Prince Albert area.

Cretaceous deposits overlying the Manville Group in the Prince Albert area consist mainly of clay shale. The lower clay shale deposits are composed of what is referred to as either the Ashville Formation or Lower Colorado Group. This unit is composed of dark grey non-calcareous clay ranging in thickness from 0 to 85 m in the Prince Albert area. This unit can sometimes be separated into a lower and upper zone where separated by a silt and sand layer (Millard 1990).

Millard (1990) describes the Lea Park Formation or Upper Colorado Group as a single unit with two distinct zones. The lower zone of this unit is composed of calcareous grey marine silt, clay and bentonite beds; whereas, the upper portion is differentiated by being non-calcareous. The lower calcareous zone is sometimes referred to as the White Speckled Shale. The Lea Park or Upper Colorado formation was thickest in the west central part of the Prince Albert area reaching a maximum thickness of 95 m near Weldon, Saskatchewan.

2.2.1.2 Quaternary Geology and Geomorphology

According to Fenton et al. (1994), 70% of the surficial deposits of the interior plains of western Canada are of glacial origin. Advancement of a glacier resulted in erosion and transportation of material, while a retreating glacier was responsible for the deposition of material. Each advance

and retreat resulted in the deposition of tills, which consist of an unsorted mixture of clay, silt, sand, cobbles, and boulders (Millard 1990).

Fenton et al. (1994) also stated that 20 percent of the interior plains are of lacustrine origin. Material of lacustrine origin can include any one or combination of clay, silt, sand, and gravel originating from aeolian, glaciolacustrine, glaciofluvial, and alluvial processes (Millard 1990).

The Empress Group overlies the Lea Park formation. The Empress Group is of late Tertiary to Quaternary Period and is present in some parts of the Prince Albert area (Whitaker and Christiansen 1972). Where found, this group lies directly on top of the clay shale and is composed of gravel, sand, silt and clay. This material was deposited through colluvial, fluvial and lacustrine processes immediately prior to and during glaciation.

The Empress Group has been found to be 30 m thick in the Prince Albert area and less than that near the town of Shellbrook and in the extreme southwest portion of the Prince Albert area. Christiansen and Sauer (1993) show that Empress Group is very thin to non-existent just to the west of the City of Prince Albert in the vicinity of the North Saskatchewan River.

Glaciation provided means to deposit till material, but at times disturbed the existing geological sequence of materials. Sauer (1978) describes glacial thrust features, where entire blocks of soil were moved by glaciers, and their presence in southern Saskatchewan.

Christiansen and Sauer (1993) investigated a drumlin feature 15 km south west of the City of Prince Albert named Red Deer Hill. Subsurface investigation of the 5 km long, 3 km wide, and 70 m high hill found cretaceous bedrock material overlying younger till material. This disturbed geological sequence was determined to be caused by a glacial thrust. This was determined through mapping the regional till where a depression in the till to the north east of Red Deer hill was shown to be a reasonable source for the material. This glacial thrust feature may have been caused by a weak zone such as a bentonitic zone, which can occur in the Cretaceous clay shale. This material was carried as a block by the glacier and thrust over stronger till material leaving a hill when the glacier retreated.

Results of glacial thrusting in the Prince Albert area are shown in Figure 2.4. Depressions in the till surface map highlight locations where blocks of material were removed and the associated uplands represent locations where the material was re-deposited. The cross-section in Figure 2.5 provides an overview of the geology of the Prince Albert area. Note the thickness and extent of the stratified drift. The thickness and pinching out of the unit represents the extent of the glacial lake during the last deglaciation where surficial stratified drift was deposited.

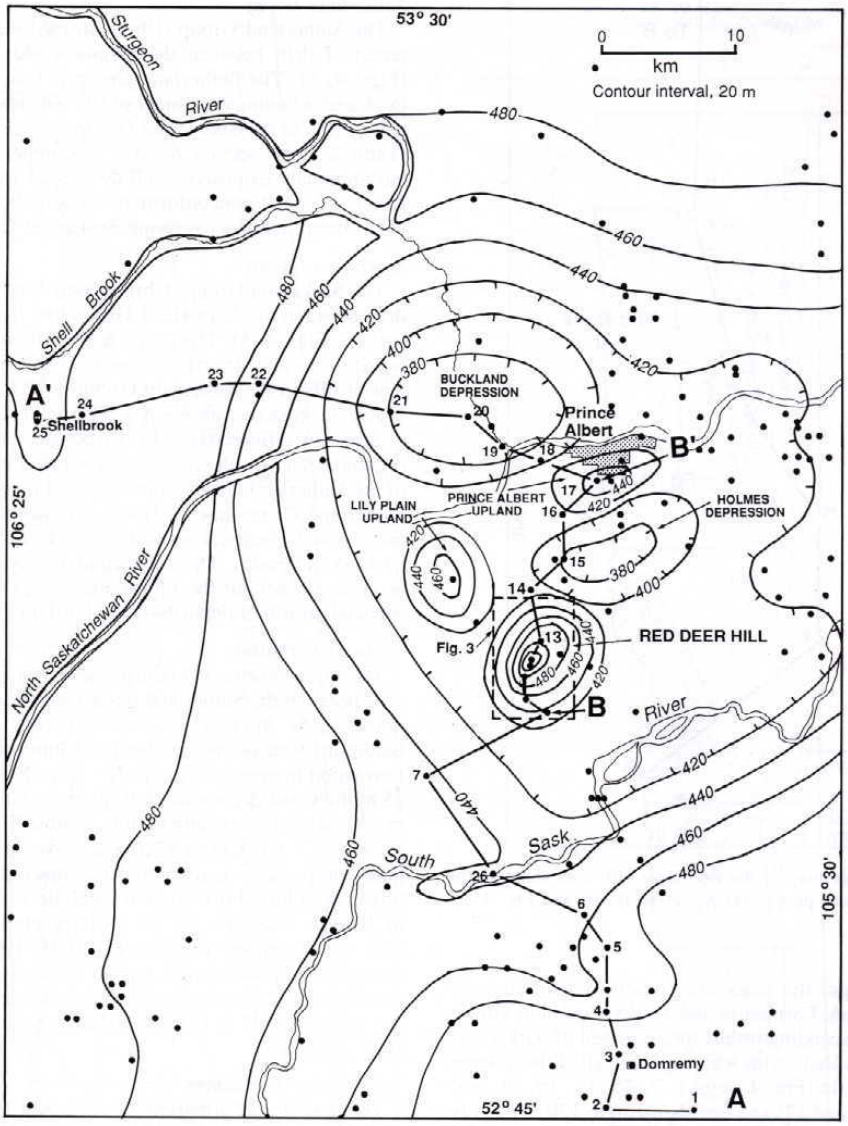

Figure 2.4: Till surface elevation contours represented as meters above sea level in the Prince Albert Area (from Christiansen and Sauer 1993).

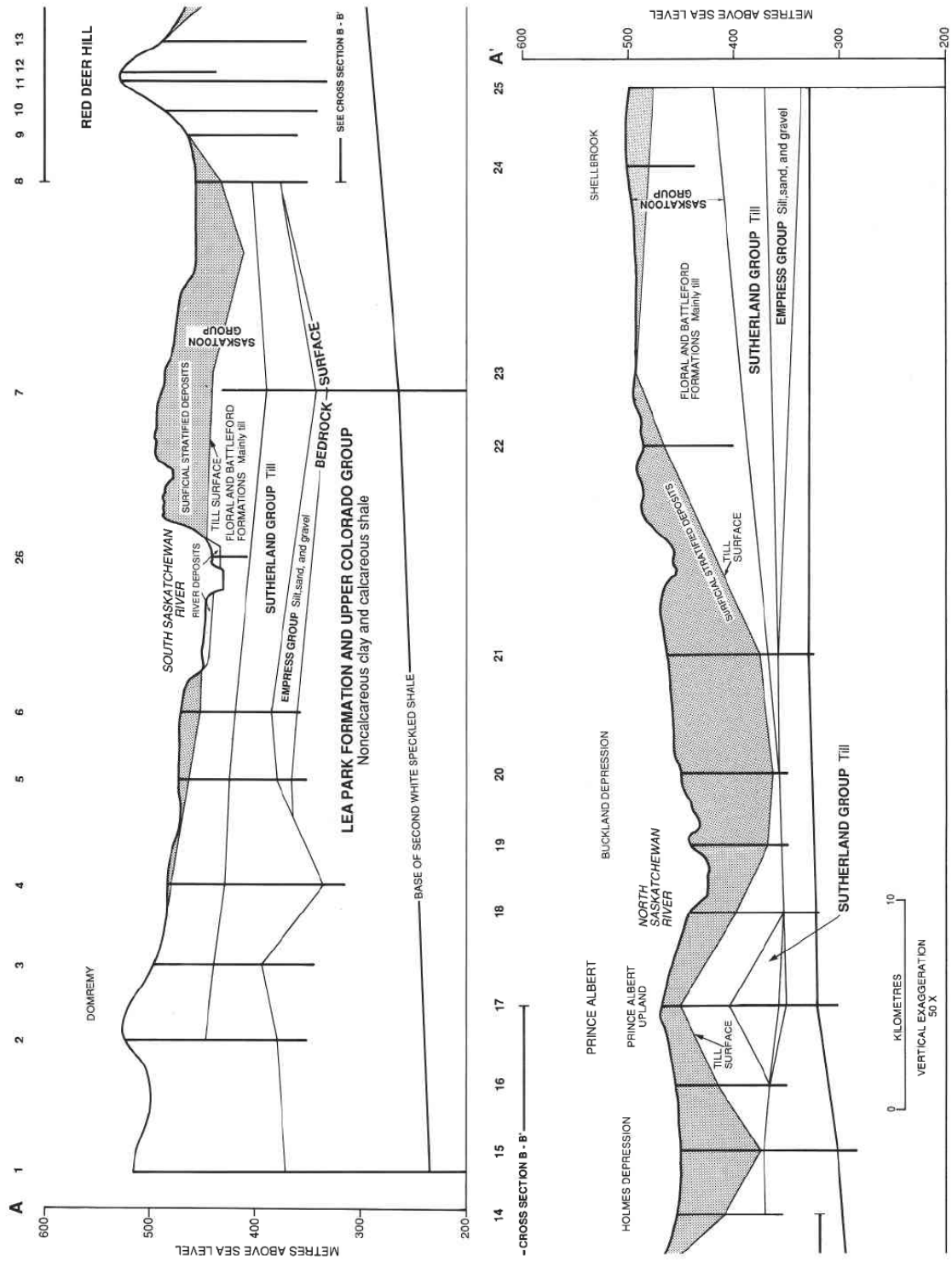

Figure 2.5: Cross Section A-A' and B-B' as represented on the till surface map (from Christiansen and Sauer 1993).

Christiansen (1979) highlighted the sequence of deglaciation by separating it into nine distinct phases. Phase 1 began approximately 17,000 years ago when the final layer of till material was being deposited. Between Phase 3, 15,500 years ago and Phase 4, approximately to 14,000 years ago, Glacial Lake Saskatchewan was formed at the retreating ice front. Further glacial retreat caused Glacial Lake Saskatchewan to envelop the Prince Albert area between Phase 6 and Phase 7 approximately 12,000 to 11,500 years ago (Figure 2.6). Upstream fluvial processes of erosion and down cutting of the melt water spillway channels supplied fine material such as sand, silt and clay which were deposited in Glacial Lake Saskatchewan. This process was responsible for the surficial stratified material or lacustrine deposits in the area.

Between Phase 7 to Phase 9, which span from 11,500 to 10,000 years ago, Lake Saskatchewan drained east via the Assiniboine Spillway into Lake Agassiz. The draining of Glacial Lake Saskatchewan created a series of deltas between what eventually became the North and South Saskatchewan Rivers. Christiansen et al. (1995) describe the formation of the Prince Albert delta located between the mouths of the North and South Saskatchewan Rivers. This occurred from approximately 10,200 to 9,500 years ago and was the first in a series of five interrelated deltas created during the draining of Lake Saskatchewan. This deltaic environment formed the near-surface geology of the Prince Albert area. This includes deposits of typically fine-grained materials such as silt, clay and sand.

Lowering of the glacial lakes caused further down cutting and erosion of the spillway channels. Christiansen and Sauer (1984) explain that landslides in the North and South Saskatchewan Rivers were initiated where channels cut through the Quaternary sediments into Upper Cretaceous clay shale, or through thick beds of glacial lake clays.

Fung et al. (1999) displayed a map describing surficial geology of Saskatchewan. The Prince Albert area in the vicinity of the landslide indicated glaciolacustrine plains to the south, hummocky aeolian terrain to the west and southwest, and a glaciolacustrine delta to the east. The river has been responsible for depositing alluvium within the river valley. Christiansen (1983), suggested that deposition of alluvium was occurring at a rate of 35 mm per year. This was based on an investigation of the Denholm landslide site approximately 250 km upstream from Prince Albert.

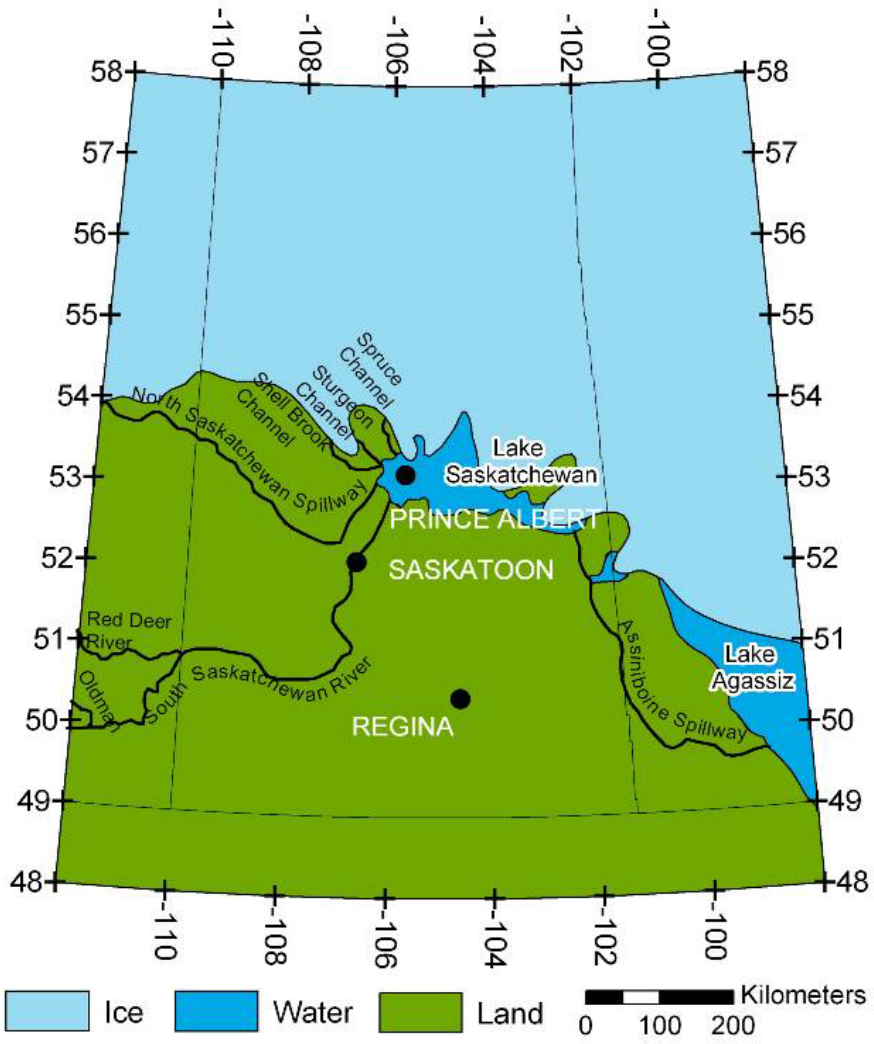

Figure 2.6: Glacial Saskatchewan in the Prince Albert Area approximately 11,500 years ago (from Christiansen, 1979).

2.2.2 Hydrogeology

The major topographic low in the Prince Albert area is the North Saskatchewan River, which acts as a drain for the regional aquifers. North of the river the land gradually dips south towards the river. The Buckland depression created by a glacial thrust caused a depression in the till surface that was subsequently in-filled with clays and silts from Glacial Lake Saskatchewan and other morphologic processes (Christiansen and Sauer 1993). Running through the middle of the depression is the Sturgeon River which also acts as a regional topographic low and drains into the North Saskatchewan River approximately 1 km to the north east of the landslide site.

Approximately 5 km south west of the landslide site is the topographic high of the Lily Plain Upland and 15 km south west is the location of Red Deer Hill. These regional topographic highs are potential areas of groundwater recharge, with discharge at the river.

Immediately south of the landslide site is a glaciolacustrine plain. The hummocky topography has localized relief of 10 m (Elev. 450 m to 460 m). Small ponds existing in the low lying areas and depressions of the fields indicate the potential of a near surface groundwater level.

The regional hydrogeology of the Prince Albert area is described by Millard (1990). It consists of many aquitards and a few aquifers. Cretaceous silt and clay shale, till and surficial stratified clay and silt units act as low permeability units, or barriers to groundwater flow. Major aquifers in the area consist of more permeable sands and gravels within these low permeability units.

The Mannville Group is considered a bedrock aquifer. Confined above by clay shale, it is composed of coarse and fine quartz-rich sand. This formation is described as a significant groundwater resource especially in the extreme eastern part of the Prince Albert area where it is located at shallower depths.

The Mannville Group aquifer has high heads in the east central portion of the province that diminish westward (Millard 1990). According to a potentiometric surface map, the freshwater heads are as high as 500 metres above sea level (masl) in the Prince Albert area. The city itself is straddled by total fresh water head contours of 450 masl and 400 masl (Christopher 2003).

The Empress Group aquifer is described as having limited extent; therefore, it is not considered a significant ground water resource in the Prince Albert area (Millard 1990). It is identified as a thin unit near the city of Prince Albert by Christiansen and Sauer (1993), but is pinched out in the vicinity of the North Saskatchewan River. This unit is confined by underlying clay shale and overlying till where it is found to exist.

Deep intertill sand and gravel aquifers are located within the Sutherland Group as well as in the deeper portion of the Saskatoon Group Floral Formation. These aquifers are neither numerous nor extensive in the Prince Albert area. Shallow sand and gravel intertill aquifers are located within the upper part of the Floral Formation. These are usually at depths less than 50 m.

Surficial aquifers are more common in the Prince Albert area and comprise any coarse-grained unit within the Battleford Formation till and surficial stratified drift. Surficial aquifers are described as being common in the southern portion of the Prince Albert area (Millard 1990).

2.3 Significance of Geology and Hydrogeology for Landslides

Understanding the geology and hydrogeology of a landslide site is a significant factor in determining the location of the failure surface(s) and the potential mechanism causing failure.

Hodge and Freeze (1977) recognized the implication of groundwater regime on slope stability. This paper highlighted that slope stability relies on the effective stress conditions in the ground. The effective stress conditions rely on the characterization of the groundwater flow regime. For both regional and groundwater review may be required which requires a review and understanding of the regional and local geology.

Haug et al. (1977) showed that the landslide at Beaver Creek, Saskatchewan was occurring in glaciolacustrine clays. A geologic investigation was still carried out in units below to allow for the characterization of the geology and hydrogeology on a regional and local scale even though the general conclusion was that river erosion was the main trigger for slope stability.

Christiansen and Sauer (1984) summarized landslides in the Saskatchewan Rivers plain. In doing so they highlighted the importance of geology with respect to each landslide they presented. Although typically the landslides were shown to exist in clay shale and glaciolacustrine clay, they highlighted failures in unexpected, stronger material such as till. This showed that understanding the geology, geomorphology and hydrogeology were of great importance when reviewing landslide failures.

Christiansen and Sauer (1993) in reviewing the geology of Red Deer Hill in the Prince Albert area showed that the geologic sequences can be disturbed. This highlighted the significance that geomorphology played in the region. Glacial thrust features such as that described provide explanation to unexpected geologic sequences, potential weakened zones that could be susceptible to landslides and potential localized changes in the groundwater flow regime.

Kelly et al. (1995) showed that multiple slip surfaces existed in clay shale where a landslide was affecting the Deer Creek Bridge. A detailed review of geology and hydrogeology provided a hypothesis as to the slip surfaces and triggering mechanism. A review of the geology and geomorphology of the region attributed the multiple slip surfaces to glacial shearing and regional tectonism. The triggering mechanism was then tied to an upward gradient in the groundwater regime.

Without understanding the entire geologic sequence including that below the shear zone the landslide mechanism related to regional and local groundwater regimes would not be reviewed. Presentation of the geologic data was shown to be important to help review potential mechanisms of failure and to determine the most reasonable cause.

2.4 Manual Monitoring of Landslides

2.4.1 Slope Inclinometer System

A slope inclinometer system typically includes the following four components:

1. Inclinometer casing (guide casing) constructed of acrylonitrile butadiene styrene (ABS) plastic, aluminum alloy, fibreglass, or steel with tracks that control the inclinometer probe orientation;

2. A traversing slope inclinometer probe containing gravity sensitive transducers that are calibrated to measure tilt and are encased in a protective steel shell with a wheel assembly;

3. A power supply/readout unit to record probe inclination; and,

4. A graduated electrical cable with equally spaced intervals (0.5 m or 2.0 ft.) connecting the probe to the readout unit.

2.4.1.1 Capabilities

A traversing slope inclinometer probe is capable of measuring tilt at specified intervals as it traverses up the inclinometer casing. If the measurement interval matches the probe length the tilt measurements can be used to define the casing shape incrementally over its entire length.

Each probe is calibrated from vertical to a range set by the manufacturer depending on the monitoring requirements (typically ± 10°). The orientation of the inclinometer probe is controlled by the tracked inclinometer casing and the length between the probe wheels that ride the grooves of the casing. Figure 2.7 illustrates the A-Axis and B-Axis of the traversing slope inclinometer probe in plan view and the corresponding direction references. Typically the probe is oriented such that the A-Axis is aligned in the expected direction of movement. The A_0 readings are positive, A_{180} negative, B_0 readings are positive and B_{180} readings are negative. Movement in the B-Axis should be minimized if the casing was successfully aligned in the expected direction of movement.

Casing deflection is obtained over each measurement interval. The tilt of the probe at each measurement interval is used to calculate displacement of the traversing slope inclinometer probe. At a single interval, displacement is calculated as the sine of the tilt angle, θ, of the probe, multiplied by the probe length (distance between the wheels). Incremental displacement can be summed from starting from the bottom-most reading to the top to determine the cumulative casing displacement.

The initial casing survey is called the baseline survey. The baseline survey provides the initial casing shape after installation. This survey is used to compare each subsequent survey against, to determine if there is a change in tilt at a discrete interval which corresponds to movement. Summation of the subsequent readings can redefine the casing shape caused by movement.

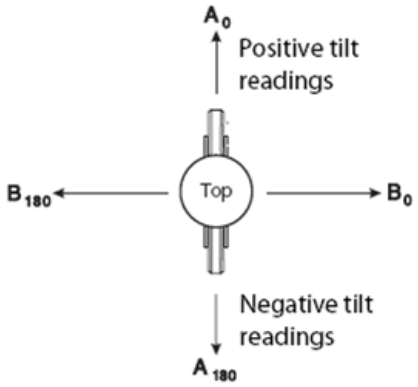

Figure 2.7: Axis orientation of a traversing slope inclinometer probe (from DGSI 2006).

2.4.1.1 Operating Principles

Accurate traversing slope inclinometer probe readings require careful installation of the slope inclinometer casing. Dunnicliff and Mikkelsen (2000) state that most inclinometer casing installations in North America rely on Acrylonitrile Butadiene Styrene (ABS) plastic casing. ABS plastic casing is corrosion resistant, flexible and does not easily deform or break under a range of temperatures. One particular benefit in cold regions is the casing's durability at low temperatures.

Dunnicliff (1993) explains that instrument precision and life can be increased with a larger diameter casing since the casing can undergo a greater amount of deformation and yet still allow the inclinometer probe to pass unimpeded (i.e. increased annular space between casing and probe). For long term monitoring of landslides, manufacturers (DGSI 2009; RST Instruments 2008) suggest the largest, 85 mm outside diameter ABS plastic casing to accommodate deformation.

Casing assembly requires proper joints, connectors and an end cap for the base. Each casing segment is connected with a variety of techniques including snaps, rivets, glue or threaded ends (DGSI 2009; RST Instruments 2008; Roctest 2008). One section of inclinometer casing is placed at a time down a vertical open borehole. Orientation of the casing tracking grooves must be controlled during installation. Mikkelsen (1996) recommends drilling the hole 6 m deeper than the zone of suspected movement to anchor the casing into competent strata. ASTM (1998)

suggests an anchor depth of at least 5 m while Mikkelsen (2003) suggests a range of 3 m to 6 m as being acceptable. Casing has been successfully installed to depths of more than 200 m (Mikkelsen 1996).

The graduated traversing slope inclinometer probe cable allows the location (depth) of the probe to be controlled so that readings are taken at the same depth interval each time. Each survey begins by lowering the traversing slope inclinometer probe to the bottom of the slope inclinometer casing, which is assumed to be in a fixed position (below the zone of movement). This is a critical assumption that provides a control check that the same fixed position can be referenced for each reading. A reading is recorded at each graduated interval as the probe is moved up the casing. Since the baseline survey of the casing is used to compare to all subsequent readings, it is recommended that the same probe be utilized for each subsequent reading. Using the same probe for each reading would avoid any potential errors that may result from switching probes (Mikkelsen 2003).

2.4.1.2 Limitations of the Technique and Sources of Error

Dunnicliff (1993) provides an overview of the factors affecting inclinometer precision. These factors include transducer precision, the design and condition of the wheel assembly, casing alignment, casing diameter, borehole backfilling procedure, casing spiral, reading repeatability (depth control), reading interval spacing, temperature effects and handling of the probe.

Table 2.1, created by DGSI (2008a), summarises sources of error as they relate to particular components of the inclinometer system. A significant number of errors are possible, especially those related to the installation of the inclinometer casing.

Mikkelsen (2003) describes two types of errors and quantifies their contribution to traversing slope inclinometer probe error. The errors were determined from observations of a number of field data sets by DGSI. Errors were classified as either random or systematic. Random error represents system precision. Systematic error represents biases in measurement. The influence of random and systematic error on probe readings was determined from a 30 m casing installation that was monitored with a 0.5 m probe. Random error was found to be no more than ±0.16 mm multiplied by the square root of the number of reading intervals. Systematic error was

found to be cumulative at ±0.11 mm per reading interval. Figure 2.8 provides a representation of total inclinometer error, where the systematic error is the difference between total and random.

It should be noted that optimum system precision can be achieved by eliminating systematic error. Random error is controlled by the instrument precision and can only be reduced by increasing the number of readings and averaging out the data sets (Mikkelsen 2003).

Systematic error can be corrected, but in order to do so the source of the error must be identified. Four common systematic errors include:

1. Bias Shift: a shift in the sensor calibration factor, b, between opposite traverses (i.e., a shift in the sensor reading between a traverse in the A_0 and A_{180} readings).

2. Sensitivity Drift: a change in the factory calibration value, k, or probe damage.

3. Rotation Error: rotational shift of the probe or sensors within the traversing slope inclinometer probe.

4. Depth Positioning Error: poor depth control due to a change in length of the cable, shortening of the inclinometer casing, or change in top reference mark.

Since systematic errors appear as displacement in a traversing slope inclinometer probe survey, they may cause unnecessary concern or mask actual deformation (Mikkelsen 2003). Bias shift, sensitivity error, and rotation error result from issues with the probe itself. Depth position error can be attributed to poor depth control that can stem from user error, casing distortion or changes in the top reference mark for periodic surveys. Bias shift can be recognized by observing the checksum plot. The checksum plot is created by summating and comparing the readings in the A_0 and A_{180} axis. That is a casing is surveyed with the probe in one direction and again in the opposite by rotating the probe 180°. The readings in the A_0 and A_{180} axis should be equal and opposite. Typically a bias towards one direction or the other exists. If there is a shift at one interval, reading it will show up as displacement. Checksums will also be have greater bias in the B-Axis since the bi-axial traversing slope inclinometer probe is controlled by the wheels running in the grooved casing. The grooves allow a little more movement in the B-Axis, this is known as the groove/wheel tolerance (Mikkelsen 2003).

Table 2.1: List of potential sources of error for inclinometer readings (from DGSI 2008a).

Accelerometer	Probe Body	Cable	Readout	Casing
Offset	Connectors	Markings	Calibration	Inclination
Sensitivity	Alignment of Mechanical Components	Handling		Curvature
Alignment		Stretching		Backfill
				Non-Parallel Grooves
				Joints
				Debris
				Displacement
				Groove Width
				Top Reference

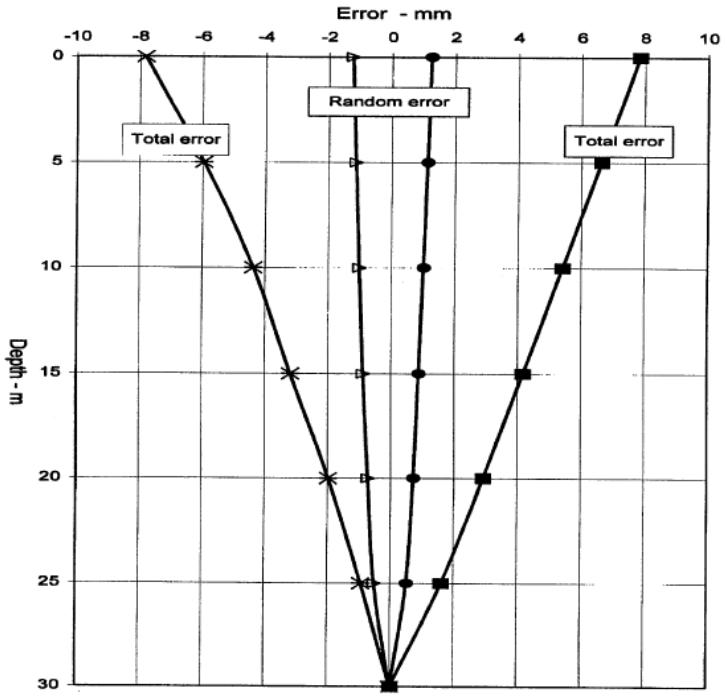

Figure 2.8: Total error represented and random for traversing slope inclinometer probe readings to 30 m (from Mikkelsen 2003).

Rotation error occurs when a probe tilt sensor rotates slightly. When this happens tilt in the cross-axis affects the readings. For example tilt in the B-Axis would affect the A-Axis readings if, between readings the tilt sensor in the probe rotates slightly. Very little rotation between readings causes this error. It is identified when viewing the cumulative displacement plot. The plots will typically show tilt values accumulating to very large values. Additionally it will likely show a drastic shift in the entire casing from previous readings.

An example of depth position error was provided by Mikkelsen (2003) in which a depth position error was intentionally introduced. The test was conducted to determine the result of 'high' and 'low' readings. A baseline survey was completed followed by a second 'low' reading during which the probe was slightly deeper for each reading interval compared to the probe depth for each reading interval on the baseline reading. A third 'high' reading was taken in which the probe was slightly shallower for each reading when compared to the baseline reading. It was shown that the 'low' readings provided positive changes, while the 'high' readings provided negative readings. In reality the tilt was a product of poor depth control.

Another depth position error was highlighted in one case study reported by Mikkelsen (2003). In this instance, movement was detected from a traversing slope inclinometer probe survey. No physical signs of movement could be determined within the structure; therefore, a detailed analysis of the data was conducted. It was determined that the depth position error was the issue and it had occurred due to the shortening of a graduated cable by just 60 mm. This error was difficult to correct and required checks on vertical control, not landslide movement.

If casing settlement is expected, a telescoping coupler is recommended. It was shown to be required if the settlement of the ground surrounding the casing is expected to be greater than 1% to 2% of the casing length.

Ultimately, with enough movement the slope inclinometer casing would be destroyed. Mikkelsen and Wilson (1983) had direct observations of the failure modes for PVC standpipe piezometers. These were observed by excavating an exploratory shaft in a large dam. The failure modes observed are displayed in Figure 2.9. Failure modes were the direct result of movement in the horizontal and vertical direction (settlement), or combination of the two. These

failure observations are relevant since they provide an indication of the failure a slope inclinometer casing may undergo at large deformation.

The quality of traversing slope inclinometer probe readings is reduced and eventually cannot be taken due to casing deformation. Casing curvature defines the tracking and passage limits of the probe. Tracking limits are reached when the curvature of the casing is greater than 5.5° between reading intervals. This causes the wheels of the probe to be pulled out of the casing tracks, thus reducing the quality of the readings. A tracking limit refers to a probe being unable to pass through the casing. This occurs when a change of 10.3° exists between two consecutive reading intervals (DGSI 2008a). An example of a traversing slope inclinometer probe passage issue is highlighted in Figure 2.10. The figure highlights the effect of probe length, diameter and casing curvature. A comparison of two probes shows that the shorter instrument length and smaller instrument diameter can navigate a casing with sharper curvatures. This translates into longer casing life and useable life of the casing (RST Instruments Ltd. 2008).

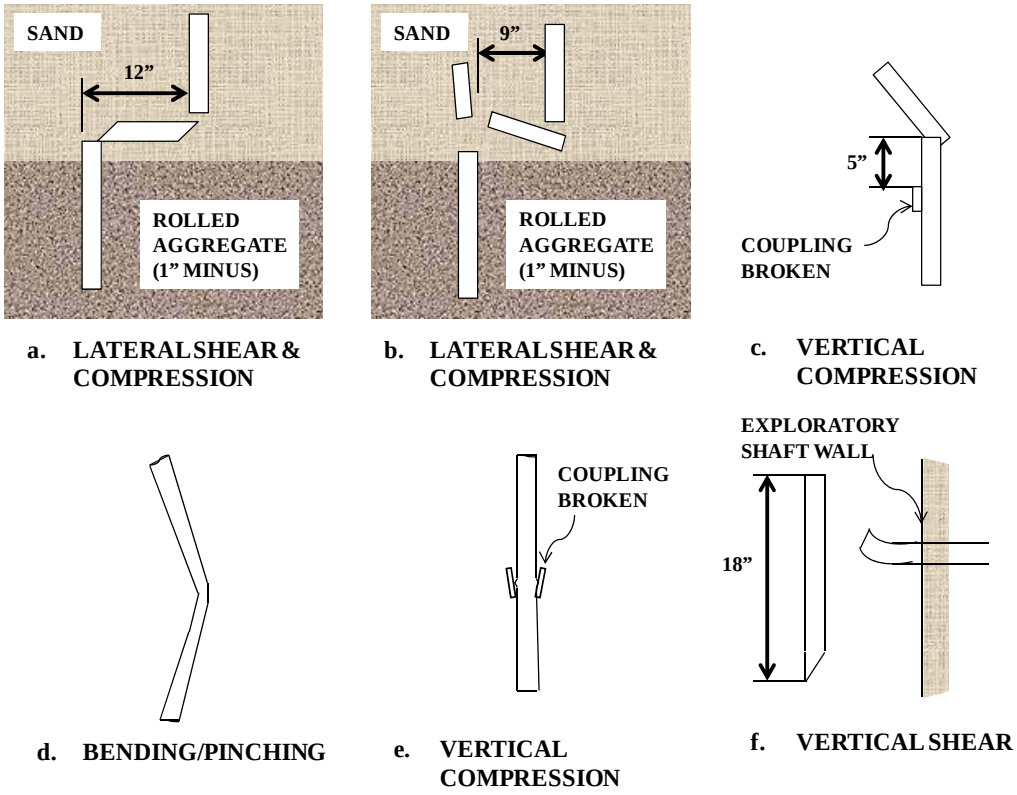

Figure 2.9: Failure modes of standpipes in an earth dam (reproduced from Mikkelsen and Wilson 1983).

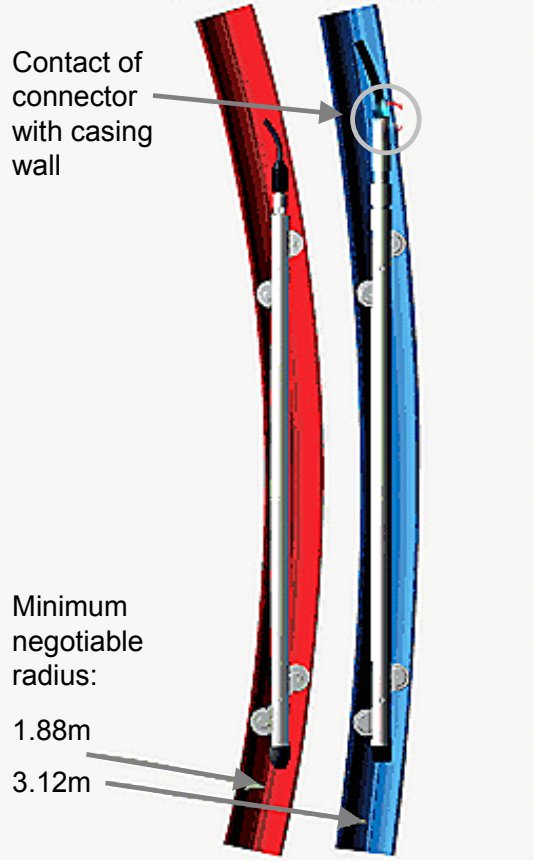

Figure 2.10: Inclinometer probe navigating casing (from RST Instruments Ltd. 2008).

2.4.2 Manual Monitoring Case Studies

The following case studies focus on landslides in Saskatchewan and Alberta and associated landslide monitoring techniques. Most, but not all case studies reviewed involve multiple retrogressive landslides.

Thomson and Hayley (1975) investigated a multiple retrogressive landslide that affected a highway and bridge located in the Peace River Valley in Northern Alberta. They relied on reading slope inclinometer casing with a traversing slope inclinometer probe to locate the slip surface of the landslide and a topographic survey to determine surface movement. Periodic monitoring of the slope inclinometer casing indicated a relatively planar slip zone, with minor slip zones nearer to the surface. The minor slip surfaces were described as the extension of the failure surface of a single block down to a common planar failure surface. Traversing slope inclinometer probe data were not used to describe relative movement of the slope blocks, but the

periodic topographic survey indicated that control points at the toe moved more than those at the crest of the slope.

At the Beaver Creek landslide site, Haug et al. (1977) identified the shear zone by inspecting cored soil samples. Piezometric levels were measured in a stable zone directly behind the slide mass as well as within the landslide mass. Air photos and topographic maps were used to identify the extent of sliding and a control line was created to observe the movement of surface targets and the location of the river over time. It was concluded that river erosion played a large role in slope movement and it was hypothesized that the blocks moved at different rates with the greatest movement being at the toe. This was verified by Churisinoff (1980) who performed periodic precise surveys using surface monuments to determine relative movements on the multiple blocks of the active slope.

Yoshida and Krahn (1985) further improved on the monitoring and understanding of the Beaver Creek landslide through the installation of slope inclinometer casing adjacent to standpipes. This was done to verify the location of failure planes as determined in previous studies. The traversing slope inclinometer probe readings were used verify the location of the slip surfaces. It was determined that they were approximately 6 m below that defined by Haug et al. (1977). The addition of standpipe piezometers was used to establish the pore-water pressure conditions in the vicinity of the shear zone. It was found that the rate of movement of each slide block varied with pore-water pressure conditions. Higher pore-water pressure conditions and movements were typically observed during spring and summer. Movement was observed to be greatest at the toe and reduced upslope. This observation was verified by comparing both periodic topographic survey results and slope inclinometer surveys. Figure 2.11 highlights the inferred slip surfaces and resultant cumulative slope inclinometer casing profiles for the A-Axis which was aligned down slope in the expected direction of movement.

Thomson and Tweedie (1978) installed and monitored slope inclinometer casings at various locations throughout a new landslide block forming at the Edgerton landslide site near Wainwright, Alberta. After a 2.3 m scarp formed at the crest of the slope it was observed that the inclinometers were destroyed progressively from crest to toe indicating that movement progressed in a top down fashion during this period of time. The tilt meters were destroyed

because the casing was pinched or sheared and the traversing slope inclinometer probe could no longer pass through the casing. The shape of a slope inclinometer casing placed near the toe of the slope for two monitoring increments is displayed in Figure 2.12. The increased rate of movement at this landslide highlights the potential for a more rigorous monitoring system that could limit temporal gaps. Note in observing Figure 2.12 that the shape of the casing changes substantially between periodic readings during a time of rapid movement.

Construction of a new bridge crossing over the North Saskatchewan River near Maymont, Saskatchewan required a large cut to accommodate the approach. Shortly after the 20 m cut was completed a large failure occurred. No monitoring of this cut slope was conducted prior to failure. After the failure Krahn et al. (1979) used air photo studies and a precise ground survey to create slope sections and develop contour maps. Open standpipes were installed to measure piezometric levels. Slope inclinometer casing was placed in the failed zone and in the stable portion behind the failed zone to track the failure surface and monitor if it retrogressed. Since this was an active construction site, daily inspection was possible to ensure movements that were detrimental to construction were captured.

Clifton et al. (1981) reported that the first landslide problem recorded by the City of Saskatoon situated on the South Saskatchewan River bank dates back to 1913. Continuous monitoring with piezometers and a traversing slope inclinometer probe has been conducted at sites throughout the city's river valley in order to plan, protect and maintain infrastructure. Throughout the city; roadways, bridges, housing and other infrastructure encroach on these unstable sites.

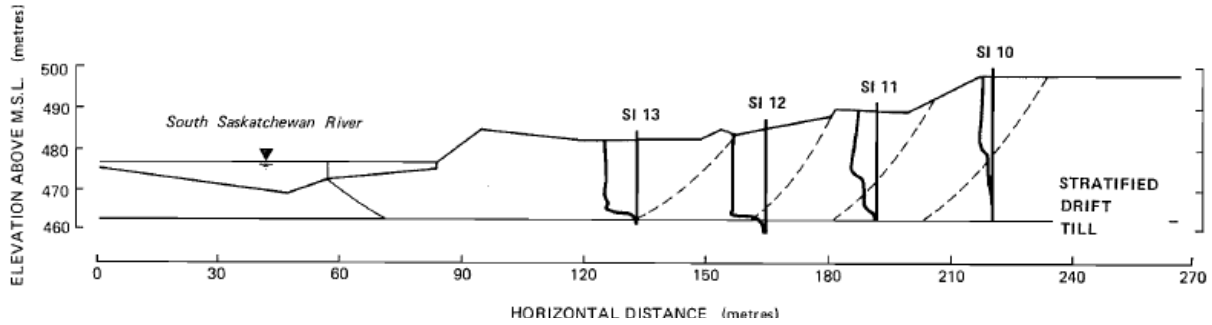

Figure 2.11: Inclinometer results, slope profile and inferred slip surfaces from the Beaver Creek Multiple Retrogressive landslide (from Yoshida and Krahn 1985).

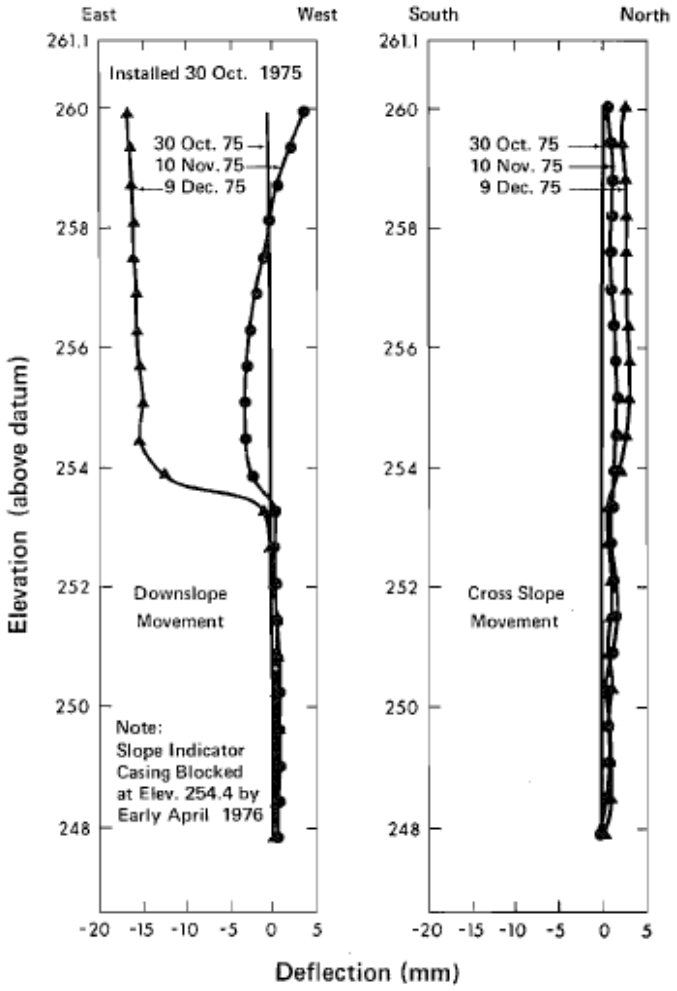

Figure 2.12: Inclinometer casing deformation for a landslide near Wainwright, Alberta (from Thomson and Tweedie 1978).

Clifton et al. (1986) studied the area of Regina Beach, Saskatchewan. This town is located along the Last Mountain Lake valley. This valley represents an old glacial melt water channel. Horizontal movement was measured with a slope inclinometer system. It was observed that grading the toe of the slopes (removing toe material), and increasing pore-water pressure correlated with an increase in landslide activity. Increases in pore-water pressure occurred through irrigation of developed lots, infiltration, and water main breaks. This site highlighted the effect of human development on the stability of slopes and the use of monitoring to determine the triggers of the movements.

Kelly et al. (1995) used stratigraphic characterization and the installation of slope inclinometer casings and piezometers nests, to monitor a landslide that affected the Deer Creek Bridge near Deer Creek, Saskatchewan. Monitoring for this site was conducted sporadically, so assumptions had to be made for temporal gaps in the readings and relative movement on the slip surfaces.

Boutwell and Schmidt (1998) described an instrumented slope failure along the Tombigbee River in the Coastal Plains region of Southwest Alabama. Manual instrumentation readings were taken just two days prior to a major slope failure. It was concluded that the monitoring of surface cracks, pore-pressures (piezometers) and slope movement (inclinometers) did not provide any indication of the incipient failure.

Pauls et al. (1999) studied a landslide site near Carrot River, Saskatchewan that affected a bridge crossing. It was hypothesized that rapid drawdown of the river after flooding could increase slope movement. Traversing slope inclinometer readings determined that movement rates did not increase before, during and or shortly after periods of flooding.

Kelly et al. (2005b) monitored twelve slope inclinometer casings with a traversing slope inclinometer probe, and five pneumatic piezometers. The result of fill placement at the top of the Frenchman River Valley showed that movement progressed at greater rates and magnitudes at the crest of the slope compared to the toe. In general, piezometers indicated a downward flow gradient and varied little over time with the exception of the changes that were induced by fill placement and removal. Monitoring of this instrumentation showed movement triggered by construction activity.

Instrumentation using periodic measurement techniques has provided a means to determine the locations and rates of movement. The main triggering mechanism was briefly discussed in section 2.1.1 and re-iterated here as groundwater levels (increasing pore-water pressures due to infiltration, increased precipitation, spring melt, irrigation, etc.), river level change (causing erosion and/or rapid drawdown) and construction (grading, excavation). In general the monitoring instrumentation has been used to provide indication of movements and to determine possible triggering mechanisms.

All hypotheses with regards to movement of multiple retrogressive landslides indicate movement from the toe retrogressing (and lesser) to the crest of the slope. In two cases periodic monitoring indicated greater movement from the crest of the slope and lesser at the toe. This showed that depending on the ground conditions it may be possible to trigger movement in a multiple retrogressive landslide from the crest of the slope.

2.5 Automated Monitoring of Landslides

2.5.1 In-Place Inclinometers

In-place inclinometers (IPIs) share similar characteristics with the traversing slope inclinometer probe. Dunnicliff (1993) describes the IPI as an instrument that collects essentially the same data as a traversing slope inclinometer probe and uses standard slope inclinometer casing, but is left suspended in the casing to monitor a specific zone.

Similar to the traversing slope inclinometer probe a tilt transducer is used to measure tilt in the IPIs. Transducers include force balance accelerometers, vibrating wire, electrolytic transducers, and most recently Micro-Electro-Mechanical-System transducers (MEMS). All the tilt sensors produce an output voltage that is proportional to the sine of the tilt angle, θ.

If the location of the shear zone of a landslide is known, then an IPI sensor placed within that shear zone is spanned with a specified gauge length. Ideally the gauge length should entirely intercept the zone of movement. Sensor gauge lengths are provided from 1 m to 3 m. Any movement of the casing where the IPIs is located will create a change in tilt over time and this can be multiplied by the gauge length to obtain horizontal displacement across that zone.

2.5.1.1 Operation

ISRM (1981) provides a suggested method for monitoring rock movements using IPIs. The recommended casing is an ABS plastic casing with an outside 85mm diameter (3.34”). Figure 2.13 highlights the components of the IPIs system. Casing installation requirements are the same as for the traversing slope inclinometer probe described in Section 2.4.1.1.

It is recommended that the initial casing profile be measured with a traversing slope inclinometer probe to determine the location of the slip surface (ISRM 1981) prior to installation of the IPIs. A baseline survey with a traversing slope inclinometer probe will also allow for full casing surveys if IPIs provide unexpected data. This provides the ability to compare results from a traversing slope inclinometer probe to that of the IPIs.

A top assembly holds the IPIs, via a steel cable, at a fixed depth down the borehole to intercept movement zones. The IPIs should be installed not only to span the zone(s) of movement, but to measure the maximum displacement (ISRM 1981; Dunnicliff 1993; Simeioni and Mongiovi 2007).

ASCE (2000) describes guidelines for instrumentation installed to monitor the performance of dams. It describes that IPIs sensors suspended in a casing using a cable should be in constant tension. This can be ensured by adding additional weights to the bottom of the probe or by lowering the installation past its required depth and pulling the sensors back up to the correct depth.

Multiple IPIs can be attached together using universal joints, or a single IPI sensor can be placed in the slope inclinometer casing. The use of a single IPI sensor was suggested by Johnson (2002) and was used by Flentje et al. (2005) as well as Simeioni and Mongiovi (2007).

2.5.1.1 Capabilities, Limitations, Sources of Error and Automated Monitoring Case Studies

Due to a limited number of case studies and the relevance of the case studies, this section will combine automated monitoring case studies with the capabilities, limitations, and sources of error for the IPIs.

IPIs enable displacements to be monitored in near real-time through connection to an automatic data acquisition systems (ADAS). The ability to connect to an ADAS can be an excellent risk management tool for continuous monitoring with alarm pre-sets. Since ADAS can record data on a pre-set time interval, the system may capture slope movements that help further explain slope kinematics and mechanism.

Geokon Ltd. (2008a) has IPIs utilising vibrating wire transducers. Both Geokon Inc. and RST Instruments Ltd. now use Micro-Electro-Mechanical Systems (MEMS) to produce a force balance accelerometer transducer in their traversing slope inclinometer probe and IPIs (Geokon Inc. 2008b; RST Instruments 2008). A MEMS transducer is much smaller allowing for the construction of smaller probe bodies. It can be concluded that the capability of IPIs is dependent on the annular space in the casing. By increasing the annular space by making the IPIs body smaller the useful life of a casing installation and IPIs is achieved.

Dunnicliff (2002) suggests that selection of the IPIs gauge length is important. The author warns that if the gauge length of the IPIs spans a shear zone significantly smaller than the gauge length, it is likely to provide false data since the gauge tubing can contact the distorted casing as shear progresses.

Johnson (2002) suggested that a single IPIs placed to span zone of maximum displacement would be sufficient to monitor slope movement. This would reduce the complexity and cost of using multiple IPIs installations but can only be utilized where the location of the shear zone is well defined. Slope inclinometer casing readings are generally used to define the shear zone.

Mikkelsen (2003) described both random and systematic errors in traversing slope inclinometer probes. Simeioni and Mongiovi (2007) attempted to apply some of the sources of error to the IPIs in the field study of the Castelrotto Landslide in Italy. They were using their system to correlate rainfall and slope movement. When data from traversing slope inclinometer probe readings and IPIs were found to vary by up to 100% between displacements and up to 91° in direction, they developed the following potential sources of error:

1. Instrument noise from the data acquisition unit.

2. Systematic error due to damage to the acquisition unit or probe.

3. Errors due to disturbance of the system. (For example, the removal of IPIs for traversing slope inclinometer probe measurements). Errors due to unforeseen or unknown phenomena.

4. Errors due to unforeseen or unknown phenomena.

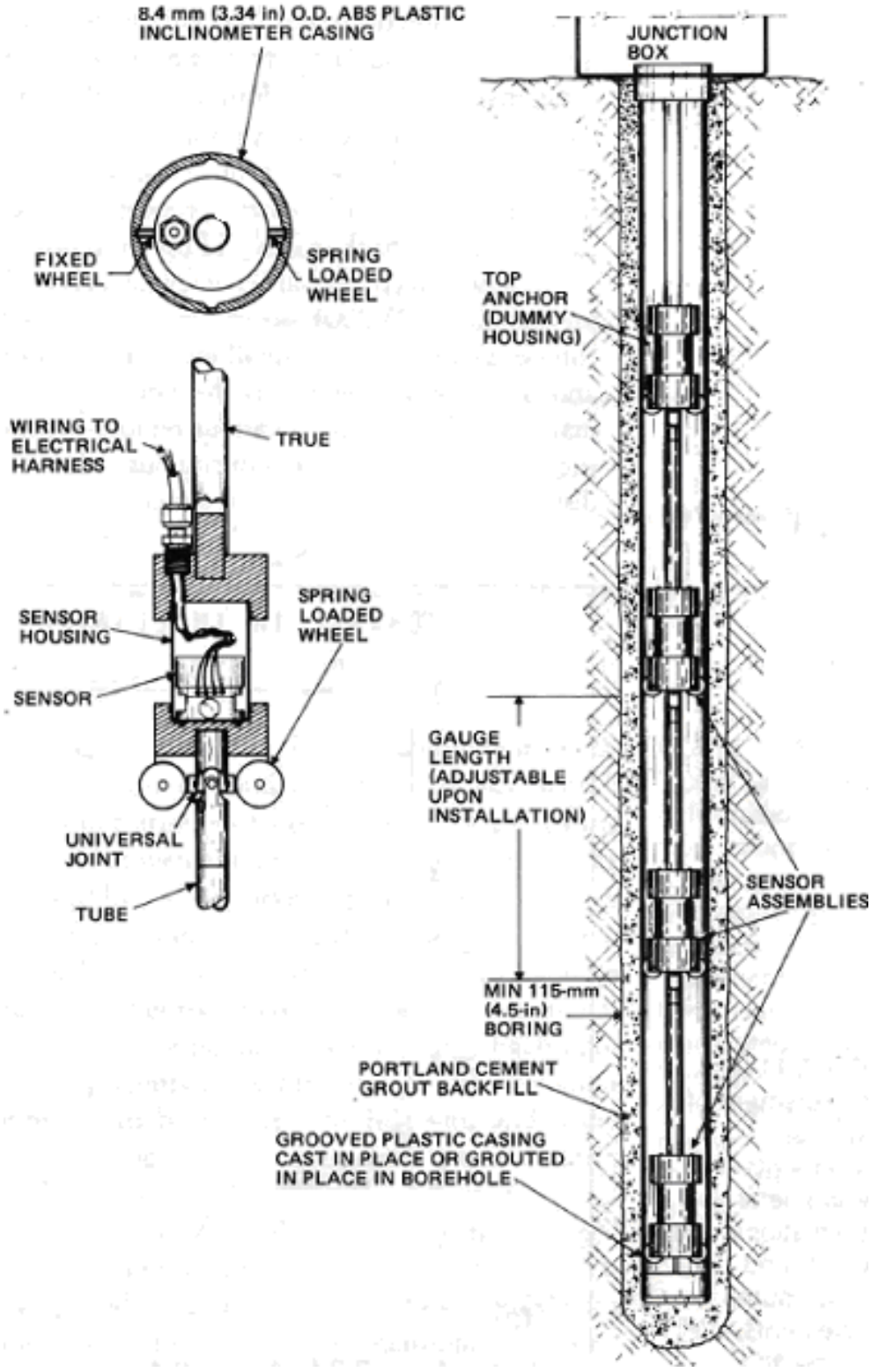

Figure 2.13: Installation details for a string of IPIs sensors (from Wilson and Mikkelsen 1978).

Since movements at the Castelrotto landslide were less than 7 mm a depth position error as described by Mikkelsen (2003) was not considered. Mikkelsen (2003) described the depth position error as a reasonable potential error in cases where larger deformation may occur. For the IPIs this would happen if the cable holding the IPIs changed length, the casing changed length or the sensors had no fixed reference point.

Finally Simeioni and Mongiovi (2007) showed that removal and replacement of the IPIs may result in the IPIs being in a slightly different position. It was also determined that the head assembly of the IPIs could settle causing a sensor to shift ±100 mV up to two weeks after replacement. This shift appears as movement.

Flentje et al. (2005) described the use of IPIs to measure slope deformation as part of a real-time monitoring system for slope instabilities in Wollongong, New South Wales, Australia. This research explored rainfall as a trigger for slide events in Wollongong. The near real-time monitoring system utilized vibrating wire piezometers, IPIs and a rainfall pluviometer (rain gauge). Data was transferred from the data acquisition system to a server via a cell phone modem and was then uploaded to the internet where data and figures from four landslides, each with their own monitoring station, were automatically processed for viewing in near real-time. This system allowed for risk management of these sites as well as archiving data for later analysis and interpretation. The data set provided evidence to suggest that rainfall events trigger slope movement.

Although the study by Flentje et al. (2005) identified a landslide trigger, it also noted unexpected IPIs data. Upon observation of the data set, a single IPI showed upslope movement. It was removed to perform a survey with a traversing slope inclinometer probe. The traversing slope inclinometer probe survey showed that the IPI sensor, which was located on the lower 0.5 m of a 3 m long gauge length, was below the shear zone. The tilt sensor functioned to read upslope movement below the shear zone, but in order to do that, the gauge tubing above it had to flex. This is a relevant issue since the gauge tubing is assumed to be rigid. Secondly, this reinforced Dunnicliff's (2002) observation that IPIs with gauge length longer than the shear zone will cause unexpected readings.

Although the IPIs are a static instrument, large deformations in the vicinity of the IPIs could cause them to come in contact with the casing wall. Contact with the casing wall could cause unexpected readings associated with IPIs tracking and the effect of the casing on the IPIs when the casing eventually contacts it.

In general the IPIs was shown to be sensitive to tilt and provided the ability to correlate readings with movement. There appear to be concerns related to obtaining accurate readings of slope movement from the IPIs based on instrument or installation issues.

2.6 Summary

Multiple retrogressive landslides often remain active with movements of just a few millimetres per year. Landslide movement or kinematics is defined by the movement distributed through the moving soil mass. Triggers of these landslides typically include water level changes, rainfall events, or human activity. These conclusions were drawn from site investigation and field monitoring.

Landslides are a function of the geology, geomorphology and hydrogeology. Typically in the Canadian Great Plains landslides occur in river valleys. River Valleys such as the North Saskatchewan River Valley were formed during deglaciation. Rapid erosion of these channels from glacial melt water resulted in the exposure of weak geologic materials such as clay shale. Where glacial lakes were present and subsequently drained the river down-cut into glaciolacustrine clay as is the case for Highway No. 302. The over steepened side slope created by down-cutting of the river resulted in slope failure to occur in the weaker clay material which overlies the stronger till material.

Many of the manual instrumentation case studies cite the use of groundwater levels (pore-water pressure measurement), traversing slope inclinometer systems and surface surveys to monitor slope movement. Lateral river erosion and groundwater level fluctuation were the two main triggering mechanisms identified with slope movement. Another potential triggering mechanism that was explored was rapid drawdown.

In general, manual monitoring techniques have been successful to hypothesize the kinematics and mechanism for landslides. The major disadvantage of manual monitoring is the time gap between readings. Movement events or destabilizing conditions may be missed during the time between site visits and warning signs of imminent failure, or clues to mechanism of failure cannot be accounted for.

Real-time monitoring systems typically consist of electronic instruments that can be read by data loggers at user-specified time intervals. Data can then be transferred with a communications system to an internet server where data is processed and uploaded to the World Wide Web. This data is available in near real-time and greatly reduces the time gap between data acquisition intervals, forming a more rigorous data set and providing an important tool for risk management.

Current research is limited, but has shown successful use of the IPIs to correlate landslide triggers. A number of potential issues have been raised with the use of the IPIs to determine movement direction and magnitude to help define slope kinematics. Issues pertain mainly to the selection of gauge length, the position of the sensors in the inclinometer casing, and the installation of the inclinometer casing. It was suggested that, if possible, a single IPIs should be used and periodic checks of the full casing profile should be done to verify the IPIs results. IPIs have a relatively short history of use; therefore, their capabilities and limitations are still in the process of being investigated.

Chapter 3 Physical Site Description and Site Investigation

This chapter summarises information regarding the physical geography, geology, geomorphology and hydrogeology of the Prince Albert area as it pertains to the Highway No. 302 landslide study site.

3.1 Physical Geography

3.1.1 Location

Highway No. 302 is part of the Saskatchewan Provincial Highway network and runs through the city of Prince Albert. Approximately 5 km west of Prince Albert (Figure 3.1) an active landslide affected a portion Highway No. 302 resulting in cracking and deterioration of the road surface. The landslide affected approximately 1 km of the highway where it runs nearly parallel to the river approximately 250 m away. The landslide is illustrated in the aerial oblique photograph, Figure 3.2.

3.1.2 Land Use

Land to the north and south of the North Saskatchewan River in the vicinity of the landslide site is a mixture of cultivated and pasture land. The south side within the river valley itself is heavily vegetated with grasses, shrubs and trees. Some vegetation in this area has been cleared in an attempt to create land for cultivation; however, these areas are covered in natural grasses and do not appear to be cultivated at present. The north side of the river is a flood plain and is cultivated for agricultural purposes. Within the cultivated land on the north side of the river is a section of wet, heavily vegetated, and low lying land.

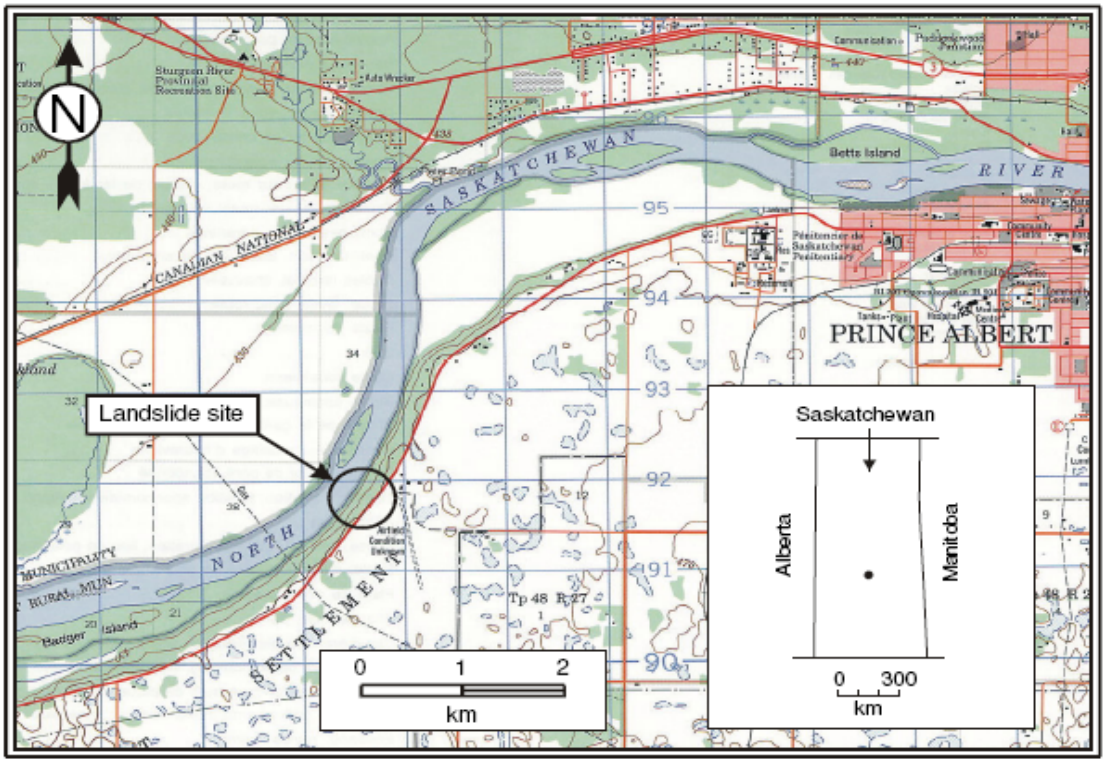

Figure 3.1: Location of landslide site (from Kelly et al. 2005a, National Topographic System Map Sheet 73/H).

Figure 3.2: Aerial view of Highway No. 302 Landslide site (Photograph courtesy of Vista Photography).

3.2 Site Geology and Geomorphology

The Saskatchewan Ministry of Highways and Infrastructure (SMHI) determined site specific geology by drilling a single stratigraphic borehole. Further information about the site was gathered through subsequent drilling for the installation of monitoring instrumentation.

Figure 3.3 presents a topographic contour map indicating ground surface elevations and the location of a stratigraphic cross section B-B' which is presented in Figure 3.4. A stratigraphic cross section was developed from boreholes (BH) BH402, BH401, and BH10 as well as the boreholes drilled to install slope inclinometer (SI) casings SI001, SI002 and SI003 (see Appendix B for borehole logs). The stratigraphic boreholes and logs were drilled and created by the SMHI and provided for use in this thesis project.

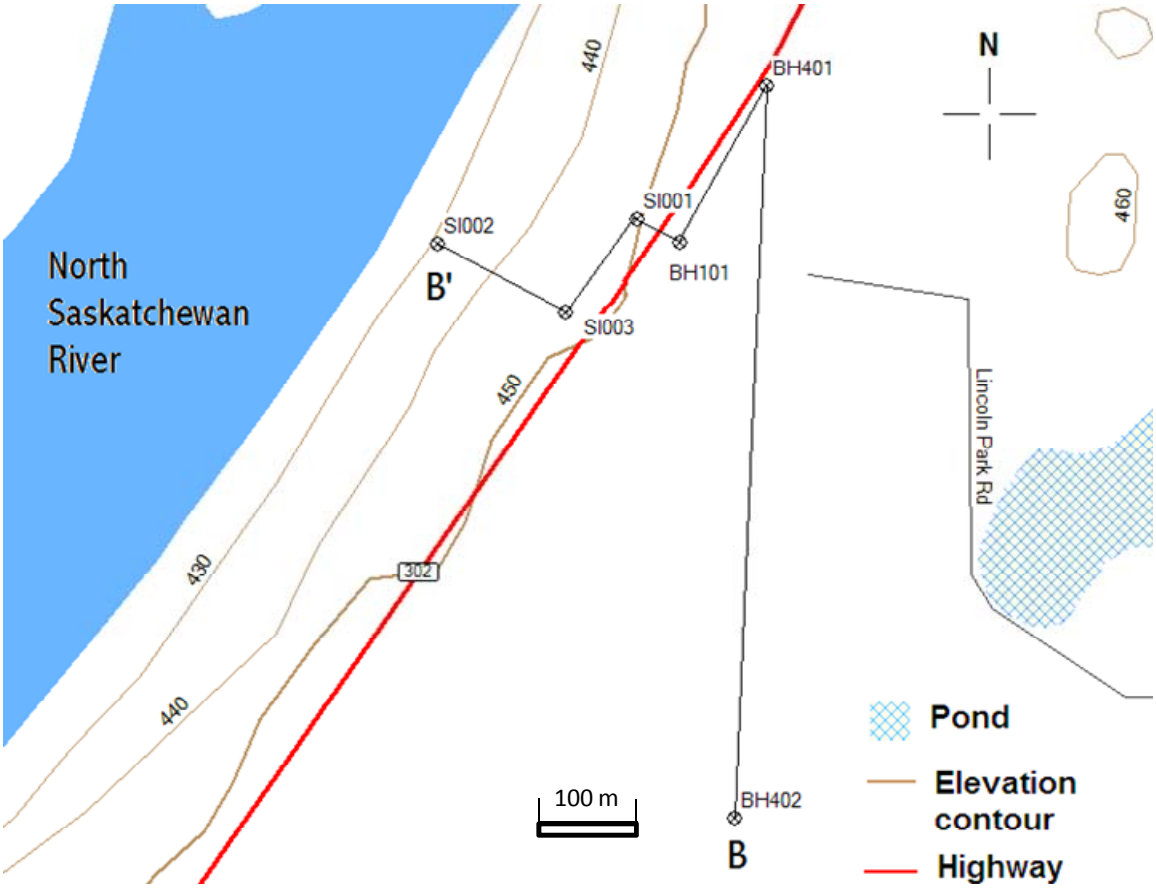

Figure 3.3: Surface contours and cross section B-B'.

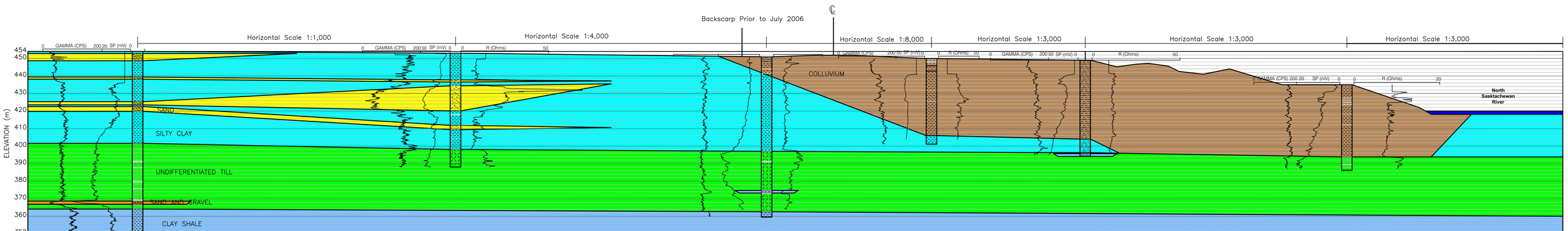

Figure 3.4: Site cross section B–B'

The failure surface is quite planar occurring near the silt/clay and till contact. Failure at this zone is likely due to the difference in strength between highly plastic clay and till material.

Presentation and discussion of the stratigraphy is important for an understanding of site specific geology and the related groundwater regimes that could exist. This provides the basic geologic and hydrogeologic framework for the site.

3.2.1 Cretaceous Geology and Geomorphology

The Upper Cretaceous Lea Park Shale was used as the base of exploration for the drilling program. No borehole extended deep enough to penetrate below the Lea Park Shale to observe the extent of shale overlying the Mannville Group. Information as to the depth and extent of the Mannville formation would have provided a more complete geologic and hydrogeologic framework for the region and the site. Although many landslides occur in the upper portion of the Lea Park Shale, a few occur where the quaternary deposits, specifically surficial stratified drifts, control slope failure (Christiansen and Sauer 1984).

3.2.2 Quaternary Geology and Geomorphology

The shale/till interface represents an unconformity and 38 m of undifferentiated till exist above it. Overlying the till surface was up to 50 m of highly plastic silty clay, which was overlain by up to 18 m of silt and clay to the ground surface.

The landslide morphology is hummocky and typical of multiple retrogressive landslides found throughout the banks of the North and South Saskatchewan Rivers (Christiansen and Sauer 1984). Figure 3.5 shows the topography formed from multiple retrogressive landslide action as well as the influence of river erosion at the toe of the slide mass. Observation of the slumping blocks at the river's edge indicates that the surficial silts and clays are being eroded by the river, causing shallow rotational failures.

Figure 3.5: Surface morphology of the Highway No. 302 landslide (from Kelly et al. 2005a).

An approximately 2 m thick shale layer was located in BH101 within the till sequence. This supports the geological thrust activity described in the Prince Albert area (eg., Christiansen and Sauer 1993). An approximately 2 m thick sand and gravel layer was discovered at the base of the till in BH402. Other findings included sand layers within the surficial stratified drift of BH401 and BH402. A 14 m thick layer of fine sand was found at a depth of 19 m (Elev. 434 m) in BH401; while in BH101, approximately 200 m to the west, no sand was found. Due to the depositional environment, the lateral extent of these sand layers is unclear; however, BH402 located approximately 570 m southwest of BH401 had a 5 m sand layer, 29 m below surface (Elev. 425 m). Significant near surface sand layers were found to exist within the highly plastic clays in the vicinity of the landslide.

3.2.3 Site Hydrogeology

The SMHI drilling and instrumentaion program provided stratigraphic information through the Quaternary deposits and into the upper portion of the Cretaceous clay shale. The depth to the top of the Mannville Group aquifer was not reached with a site specific borehole; therefore, no

information was obtained from this unit to determine the groundwater flow regime stemming from the deep aquifer.

The Empress unit was not encountered, which confirms the cross section presented by Christiansen and Sauer (1993) that suggests this unit pinches out in the vicinity of the North Saskatchewan River.

The location of the sand and gravel unit found in BH402 may be related to the intertill aquifers described by Millard (1990) since the locations of these units are within the till deposits. Since differentiation of the till units was not required for this study it can only be speculated that this unit may separate the Sutherland Group, or Saskatoon Group Floral Formation.

The 14 m thick layer of fine unoxidized sand found at a depth of 19 m in BH401 (Elev. 434 m) within the highly plastic clay may be connected to the 5 m thick sand layer discovered 29 m below surface (Elev. 425 m) in BH402 located approximately 570 m southwest of BH401. The possibility of such a significant sand layer within the highly plastic clays near the landslide would have implications for stability as it would be providing a conduit for water to enter the landslide mass. Entry of water at the crest of the landslide mass could significantly affect the stability of the upper landslide block.

3.3 Site Instrumentation and Investigation

A brief overview of the IPIs and vibrating wire piezometer instrument installations at the study site will be presented in this section.

Locations of all the instruments with reference to the unstable slope are shown in Figure 3.6. A summary of instrumentation installed near the highway is provided in Table 3.1. A summary of instrumentation installed near the river is given in Table 3.2.

It should be noted that all slope inclinometer (SI) casings were installed according to standard SMHI practice of aligning the A-axis with the North-South direction. This is not consistent with the recommendation of the SI manufacturer that the A-axis of the casing be aligned roughly along the expected direction of movement so as to enhance the sensitivity of the instrument to

slope movements. Since the unstable riverbank was aligned in the Northeast-Southwest direction (approximated 45° skew from the North direction; Figure 3.6), the movements measured along the B-axis were greater than or equal to those measured along the A-axis.

3.4 Instrumentation Background

Subsurface instrumentation was installed by the Saskatchewan Ministry of Highways and Infrastructure (SMHI) using a Failing 1250 mud rotary drill rig. Boreholes were drilled with a 4.75 inch (120 mm) diameter Walmac wash bore drill bit. Soil samples were collected and described, and geophysical tests including spontaneous potential, resistivity and natural gamma were conducted on each borehole. This information was used to confirm material visual geologic descriptions and the contact zones between them.

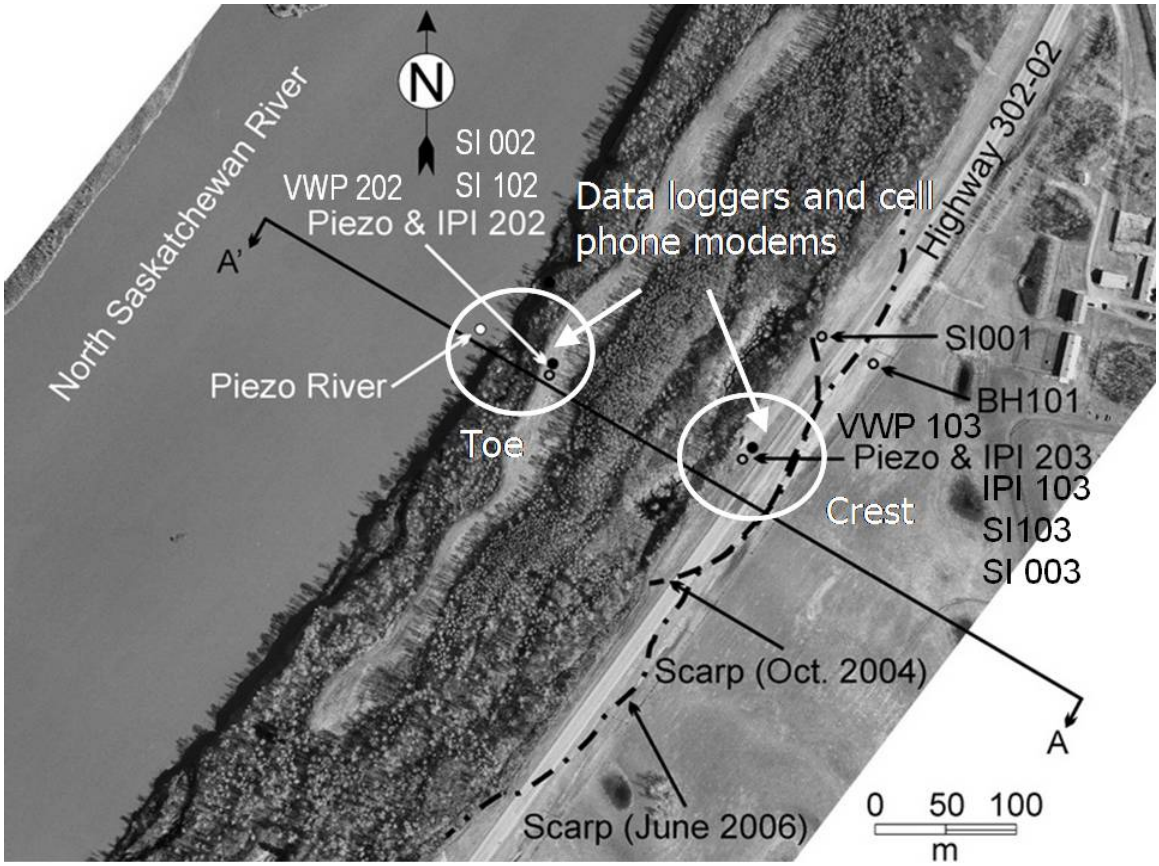

Figure 3.6: Aerial photograph showing the extent of unstable slope and the location of instruments (after Antunes et al. 2006).

Table 3.1: Summary of instrumentation installations near the highway.

Name	Instrument	Serial No.	Completion Date (dd/mm/yyyy)	Elevation (masl)			Measurement Method and *Type*
				TOC	Surface	Instrument Tip	
SI001	SI	N/A	16/10/2002	450.76	450.26	401.96	Manual Monitoring *Displacement*
SI003	SI	N/A	26/07/2005	449.45	448.95	394.5	
SI103	SI	N/A	31/08/2005	449.25	448.75	392.25	
IPI103	IPI	IPI12783	18/09/2005	449.25	448.75	406.40	Automated Monitoring *Displacement*
		IPI12784				404.40	
		IPI12785				402.40	
IPI203	IPI	IPI12912	15/05/2005	449.25	448.75	408.40	
		IPI12913				405.90	
		IPI12914				403.40	
PZO103	VWP	PZO83404	30/08/2005	N/A	448.92	409.32	Automated Monitoring *Pore-water Pressure*
		PZO83405				404.27	
		PZO83406				399.37	

[**Legend:** SI = Slope inclinometer; IPI = In-place inclinometer; VWP = Vibrating wire piezometers; TOC = Top of casing]

Table 3.2: Summary of instrumentation installations near the river.

Name	Instrument	Serial No.	Completion or Installation Date	Elevation (masl)			Measurement Method and *Type*
				TOC	Surface	Instrument Tip	
SI002	SI	N/A	5/26/2004	435.45	434.95	386.15	Manual Monitoring *Displacement*
SI102	SI	N/A	7/27/2005	435.72	435.22	387.22	
SI202	SI	N/A	08/29/2005	435.7	435.2	387.20	
PZO201	PP	N/A	05/16/2004	N/A	435.05	425.05 408.70	Manual Monitoring *Pore-water pressure*
PZO202	Vented VWP	PZO83513	8/17/2005	N/A	N/A	418.60*	Automated Monitoring *River Level*
IPI202	IPIs	IPI12786 IPI12787 IPI12788	09/18/2005**	435.7	435.2	395.70 393.70 391.70	Automated Monitoring *Displacement*
PZO202	VWP	PZO83401 PZO83402 PZO83403	09/18/2005**	N/A N/A N/A	435.22	399.07 395.07 389.07	Automated Monitoring *Pore-water Pressure*

*Estimate of river bed [**Legend:** SI = Slope inclinometer; PP = Pneumatic Piezometer; IPI = In-place inclinometer; VWP = Vibrating wire piezometer; TOC = Top of casing]

3.4.1 Electrolytic In-Place Inclinometer

The electrolytic in-place inclinometer (EL IPI) from DGSI (Figure 3.7) was used for all IPIs installations. Three IPIs were connected and installed in each casing to span the zone of movement. Each IPI was 2.0 m in total length with a 0.55 m probe and 1.45 m gauge tubing.

3.4.1.1 Installation

The installation of the IPIs first required the installation of 85 mm ABS plastic inclinometer casing supplied in 3 m sections. A typical casing installation procedure was carried out by SMHI as follows:

1. A mud rotary borehole was drilled into stable strata.
2. The drilling fluid was replaced with a cement-bentonite grout.
3. A bottom cap was placed on the base of the first piece of casing, to seal the inclinometer casing before it was pushed down hole and filled with water for weight to overcome buoyancy.
4. Each subsequent section was snapped in place, riveted, taped, filled with water and lowered into the hole.
5. Once all the casing was installed it was held at surface with the drill rig overnight to prevent the casing from 'floating' out of the borehole while the grout set.
6. Once the grout set, initial traversing slope inclinometer probe readings (baseline readings) were conducted followed by additional monitoring with the traversing slope inclinometer probe or through real-time monitoring with the installation of the IPIs.

DGSI (2006) recommends the casing be installed with the A-Axis aligned in the direction of suspected movement (Figure 3.8). SMHI standard procedure is to install all A-Axis to the north to achieve consistency in all the installations of inclinometer casing in the province. This was also done at the Highway No. 302 site. The typical components required for installation of the IPIs are displayed in Figure 3.9 and the top assembly termination is shown in Figure 3.10.

A single IPI or multiple IPIs are 'fixed' at a depth relative to the top of the inclinometer casing as required. Minor depth adjustments can be achieved by using a chain and s-hook. Retrieval of the IPIs is possible as long as the deformation of the casing has not reached a point where the IPIs cannot navigate the casing. Removing the IPIs sensors periodically may be required to perform a traversing slope inclinometer probe survey, repair malfunctioning IPIs, or to retrieve the sensors for reuse.

Figure 3.7: EL IPI from Durham Geo Slope Indicator (DGSI 2008b).

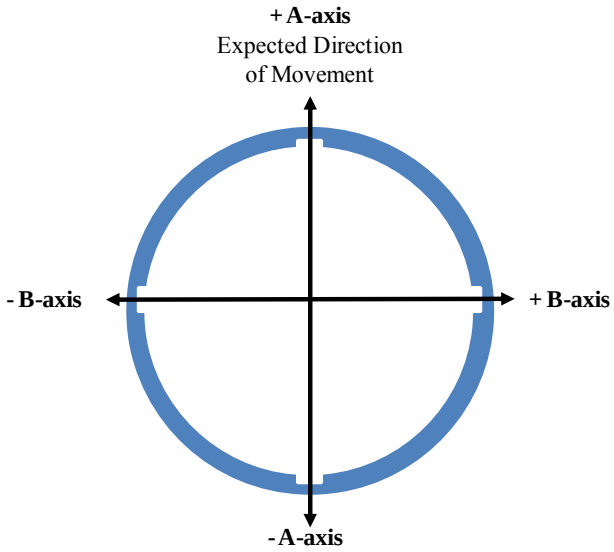

Figure 3.8: Orientation of the slope inclinometer casing during installation.

Three IPIs were installed in each borehole casing for SI103 (renamed IPI103), IPI203 at the crest and SI202 (IPI202) at the toe. The third IPIs (IPI203) was installed at the crest of the slope to replace IPI103 after it was destroyed. Manual readings were conducted for IPI103 and IPI202 prior to installation of the IPIs, but a preliminary traversing slope inclinometer probe survey was not conducted for IPI203 prior to installing the IPIs. The gauge length of IPI203 was increased to 2.5 m to allow the installation to span a longer zone compared to previous installation of IPI103, which had 2.0 m gauge lengths.

3.4.1.2 Calibration and Calculations

Calibration of IPIs was performed by the manufacturer prior to shipping the probe. The IPIs installed at IPI103 and IPI202 underwent an eleven point calibration at three temperatures from 4°C to 20°C over a tilt range of ±10° (tilt of ±350 mm from vertical). Additional calibration to ±30° (tilt of ±1155 mm from vertical) was completed on IPIs installed at IPI203.

The output signal from the IPIs is recorded in terms of voltage. All calibration factors were provided on a unique calibration sheet for each sensor based on serial number. Six conversion factors for each axis were provided to convert the voltage reading directly to engineering units of mm/m.

Electrolytic tilt sensors are sensitive to changes in temperature and a thermistor was included in each sensor. Temperature changes can affect both the sensor calibration as well as the sensor offset; however, if the temperature remains constant these factors are negligible. In total 12 calibration factors exist for one axis of one IPI.

Conversion of the sensor reading, *EL* (Volts), to the *mm/m* reading requires the following equation:

$$mm/m = C5 \times EL^5 + C4 \times EL^4 + C3 \times EL^3 + C2 \times EL^2 + C5 \times EL + C0 \quad \text{..... (3.1)}$$

where *C0* to *C5* are unit less calibration factors.

If the temperature fluctuates then the following sensor and offset (*SENSTC and OFFSTC*), corrections would be required:

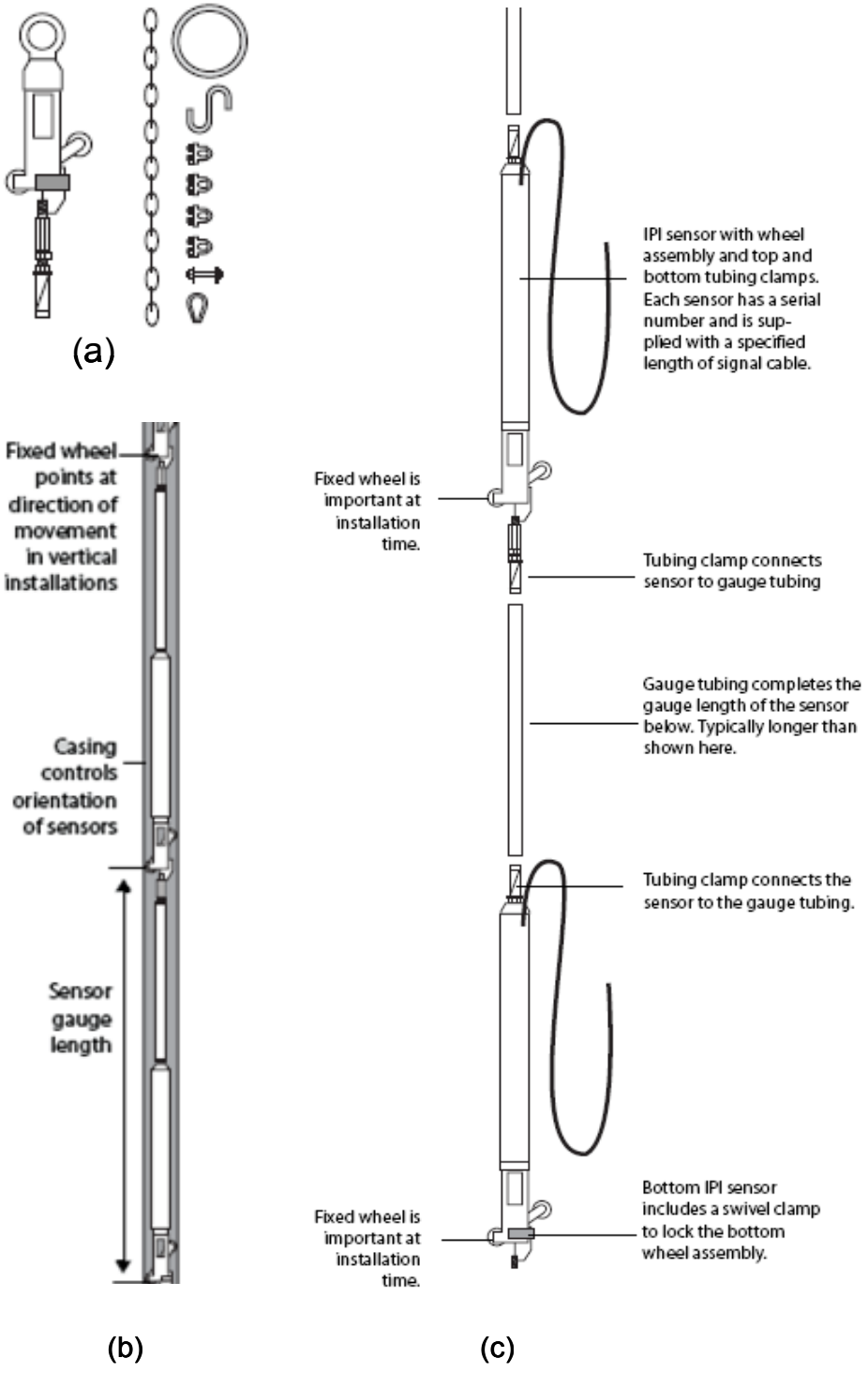

Figure 3.9: Components the EL In-Place Inclinometer (a) Top suspension assembly, (b) Orientation and gauge length definition, and (c) Sensor assembly (DGSI, 2008b).

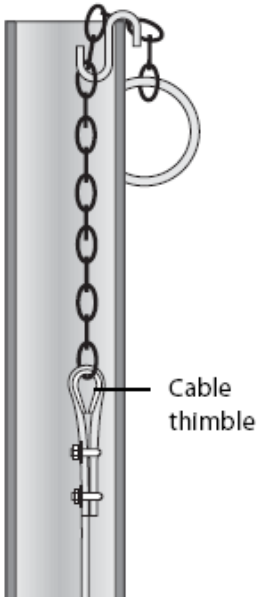

Figure 3.10: Top assembly termination of in-place inclinometers suspended in inclinometer casing (DGSI 2009).

$$SENSTC = S2 \times \delta T^2 + S1 \times \delta T + S0 \quad \text{.....(3.2)}$$

$$OFFSTC = F2 \times \delta T^2 + F1 \times \delta T + F0 \quad \text{.....(3.3)}$$

where *S0* to *S2* and *F0* to *F2* are unit less calibration factors and δT is the temperature differential from the calibration temperature (*Tnom*), of 12°C. Equation 5.4 includes the temperature correction factors

$$mm/m = [(C5 \times EL^5 + C4 \times EL^4 + C3 \times EL^3 + C2 \times EL^2 + C5 \times EL + C0) * SENSTC] + OFFSTC \quad \text{.....(3.4)}$$

Once the value is in the form of *mm/m* the total displacement can be determined simply by multiplying the value by the gauge length of the instrument. These calculated values are valid based on two main assumptions:

1. The top of the casing provides a fixed reference point; and

2. The entire gauge length of 2.0 m is rigid.

Equation 5.1 was programmed into ARGUS by SMHI and DGSI to calculate displacement of the IPIs. Since the depth of the IPIs at the Highway No. 302 was so great the temperature fluctuated very little (between 5.00°C and 5.16°C at the toe of the slope and 4.88°C and 4.96°C at the crest of the slope). Constant temperature of the IPIs eliminated the need to incorporate the more complex formula that includes temperature correction.

3.4.2 Vibrating Wire Piezometers

Two types of vibrating wire piezometers (VWPs) were installed at Highway No. 302. All borehole installations used 345 kPa to 3450 kPa rated non-vented VWPs supplied by DGSI. The single alternate installation required the use of a 150 kPa pressure rated vented VWP to monitor river level. A typical VWP is displayed in Figure 3.11.

A vented VWP was used to monitor river elevation. A vent tube extending from atmosphere and extending to the instrument applies barometric pressure to the back of the vibrating wire sensor. This transfer of barometric to the instrument creates a gauge rather than absolute pressure measurement.

Figure 3.11: Vibrating wire piezometer (DGSI 2008c).

3.4.2.1 Installation

The vented VWP was installed by hand auguring a 150 mm diameter borehole into the river bed. This hole was located approximately 1.5 m from the riverbank and 2 m deep into the river bed. The instrument tip was removed and filled with water to saturate the instrument prior to placing the instrument into the hole and backfilling with silica sand. The instrument cables were run from the riverbank to the data logger in small diameter PVC tubing for protection.

Figure 3.12 shows a photograph of a string of three VWPs that are ready to be lowered into a single borehole that has been backfilled with grout. The string of three VWPs was prepared by layering lead weights, a silica sand pack for the VWP, and bentonite chip in a screen sock. These instruments were installed approximately 5 m above, 5 m below and at the shear zone which was previously determined from the traversing slope inclinometer probe survey.

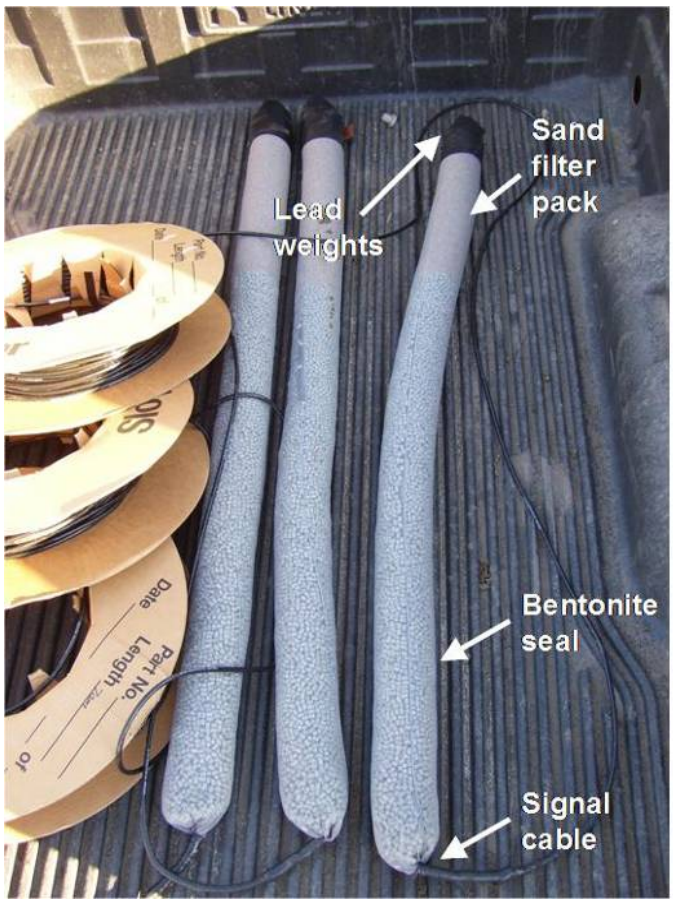

Figure 3.12: Vibrating wire piezometers prepared for installation.

Once the VWPs were installed they were tied off at surface so the grout could set. Next the instruments were connected to a data logger and read on programmed intervals to continuously monitor pore-water pressure.

Later installations of VWPs (Piezo 401 and Piezo 402) were conducted away from the real-time system outside the landslide mass and monitored sporadically.

3.4.2.2 Calibration and Calculations

Each VWP was calibrated at a specific temperature and over a range of pressures. A unique calibration sheet is provided with each instrument. A VWP is a temperature sensitive instrument and a thermistor is included in the sensor to allow for temperature measurement in order to allow the user to apply a temperature correction.

The instrument output is a frequency, recorded in Hertz, (Hz). This frequency output is converted to units of pressure in kilopascals (kPa), pounds per square inch (psi), meters of water (m), feet of water (ft.), kilogram per square centimetre (kg/cm^2), or bars using the specific factors of A, B, and C provided on the sensor calibration. If the temperature is relatively constant, temperature corrections do not need to be applied. The equation to convert the VWP output from Hz to a pressure, P, for the sensors used at site is:

$$P = A \times R^2 + B \times R + C \quad \text{.....(3.5)}$$

where R is the frequency reading (Hz) and A, B and C are unique calibration factors supplied on the calibration sheet with each VWP.

Once the pressure value is achieved changes in pressure, (ΔP), are simply determined through the following:

$$\Delta P = P_C - P_0 \quad \text{.....} \quad \textbf{(3.6)}$$

where P_C is the current reading and P_0, is the initial pressure reading.

The pressure value was then converted to a pressure head and added to the elevation of the piezometers tip to obtain a total head reading.

3.5 Real-Time Monitoring System

The advantage of using electrical instruments such as VWPs and IPIs is that they are easily connected to automatic data acquisition systems (Dunnicliff 1993). The Highway No. 302 site was the first site in the province of Saskatchewan to be instrumented with a real-time monitoring system.

The real-time monitoring system included instrumentation at the toe of the slope near the North Saskatchewan River and crest of the slope near Highway No. 302 (Clifton Associates Ltd. 2005). Two data collection stations were required due to the number and location of instruments.

3.5.1 Data Collection, Communication, Storage and Presentation

Data collection and communication was accomplished using a CR10X data logger from Campbell Scientific, Inc. This data was communicated to an off-site server at a Saskatchewan Government location in Regina where it was stored, processed, and made available for graphical or numerical presentation via a web-based user interface. The software also enabled features such as automated alarm messages where a digital report was automatically sent via email as a portable document file (pdf).

3.5.1.1 CR10X Data Logger

All instrumentation was connected to the CR10X data logger through analog inputs. The analog inputs measure an electrical signal within a defined range. Accepted signals are generally voltage, current or resistance. The IPIs, for example, sends a voltage reading that is converted to engineering units of millimetres of deflection based on tilt and geometry of the electrolytic sensor. In order to obtain the frequency readings from the vibrating wire piezometer, the data logger can be programmed to excite the coil responsible for "plucking" the vibrating wire as well as the coil responsible for "counting" the frequency. This frequency is measured over a specific time period by the data logger and the value can be converted to engineering units of pressure

based on calibration factors and if necessary temperature corrections can be applied (Campbell Scientific Inc. 2003).

Instrumentation scans can be set to meet site specific conditions. The Highway No. 302 site instrumentation was programmed to read the instruments hourly. The recorded data was stored briefly in the data logger and transmitted via a cell phone modem to the offsite location where it was processed and made available via the ARGUS monitoring website (Antunes et al. 2006).

An AM16/32 multiplexer was used in conjunction with the CR10X data logger to allow for enough input ports for the instruments. For example, the monitoring station at the river contained three IPIs, three VWP, one vented VWP and one barometer.

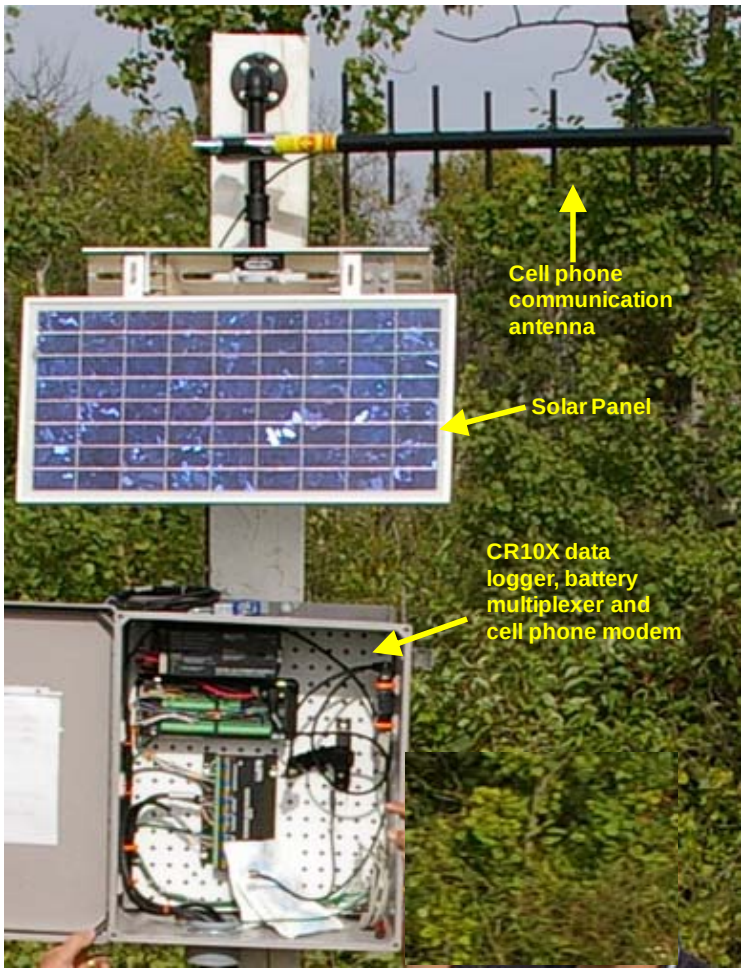

Figure 3.13: Data logger, communication and power system (after Antunes et al. 2006).

3.5.1.2 ARGUS Monitoring Software

The ARGUS monitoring software can relay the monitoring data (raw or processed using the instrument calibrations) and a graphical representation of this data (e.g., time sequence of measurements). This software system (Figure 3.14) allows data to be communicated from single or multiple project sites via satellite or cell phone modem to a MySQL database where the information is stored, processed, and made available to users to view in near real-time. ARGUS is capable for use on a single project with a few sensors, or multiple projects with many sensors creating a web-based data management system (Boart Longyear 2005).

The monitoring data from the study site was immediately available to download from ARGUS, a password protected website. Data was available in raw and processed forms. All data provided in this document were monitored via the website and downloaded to create graphs using Microsoft Excel®.

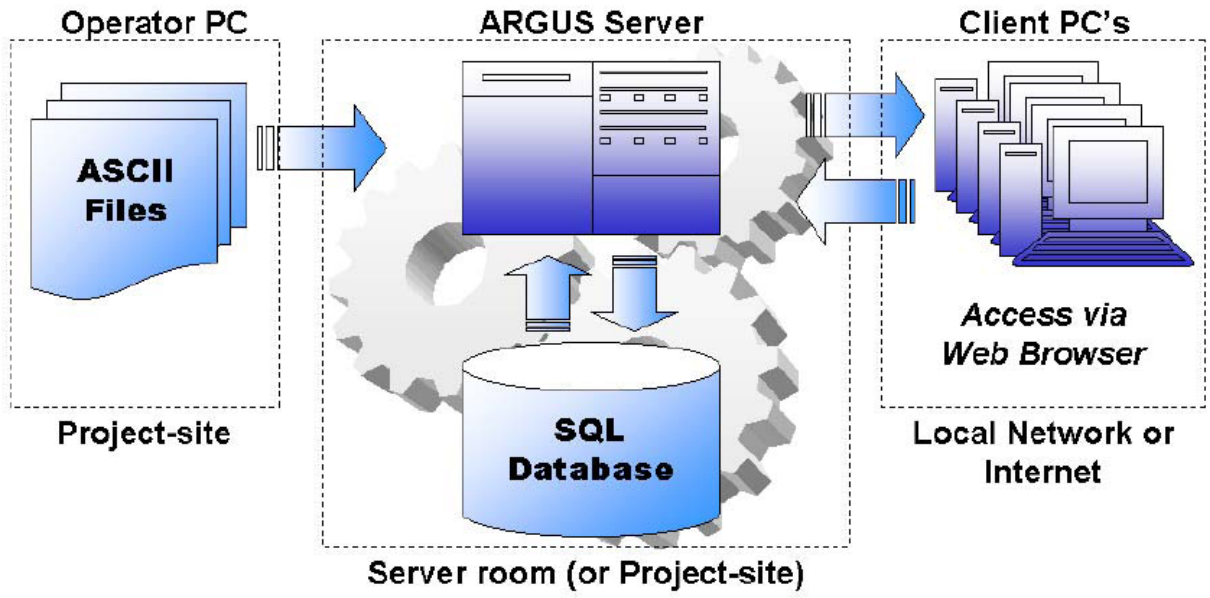

Figure 3.14: ARGUS Monitoring Software (Boart Longyear 2006).

Chapter 4 Presentation of Monitoring Data

4.1 Overview

Data in this section are presented in chronological order. The results from the traversing slope inclinometer probe are presented first. The traversing slope inclinometer (SI) probe readings required a site visit and were conducted on a routine basis as part of the Saskatchewan Ministry of Highways and Infrastructure (SMHI) monitoring schedule. Increased frequency of readings was scheduled as needed based on the results of each survey. Data collected from the traversing slope inclinometer probe are referred to as manual monitoring. Real-time monitoring data from the in-place inclinometers (IPIs) and vibrating wire piezometers (VWPs) will follow. All IPIs and VWPs data were collected using the ARGUS monitoring system and are referred to as automated monitoring.

4.2 Manual Monitoring

Since the slope inclinometer casings were installed with the primary axis facing north as opposed to the expected direction of movement, the B-Axis of the probe typically carried an equal or greater amount of movement compared to the A-Axis. As a means of simplifying the presentation of results, a calculated resultant value for both the incremental and cumulative displacement will be displayed in the following section. This will reduce the number of graphical representations of the data recognizing that the detailed analysis is typically carried out using the individual A-Axis and B-Axis plots. Individual plots of A-Axis incremental and cumulative displacement and B-Axis incremental and cumulative displacement are provided in

Appendix C. Generally the data from the traversing slope inclinometer probe provided good results unless otherwise noted.

The first SI casing (SI001) was installed in the north ditch of Highway No. 302 and was monitored 30 times between October 2002 and September 2005. The monitoring results (Figure 4.1) indicate the existence of a major shear zone at a depth of approximately 44.5 m (Elev. 406.2 m) within the lacustrine clay. Resultant incremental movement at the shear zone showed nearly 22 mm of movement towards the north during this time period, while cumulative movement indicates only 16 mm. The cumulative values from SI001 are considered suspect because the base of the casing shows movement.

Due to the unexpected readings in S001 the checksum plot was reviewed. A review of the checksum plot showed that the bias in the traversing probe was quite large. The first five data sets for SI001 (see Appendix C) showed a bias shift error of greater than 50 units in the A-Axis and greater than 100 units in the B-Axis. Typically these values are less than 20 units in the A-Axis and less than 50 in the B-Axis. Between the readings conducted on February 18, 2003 and April 14, 2003 the checksum values were reduced to less than 10 units in the A-Axis and less than 35 units in the B-Axis. This indicates that a new probe was used or the existing probe was repaired and re-calibrated. The readings for SI001 are conspicuous since the baseline readings contained so much error. Additionally, the casing extended through the shear zone but did not extend into till. It may be that the casing did not extend the prescribed 3 to 6 m below the shear zone. Issues with the probe and the depth of installation were corrected in the subsequent installation of SI003.

The continuing movement in SI001 led to the installation of SI002 (located at the toe of the slope) in May 2004. SI002 casing was installed to a depth of 47.5 m (Elev. 388.0 m). The incremental and cumulative resultant displacement readings for SI002 are presented in Figure 4.2. There was approximately 47 mm of movement perpendicular to the river at a depth of 41.5 m (Elev. 393.95 m) from May 2004 to June 2005. The movement at SI002 occurred in the clay just above the contact between the clay and till.

The rate of shear movement at the highway location (near the crest of the slope) has been compared with that near the river (toe of the slope). In May 2004, the rate of movement near the

crest was approximately 3.5 mm per year, whereas the rate of movement at the toe was 31 mm per year, as shown in Figure 4.3. During February 2005, the rate of movement at the toe of the slope increased to 81 mm per year. By June 2005, the rate of movement at the crest of the slope increased to 29 mm per year. The delay between the increased rate of movement at the toe (February 2005) and the increased rate of movement at the crest (June 2005) was approximately 60 days. The observation that the toe of the slope is moving more quickly than the crest of the slope is in agreement with the conclusion reached by Kelly et al. (2005a). It should be noted though that the readings from SI001 are suspect so the rate of movement at the toe was affected. Moving the installation of crest monitoring with SI003 and re-calibrating the traversing slope inclinometer probe provided more reliable readings for the subsequent installations.

Two pneumatic piezometers, PZO201 and PZO201A, were installed beside SI002 to monitor pore-water pressures at depths of 10.0 m (Elev. 425 m) and 26.4 m (Elev. 408.6 m), respectively. These pneumatic piezometers were read six times between February 2005 and September 2005. The pressure head in the upper piezometer (PZO201A) fluctuated by less than 0.5 m while pressure head in the lower piezometer (PZO201) fluctuated by up to 2.3 m. Typically, the total head values were lower in the deeper piezometer indicating a downward flow at the toe of the slope.

By June 2005, it had become impossible to pass the SI probe through casings SI001 and SI002. Consequently, in July 2005, SI003 was installed near the highway (to replace SI001) and SI102 was installed at the toe of the slope near the river (to replace SI002). The location of SI003 remained in the north ditch of Highway No. 302, although it was moved 100 m west to center the SI in the landslide mass and align it with SI102 at the toe of the slope near the river. Installation of the SI003 casing was to a depth of 54.9 m (Elev. 394.05 m) placing it nearly 2.5 m into the till. This installation provided a fixed reference point. Figure 4.4 indicates the main shear zone located at approximately 45.5 m (Elev. 404.5.0 m) approximately 10 m above the clay till contact. There are also two minor shear zones highlighted at approximately 43.5 m (Elev. 406.0 m) and 39.0 m (Elev. 410.0 m). Readings at SI003 indicated a cumulative resultant movement of nearly 40 mm at the main shear zone and an accumulation of just over 60 mm when including movement from the two minor shear zones. The sloping upper portion of the casing was likely

caused by slight rotation of the upper landslide block since there were no indications of error in the traversing slope inclinometer probe data.

SI102 was installed to a depth of 48.0 m (Elev. 387.5 m). After installation, a well-defined shear zone was observed at a depth of 42.0 m (Elev. 393.2 m), in Figure 4.5. A minor slip surface appeared to be developing at a depth of 40.0 m (Elev. 395.2). Movement rates were 541 mm per year at the toe and 483 mm per year at the crest of the slope when considering total cumulative movement at SI003 and SI102 between March 2005 and September 2005 (Figure 4.7).

Observation of slope movements as monitored by manual monitoring consistently showed that the movement at the toe was greater in magnitude and rate compared to movement at the crest of the landslide. This supports the conclusion by Kelly et al. (2005a) that monitoring movement at the toe should predict movement at the crest of the slope. Movement rates at the toe were still greater than those at the crest, but both the toe and the crest of the slope were moving at high rates.

In August 2005 two SI casings were installed to house the IPIs. Three VWPs were installed next to each SI casing. The SI casings and VWP installations were labelled as SI103, PZO103, SI202 and PZO202 at the crest and toe of the slope, respectively.

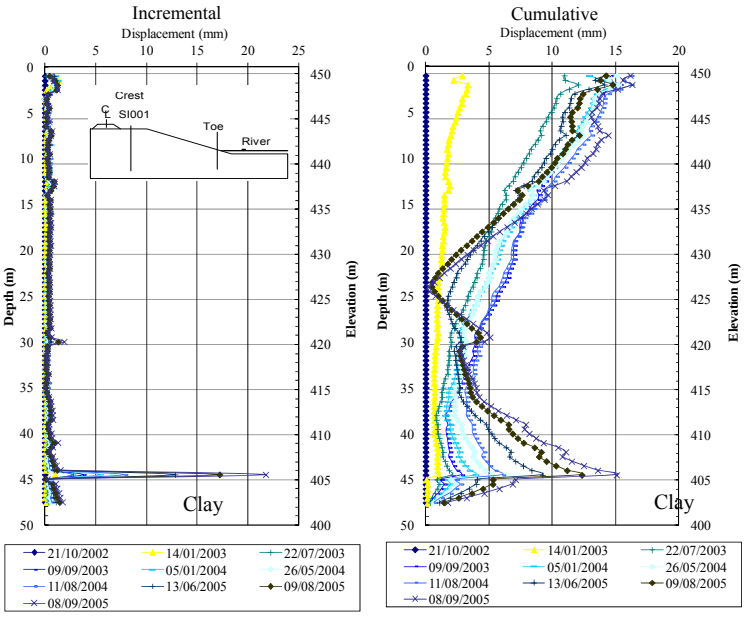

Figure 4.1: Incremental and cumulative resultant displacement for SI001.

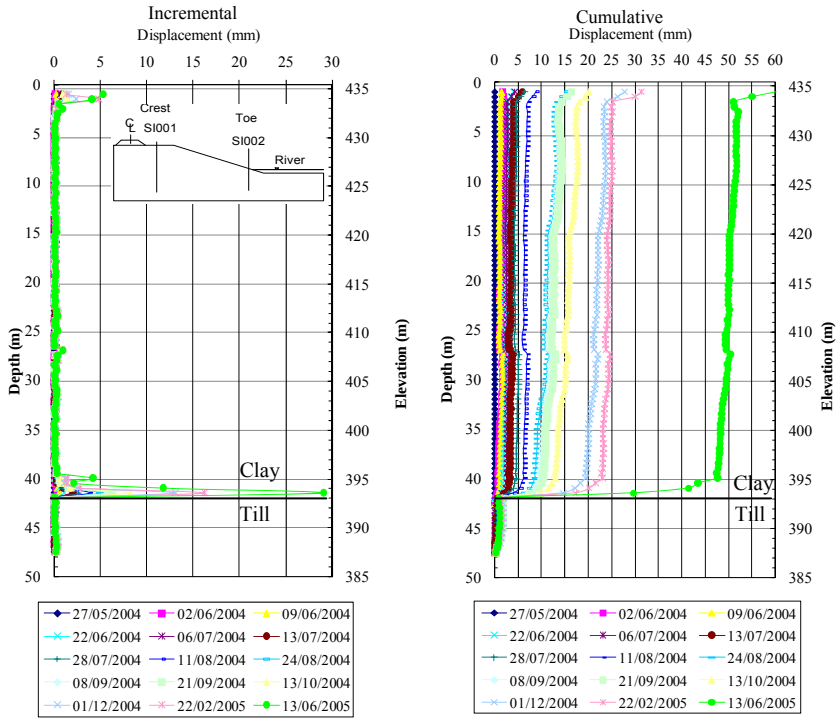

Figure 4.2: Incremental and cumulative resultant displacement for SI002.

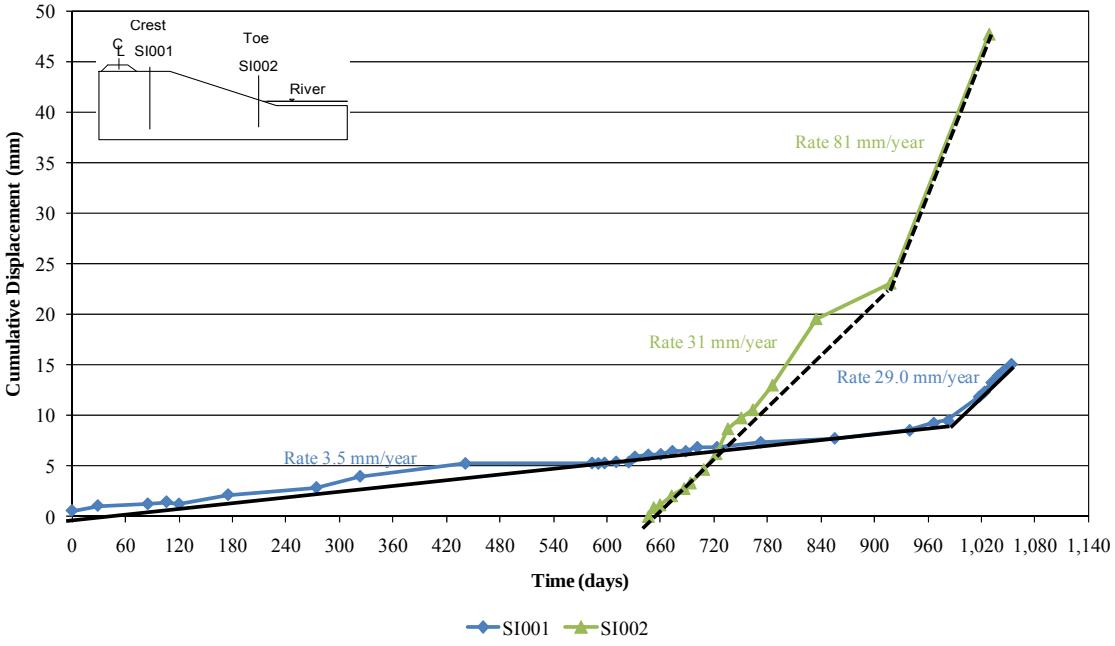

Figure 4.3: Cumulative displacement versus time at SI001 and SI002.

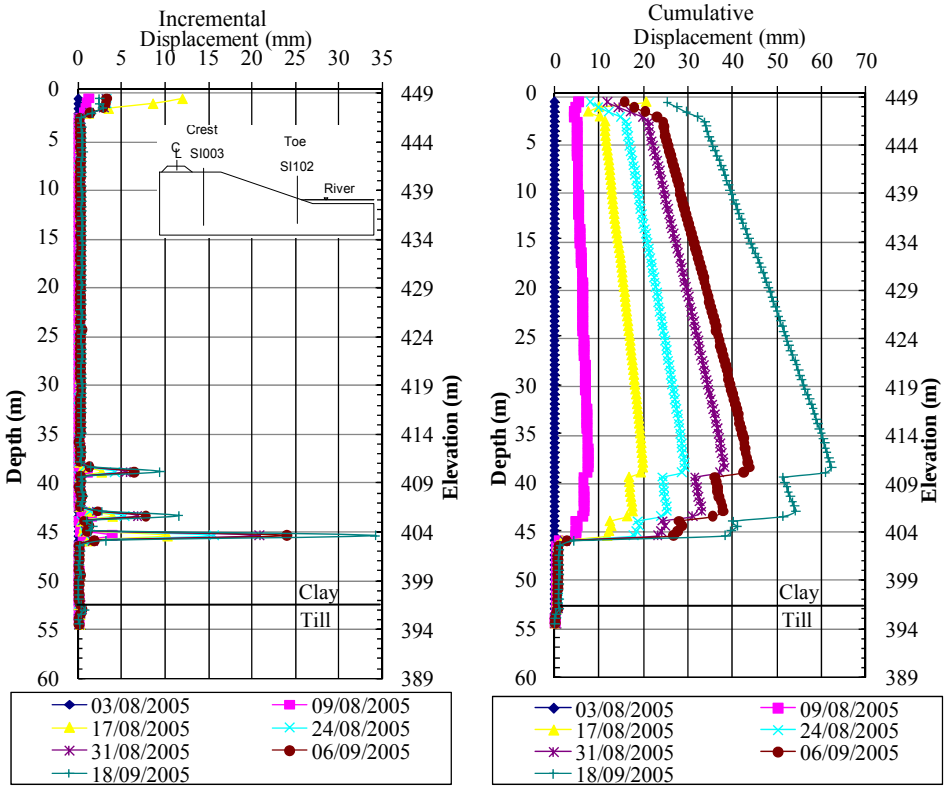

Figure 4.4: Incremental and cumulative resultant displacement for SI003.

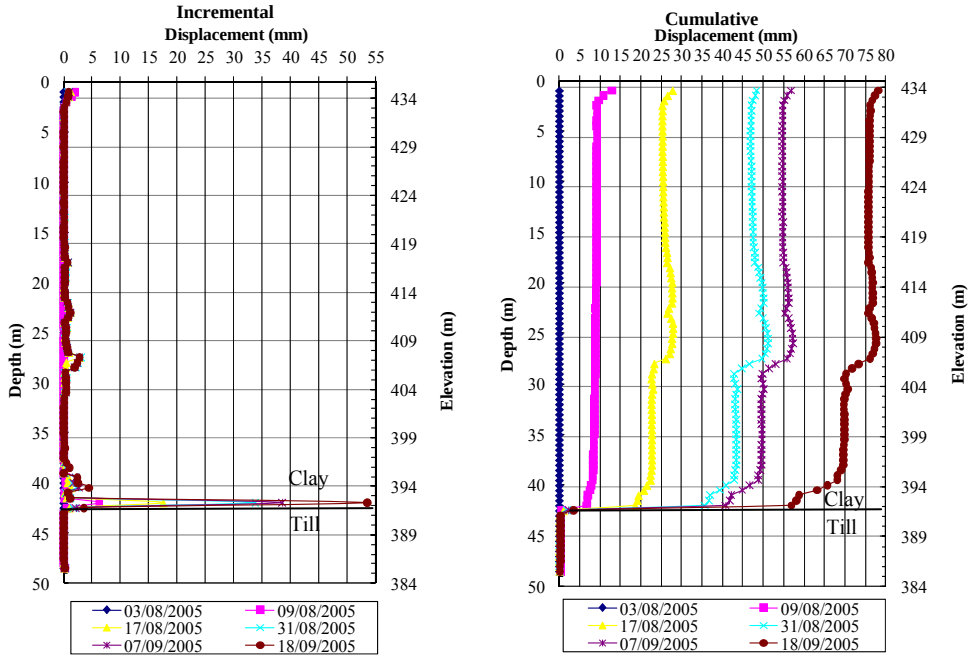

Figure 4.5: Incremental and cumulative resultant displacement for SI102.

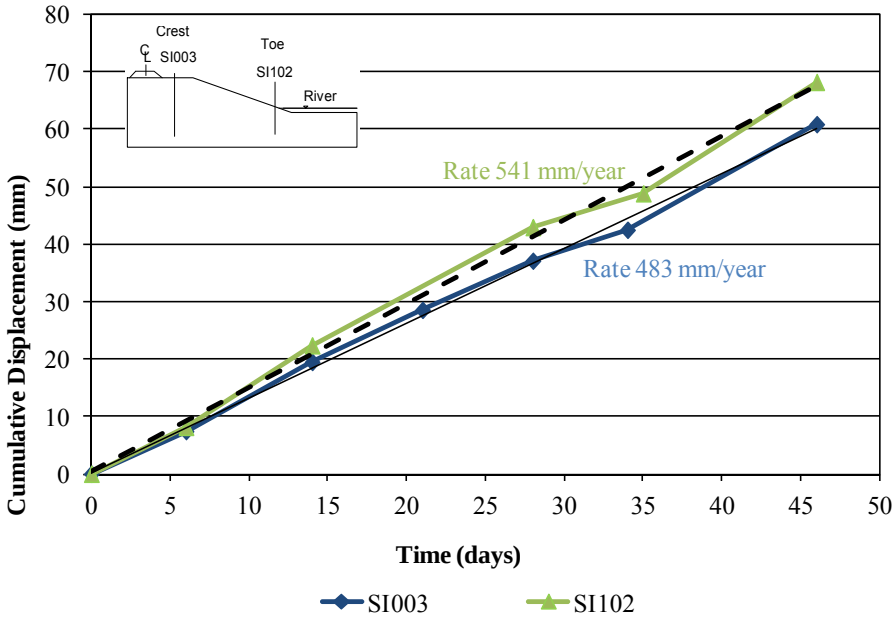

Figure 4.6: Cumulative displacement versus time at SI003 and SI102.

SI103 was installed to a depth of 57.95 m (Elev. 390.7 m). The initial survey of the casing for SI103 was conducted on September 6, 2005 and the final survey was conducted on September 18, 2005. During this 12-day monitoring period multiple shear zones developed. These shear zones are highlighted by sharp spikes on the incremental plot and by the shape of the cumulative displacement plot (Figure 4.7). The primary zone of movement was located at a depth of 44.25 m (Elev. 405.0 m). Approximately 11 mm of movement was recorded at that zone between the initial and final reading. The cumulative movement between depths of 41 m and 45 m (Elev. 403.95 m to Elev. 407.95 m) was approximately 20 mm including movement from shear zones at 42.25 m (Elev. 407.0 m) and 40.75 m (408.5 m). The perceived movement below the shear zone may be apparent due to the sharp curvature at the base of installation. Readings in the A-Axis and B-Axis switch sharply from positive to negative in every survey. The checksum values remain near zero indicating that bias-shift is not the problem. Since this curve is below the installation of the IPI, it should not pose a problem to IPI readings. Additionally, the sloping upper portion of the plot is similar to and consistent with what was witnessed in SI003.

SI202 was installed to a depth of 48.0 m (Elev. 387.2 m). The initial survey of the casing for SI202 was conducted on August 31, 2005 and the final survey on September 18, 2005. A distinct shear zone located at a depth of 41.8 m (Elev. 394.0 m) was noted after the completion of these surveys. Approximately 20 mm of movement was measured at 41.8 m depth and a total 25 mm of movement had occurred between a depth of 39.75 m and 41.8 m (Elev. 394.0 m and 396.5 m) (Figure 4.8). Between August 31, 2005 and September 7, 2005, 5 mm of movement occurred at a depth of 41.8 m, and over the next 12 days between September 7, 2005 and September 18, 2005, 20 mm of movement occurred.

Comparisons of the rates of movement at the crest and toe (Figure 4.9) showed that the rates of movement were nearly the same. This indicated that all the constituent blocks of the slope were now moving at nearly the same rate and that global failure of the slope had been triggered.

Figure 4.10(a) displays the initial position of IPI103 near the highway based on the last traversing slope inclinometer probe readings dated September 18, 2005. Using the resultant cumulative deflection plot, it was observed that the lowermost sensor was placed below the zone of movement, and the two uppermost sensors were placed within the zones of movement.

The initial position of IPI202 is shown in Figure 4.10(b). The bottom sensor gauge tube extended 0.75 m above the shear zone, while the IPIs sensor (length 0.55 m) and 0.70 m of gauge tubing remained below the shear zone. The top two sensors were located within the moving portion of the casing. It appears that the two uppermost sensors were located within an S-shape deformed portion of the casing.

Real-time data was functional for IPI103, PZO103, IPI202, and PZO202, by September 18, 2005. The datum reading was September 18, 2005 at 14h00.

IPI203 was installed to replace IPI103 after it was destroyed. No initial SI reading was taken for this installation. Due to lack of initial data, the SI casing profile and initial position for IPI203 cannot be examined. The SI casing was installed and the IPIs were placed to span the zone of movement as defined by IPI103. Gauge lengths were increased so that the sensor and gauge tube total length was 2.5 m (i.e., 0.5 m longer than the previous installation) to span a total distance of 7.5 m (as opposed to 6.0 m for the previous installation).

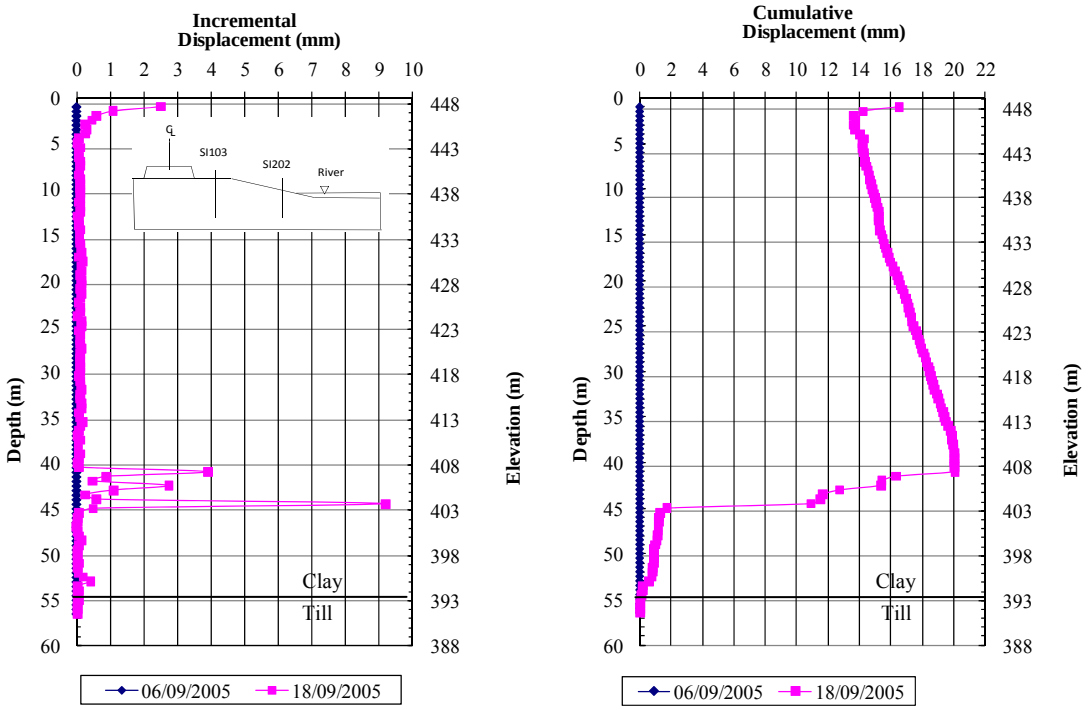

Figure 4.7: Incremental and cumulative resultant displacement for SI103.

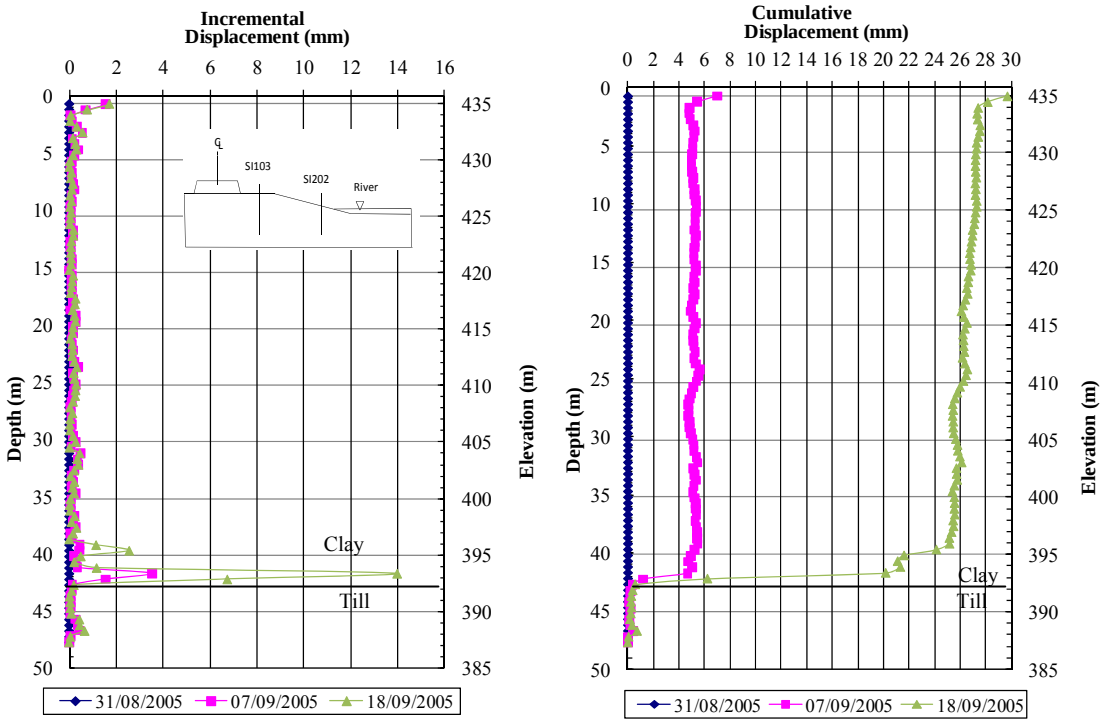

Figure 4.8: Incremental and cumulative resultant displacement for SI202.

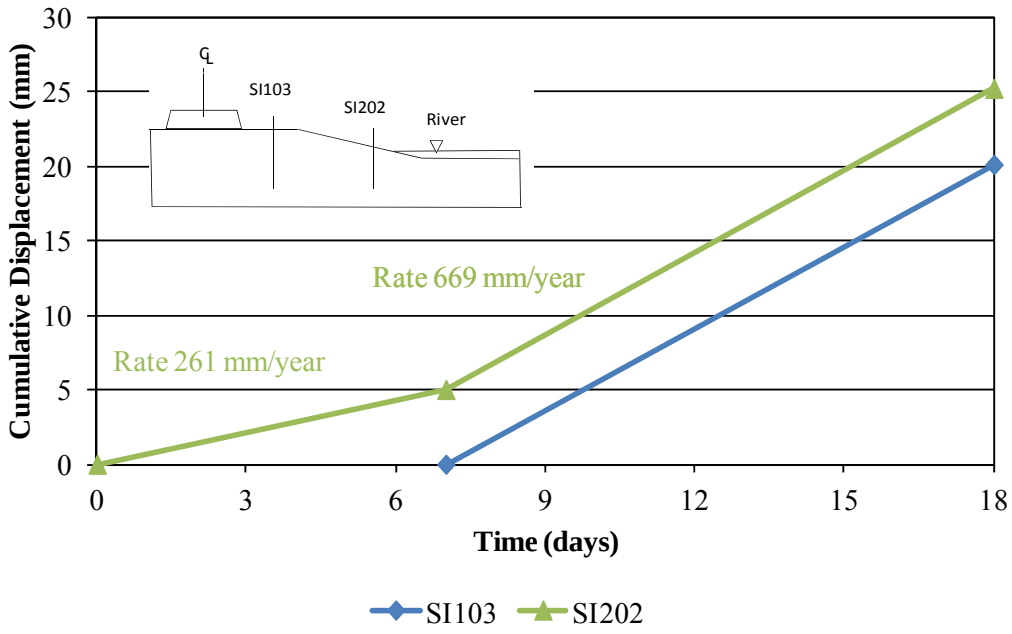

Figure 4.9: Cumulative displacement versus time at SI103 and SI202.

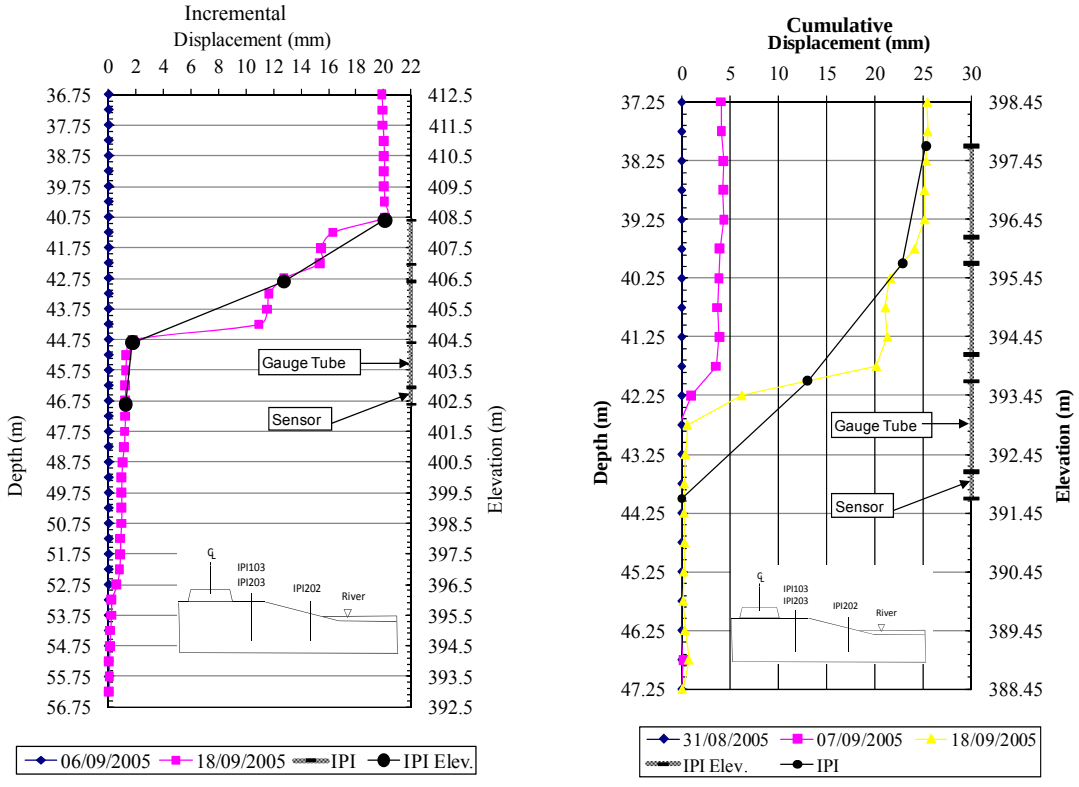

(a) **(b)**

Figure 4.10: (a) Initial placement of IPI103 (SI103) and (b) Initial placement of IPI202 (SI202).

4.2.1 Summary of Manual Monitoring

The results of manual monitoring show that movement rates increased throughout the summer and fall of 2005. Data indicated the toe of the slope was moving at higher rates than at the crest of the slope. During the last readings prior to the installation of the IPIs the rate of movement at the crest was approaching the rate of movement at the toe of the slope. When cumulative resultant movement of all slip surfaces was considered the rates of movement at the toe and the crest were nearly the same, indicating the onset of global failure of the slope. For additional plots from the SI refer to Appendix C.

4.3 Data of Real-Time Monitoring Displacement and Pore-water Pressure

Readings from the VWP and IPIs were retrieved on an hourly basis via the on-site data loggers. Data was sent to a server, processed via the ARGUS monitoring software and uploaded to a secure website for viewing. The datum reading for the IPI103, at the crest, and IPI202 at the toe, was selected as September 18, 2005 at 14h00.

IPI103 functioned between September 18, 2005 and March 15, 2006 when excessive movement caused the IPIs to stop functioning. IPI203 replaced IPI103 and functioned between May 24 and July 7, 2006.

Between September 18, 2005 and July 2, 2006, IPI202 was functional. This was the third SI casing placed at the toe of the slope and the only one to house IPIs.

Incremental resultant displacements along the A-Axis and B-Axis for IPI103, IPI203 (near the highway) and IPI202 (near the river) are plotted in Figure 4.11 and Figure 4.12, respectively. This representation indicates the difference in the resultant displacement for each sensor in one hour increments (i.e., each subsequent hour is subtracted from the last).

Figure 4.11 shows the results for IPI103 and IPI203. The general trend indicates that movement is typically an accumulation of small displacements. There are displacements on the graph where spikes of movement occur over a one hour period. For instance between 00h00 and 01h00 on October 13, 2005 all three IPIs comprising IPI103 showed displacement. The largest

displacement was 34 mm and occurred in the bottom IPIs. After this single disturbance IPI103 experienced five other spikes, all less than 5 mm, affecting the middle and upper IPIs only.

Two displacement spikes occurred in IPI203 (Figure 4.11). The upper IPIs experienced movement of 3 and 8 mm over separate one hour periods. These movements occurred in June 2006 prior to the loss of IPI203.

The movement recorded by IPI202 (Figure 4.12) also appeared to be accumulated small strains except for three significant spikes in displacement in October and November 2005. The initial spike disturbed the middle and the bottom IPIs of IPI202. The middle sensor showed displacement of nearly 55 mm while the bottom sensor showed displacement of 23 mm. This displacement occurred 20 minutes after the displacement spikes noted near the highway in IPI103 on October 13, 2005. The next major movement occurred on October 27, 2005 and November 18, 2005. The October 27 movement affected the middle and bottom IPIs while the November 18, 2005, affected the top IPIs more than the middle and the bottom IPIs.

Figure 4.13 and Figure 4.14 show the cumulative resultant displacements at locations IPI103, IPI203 (near the highway) and IPI202 (near the river), respectively. These two figures highlight the total cumulative resultant movement from the bottom sensor to the top sensor.

IPI103 (Figure 4.13) indicates movement during the fall and relatively slow rates of movement during the winter. Increased rates of movement begin again in February 2006 until destruction of IPI103 on March 15, 2006. IPI203 showed movement right after installation and this continued between May and July 2006 until it was destroyed. The majority of the movement in IPI203 was attributed to the middle IPIs with relatively little movement experienced in the upper and lower sensors.

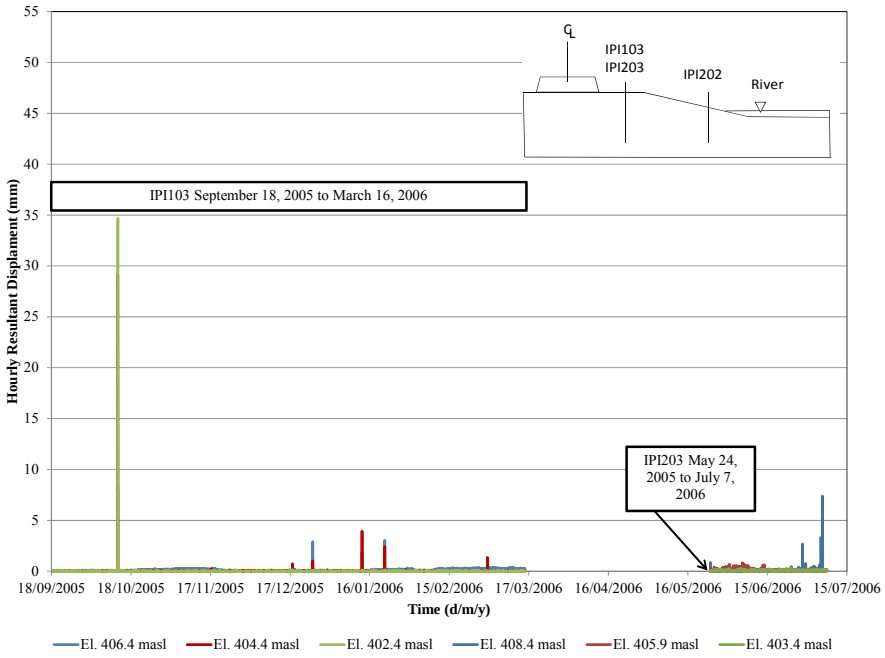

Figure 4.11: Hourly incremental resultant displacement of each sensor at IPI103 and IPI 203.

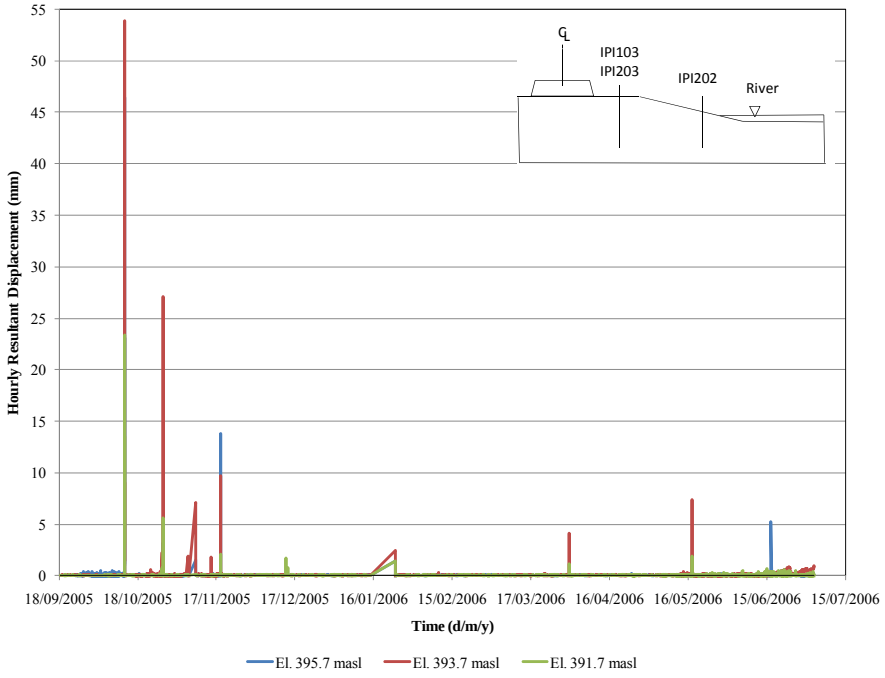

Figure 4.12: Hourly incremental resultant displacement of each sensor at IPI202.

IPI202 (Figure 4.14) showed 25 mm of movement between September 18, 2005 and October 13, 2005. After the initial disturbance on October 13, 2005 the movement reversed and became positive. This movement was associated with the high incremental hourly movements. This phenomenon will be discussed further in Chapter 5. Movement in the spring highlights the increased rate of movement until IPI202 was no longer functional by July 2, 2006.

Figure 4.15 provides the average rates of movement based on the cumulative resultant value for each IPIs installation. Prior to the disturbance on October 13, 2005 movement rates were 370 mm per year at the toe compared to 219 mm per year at the crest. No slope movement was observed at the toe during the increased movement of the crest during February 2006. According to IPI202 movement initiates during the second half of May 2006. By mid-June the movement rate increased to 3970 mm per year. A rate of 1750 mm per year was observed during May and June 2006 at IPI203. Comparing the rate of movement between the toe and the crest of the slope, the movement rate at the toe is 2.2 times that observed at the crest.

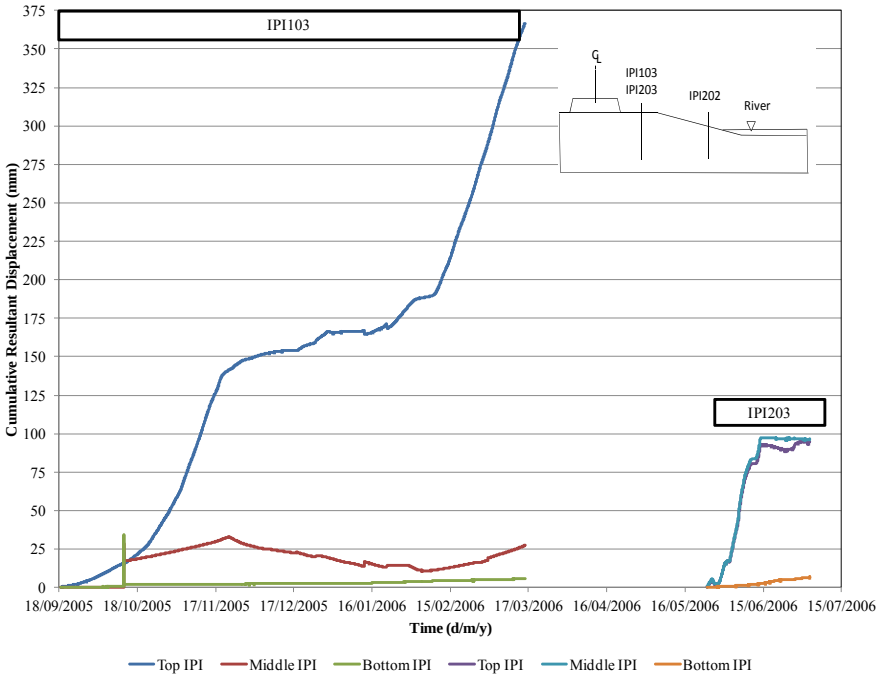

Figure 4.13: Cumulative resultant displacement of each sensor at IPI103 and IPI203.

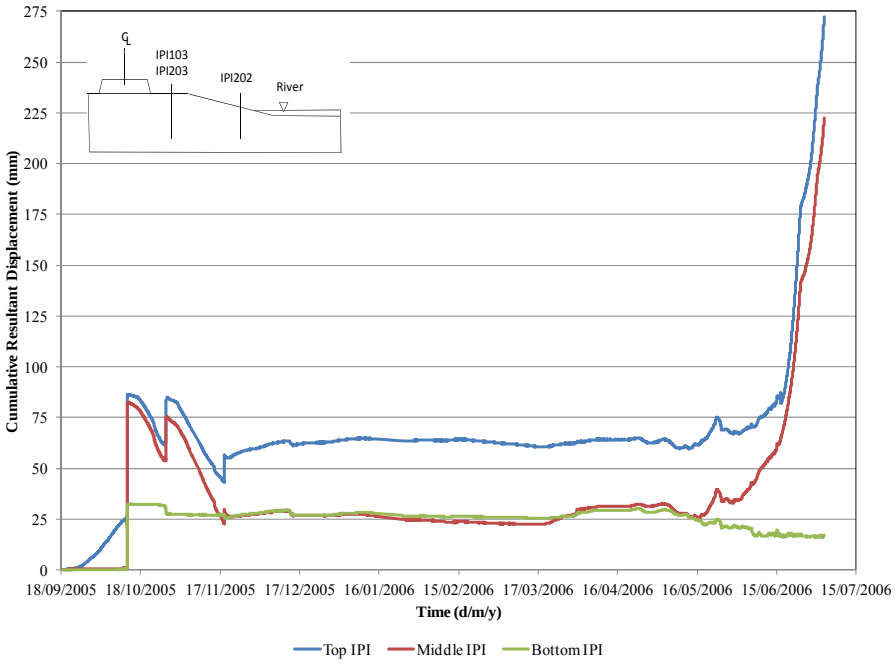

Figure 4.14: Cumulative resultant displacement of IPI202.

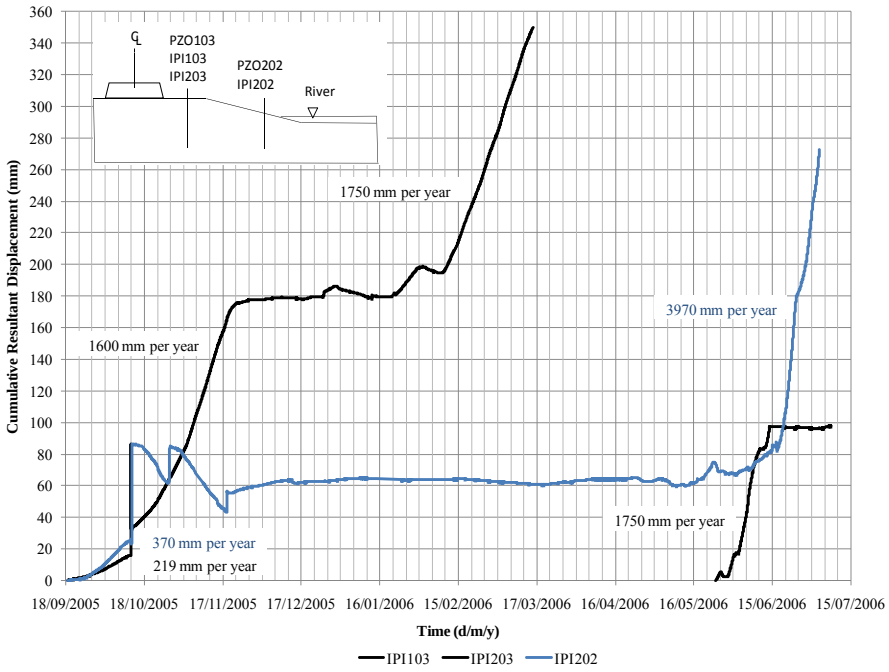

Figure 4.15: Comparison of cumulative resultant movement for IPI103, IPI203 and IPI202.

Pore-water pressures were monitored above, below and at the shear zone beside the locations for IPI103 and IPI202. Figure 4.16 and Figure 4.17 present the cumulative resultant displacement and pore-water pressure data for the crest and toe of the slope, respectively.

Periods of movement appear to have caused the increases in pore-water pressure shown in Figure 4.16. An increase movement rate from 219 mm per year to 1600 mm per year between October 13, 2005 and November 23, 2005 was associated with a 1.2 m increase in total head at the piezometer nearest to the shear zone.

During the winter period (November to February) there was virtually no movement of the slope. A dissipation of pore-water pressures at the shear zone was observed. The slope began to move again on February 6, 2006 and the rate of movement increased to 1500 mm per year. No significant change in pore-water pressure was noted with the increase in movement during the winter. IPI103 was destroyed by March 15, 2006. An additional increase in pore-water pressure of 2.5 m occurred near the shear zone between April 21, 2006 and May 11, 2006 after which time the VWPs stopped functioning. Since IPIs103 was already destroyed and IPI203 had not been installed, displacement associated with this increase in pore-water pressure was not monitored.

Over the entire monitoring period, between September 18, 2005 and May11, 2006, the total head above the shear zone increased steadily by 2.2 m. The VWPs below the shear zone indicated a total head decrease of approximately 2.0 m. In general the total head in the shear zone was the highest followed by the total head above the shear zone and the lowest values below the shear zone.

Figure 4.17 includes the data from the VWP installed above, below and at the shear zone, river elevation and IPIs displacement. The elevation of the river bed was assumed to be 418.16 m based on air photo interpretation (Kelly et al. 2005a).

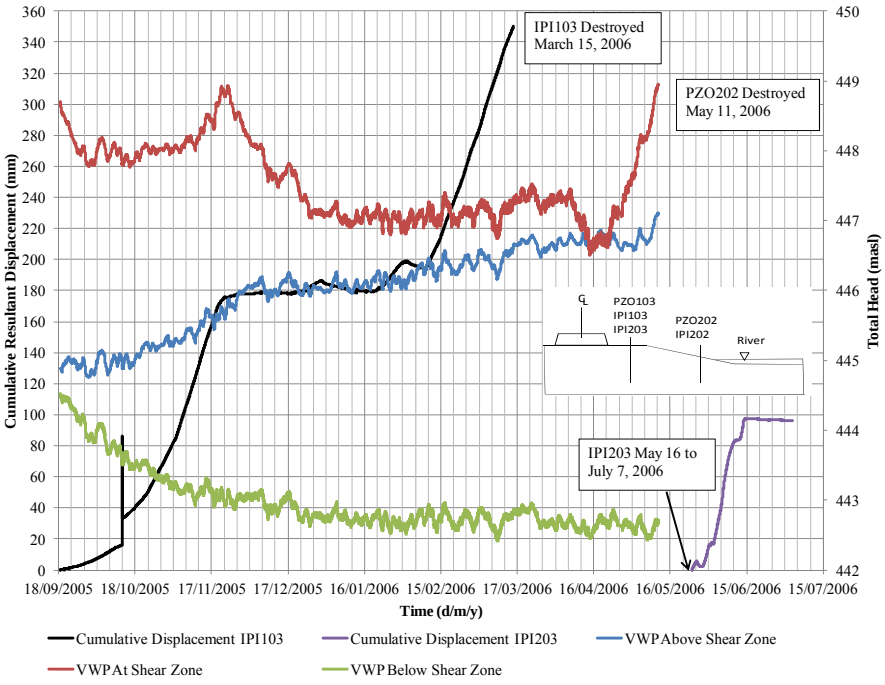

Figure 4.16: Comparison of movement at the highway (IPI103 and IPI203) with pore-water pressure measurements (PZO103).

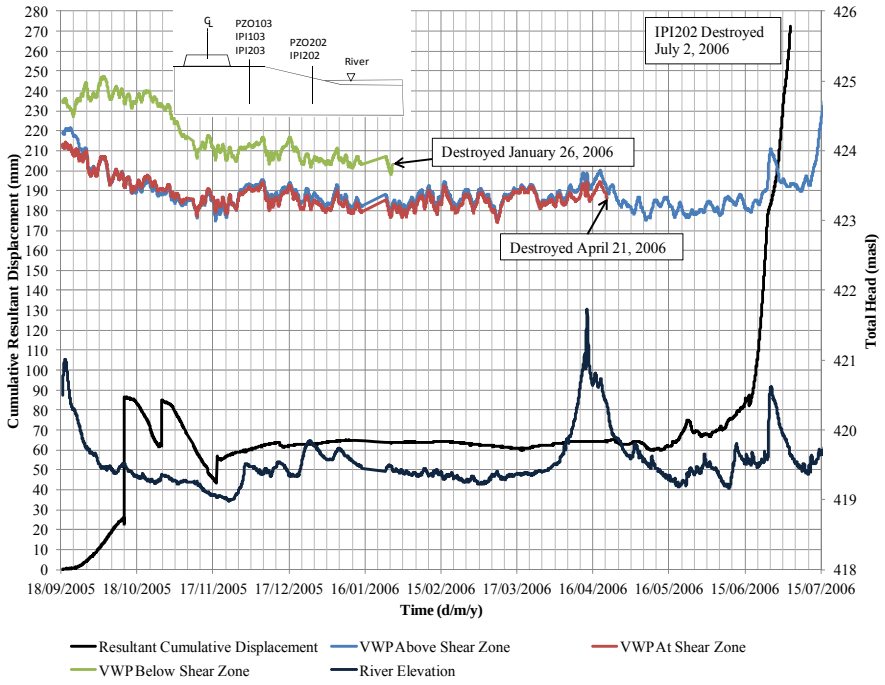

Figure 4.17: Comparison of movement near the riverbank (IPI202) to pore-water pressure (PZO202) and river level.

The pore-water pressure at the toe of the slope remained fairly stable during the monitoring period with maximum pressure heads fluctuating by less than 1 m. Levels of pore-water pressure remained high initially and dropped throughout the winter. The piezometers below and at the shear zone failed prior to the spring of 2006. The VWP above the shear zone continued to provide data throughout the monitoring period and displayed a delayed pore-water pressure increase after spring movement was initiated. Two periods of movement were observed where the rate of movement increased after a rise and fall in the river level in September 2005 and April 2006.

4.3.1 Summary of Real-Time Monitoring

IPIs readings indicate that high rates of movement, ranging from 219 mm per year to nearly 1650 mm per year, occurred during September through November 2005. The IPIs at the crest and toe recorded no movement during the months of December 2005 through January 2006. IPI103 at the crest of the slope showed an increase in movement in February 2006. By March 15, 2006 the installation was destroyed. Movement at IPI202 (near the river) was not substantial until May 2006. IPI203 replaced IPI103 at the highway and high rates of movement between 1750 mm per year (near the highway) and 3970 mm per year (near the river) were observed through the spring and early summer resulting in the destruction of all instrumentation by July 2006.

A review of the incremental movements showed that, at the toe and crest of the slope, movement was generally due to an accumulation of small displacements. Large displacements over one hour time periods were observed sporadically. The main incremental movement that occurred on October 13, 2005 caused unexpected data to emerge from IPI103 and IPI202, which were installed at the crest and toe of the slope. This movement appeared to have little effect on the continuing operation of IPI103, but IPI202 readings during the fall of 2005 were difficult to interpret. Prior to the disturbance in October 2005, the rate of movement at the toe (IPI202) was still greater than that at the crest of the slope (IPI103). During February 2006 movement at IPI103 was initiated prior to movement at IPI202. This indicates that the crest was moving at a greater rate than the toe between February and May 2006.

Pore-water pressure data and river levels were observed in conjunction with cumulative resultant displacement. In general the PZ103 (near the highway) showed increasing pore-water pressures associated with or following observable movement at and above the shear zone. The pore-water pressures dropped steadily below the shear zone at IPI103. PZO202 (near the river) had intermittent failure of the piezometers, but in general indicated that the lowest piezometer had higher pore-water pressure compared to the ones at and above the shear zone.

River level and IPI202 at the toe showed movement increase following a rise and fall in the river. This observation suggests a relationship between movement of the slope and river level fluctuation.

Chapter 5 Analysis and Discussion of Results

Traversing slope inclinometer probe measurements indicated that slope movement at the study site originated at the toe and moved towards the crest. Increasing rates of movement were observed during spring, summer and fall 2005.

In-Place inclinometers (IPIs) were installed to facilitate real-time monitoring of slope movements. The IPIs verified that movement continued at high rates; however, the magnitude and direction of movement reported by the IPIs were difficult to interpret, particularly for periods just after their installation. Data trends from the real-time monitoring indicated that the rate of movement at the toe was greater than that at the crest. After a major disturbance to the sensors it was difficult to compare movement rates; however, movements at the crest appeared to be occurring prior to movements at the toe of the slope. Movements of the slope subsequently destroyed the IPIs at the crest. The IPIs also indicated both downslope (positive) and upslope (negative) movements, which is puzzling from the viewpoint of kinematics of slope movement.

In spite of the apparent problems, the IPIs readings have been used to hypothesize landslide kinematics and potential mechanisms responsible for accelerating movement at this site. Secondly, the IPIs readings have been examined in the light of geometric limits of casing deformation to establish potential causes of the disturbances experienced by the IPIs sensors.

5.1 Landslide Kinematics and Failure Mechanisms

5.1.1 Kinematics

Kinematics of a landslide describes the movement distribution of a displaced soil mass (Cruden and Varnes 1996). Data from the horizontal deformation monitoring at Highway No. 302 showed that movement initiated at the toe of the slope and progressed towards the crest of the

slope (a retrogressive movement). This provided the general movement distribution of the soil mass.

Stauffer et al. (1990) described the extension of a land mass and illustrated the resulting topography of a retrogressive landslide (Figure 5.1). The resulting topography depended on the amount of movement from crest to toe. Figure 5.1b highlights a scenario where all landslide blocks extend equally and the surface is composed of horst and graben features at approximately the same level. Figure 5.1c shows a scenario where 30% extension occurs at the toe reducing to 10% at the crest of the slope. An oblique aerial view of the landslide (Figure 5.2), resembles Figure 5.1c confirming the retrogressive nature of the Highway No. 302 landslide.

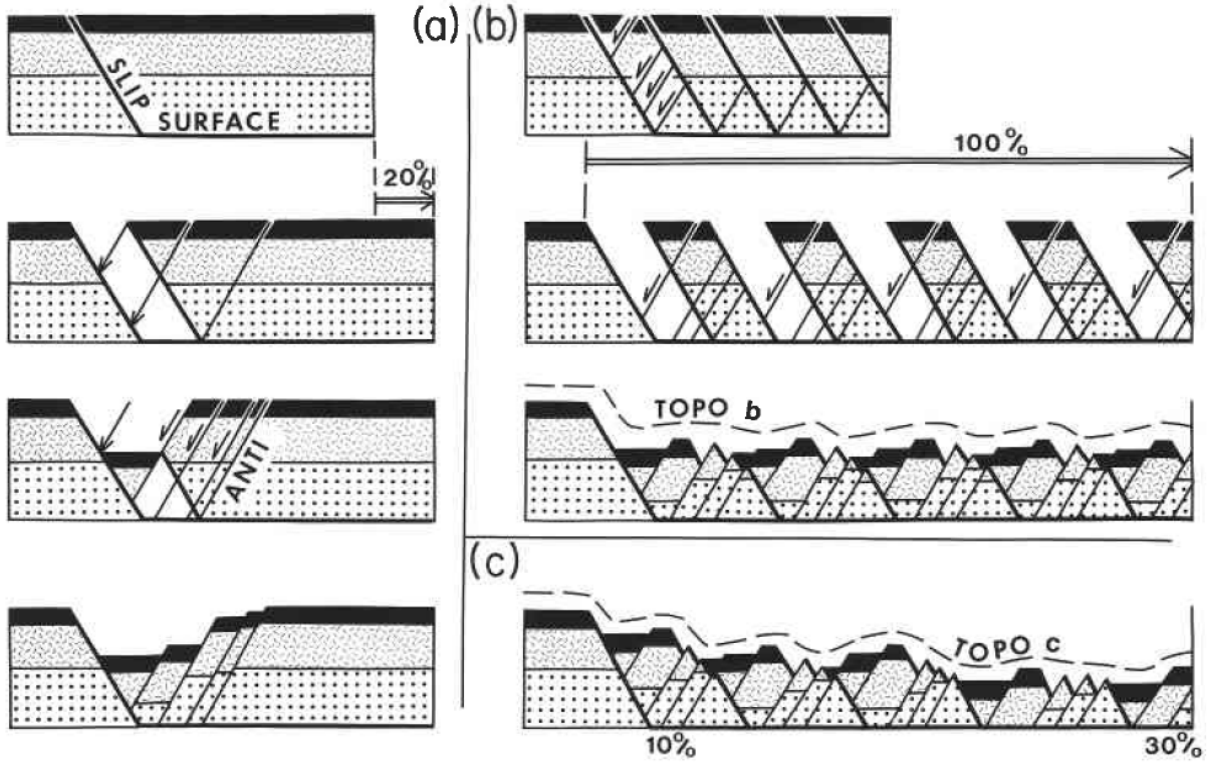

Figure 5.1: Development of multiple retrogressive landslide topography (from Stauffer et al. 1990).

Figure 5.2: Oblique aerial view of the topography of the Highway No. 302 landslide (Photograph courtesy of Vista Photography).

Comparison of all manual measurements at the toe and the crest of the slope and the initial readings from the IPIs between September 18, 2005 and October 13, 2005 support a retrogressive landslide distribution; however, after the disturbance to all the sensors at the crest and toe on October 13, 2005, this observation was no longer supported by the monitoring data. Following this disturbance, movement at the crest of the slope increased and surpassed movement at the toe of the slope. This phenomenon may be explained using one of the following three scenarios:

1. Translational movement at the crest was greater than that at the toe of the slope for a period of time (Figure 5.3);

2. The movement recorded by IPIs sensors at the crest was magnified due to a combination of horizontal shear and vertical compression of the casing (Figure 5.4); or

3. Accurate movement of the slope could not be recorded due to poor sensor position control, likely caused by the casing pushing on the sensors because of excessive deformation of the casing.

Figure 4.15 displayed the IPIs data and movement rates for the toe and crest of the slope. This figure supports scenario #1 wherein the slope, for a period of time, was moving more at the crest than at the toe. It is plausible that the movement at the toe, which had previously been occurring at a faster rate compared with the movement at the crest, had occurred prior to the triggering of the movement at the crest. Picarelli et al. (2004) describe the relationship of multiple block landslides in clayey slopes as a series of self-adjusting blocks in which, for a period of time, movement of an upper landslide block could be greater than those of the lower blocks. This was shown in Kelly et al. (2005b) for the Frenchman River Valley landslide where the movement of a multiple block failure was triggered from the crest down due to fill placement at the crest.

Scenario #2 considers vertical settlement coupled with shear displacement. Vertical settlement was observed at the site during the monitoring with the IPIs and was most significant during the spring and summer of 2006 (see photographs in Appendix A). Although no additional survey was conducted of the settlement at the instrument large settlements were noted at the crest of the slope. The manufacturers suggest that when settlements greater than 1% to 2% of the installation depth are expected, a telescoping coupling may be required to avoid buckling of the casing (DGSI 2009). This corresponds to 0.5 m to 1.0 m of settlement at the crest of the slope for the Highway No. 302 site. A combination of buckling and horizontal shear could compound casing deformation. Vertical settlement would show up as greater horizontal displacement rates and could potentially result in premature destruction of the casing.

Scenario #3 indicates that the readings of IPIs sensor could have been affected by settlement of the sensor or by having the sensor come in contact with the inner wall of the casing. Given the rigid nature of the sensor, it would be difficult to keep it away from the inside wall of the casing as the casing deforms in response to shear movements. A quantitative assessment of this effect is presented in subsequent sections.

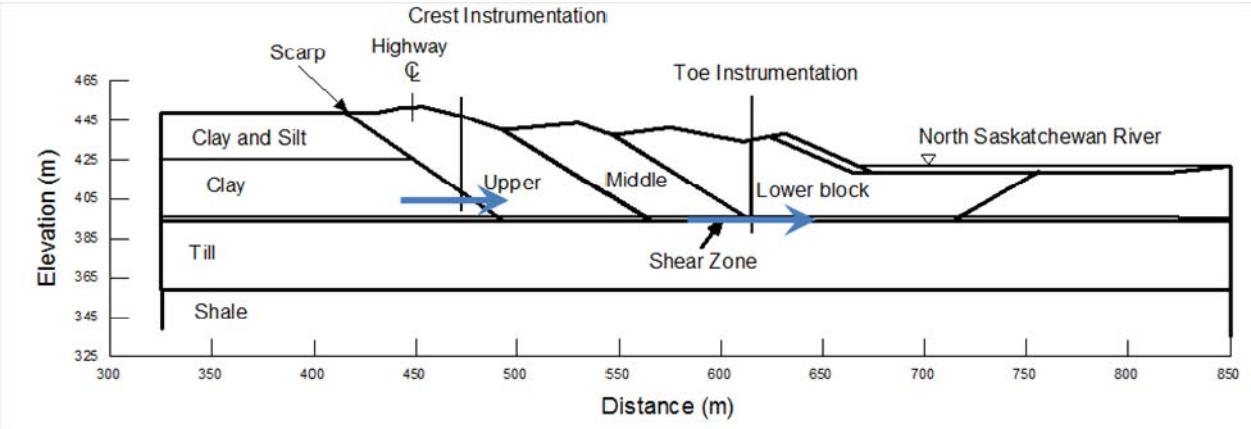

Figure 5.3: Scenario #1, horizontal shear at the slope crest greater than horizontal shear at the slope toe.

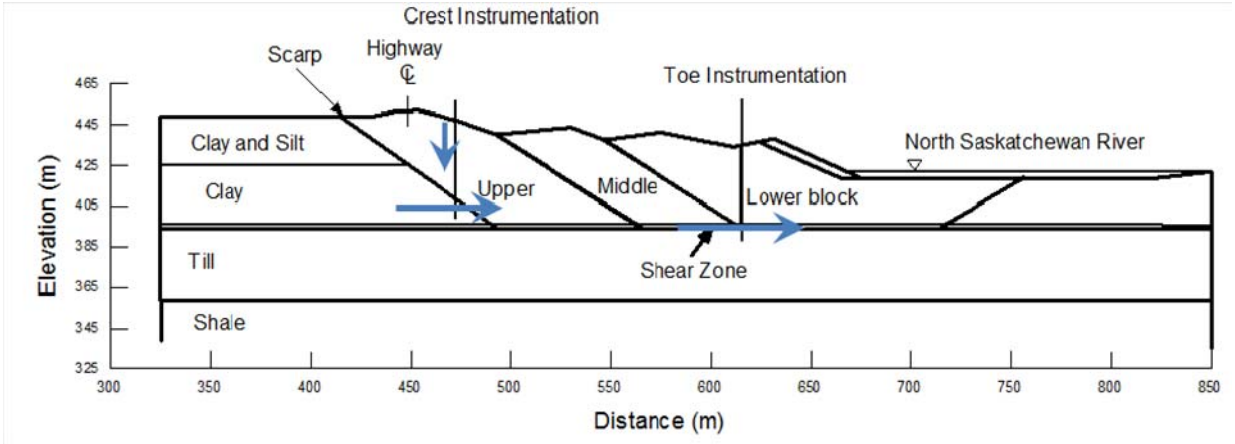

Figure 5.4: Scenario #2, vertical settlement and horizontal shear at the slope crest compounding casing deformation.

IPI103 was destroyed in March 2006 due to excessive movement. It was replaced in May 2006 by IPI203. IPI203 functioned until July 2006 at which time both IPI203 at the crest and IPI202 at the toe stopped functioning. It should be noted that prior to the destruction of the IPI203 and IPI202, the rates of movement at IPI202 at the toe of the slope increased to be much greater than those at the slope crest. This observation tends to support the observation that the toe typically moves at greater magnitudes and rates than the crest of the slope (Figure 4.15).

The manual SI data and topography of the landslide strongly support a retrogressive distribution of movement for this landslide. Based on the IPIs data, monitoring and published literature on

retrogressive landslides, it is also possible that the upper blocks could move at greater rates compared with those of the lower blocks, following a period of movement in the lower blocks. It is also reasonable to consider that the readings of the IPIs sensors are being affected by excessive deformation of the casing that would affect the magnitude and direction of the IPIs readings thus masking actual movement.

5.1.2 Trigger for Failure Mechanism

Vibrating-wire piezometers (VWP) were installed to monitor river level and pore-water pressure. The measurement of ground and river water levels was implemented to observe potential triggering mechanisms for movement. The data were presented with the displacement monitoring to determine if water levels were triggering movement.

In general, pore-water pressure conditions at or above the shear zone increased during or after movement occurred. This indicates that the rapid increases in pore-water pressure were likely shear-induced. Since records of long-term pore-water pressure monitoring at the site were not available, groundwater conditions prior to movement cannot be determined. Without pre-slide pore-water pressure data, it was not determined if a long-term pore-water pressure increase within the slope played a role in destabilizing the slope. The stratigraphic cross-section (Figure 3.4) showed sand layers behind the scarp, which may enhance the movement of groundwater into the slope, thus increasing pore-water pressures and potentially destabilizing the slope near its crest. This hypothesis cannot be confirmed because of lack of definitive pre-slide pore-water pressure monitoring data.

The second changing water level that could potentially affect the stability of the slope is the river level. Two potential concerns with the river level include active erosion and rapid drawdown. Haug et al. (1977), in the investigation of the Beaver Creek landslide near Saskatoon, SK, illustrated that lateral erosion of the river bank could be responsible for initiating movement.

Observations of the North Saskatchewan River at the Highway No. 302 landslide site show active erosion and small rotational failure at the river bank. This is expected since the landslide is located on the outside bend of a river meander.

Pauls et al. (1999) explored flooding of the Carrot River, near Nipawin, SK to determine if a rapid drawdown mechanism could be linked to slope movement. They hypothesized that a rising river level would result in saturated conditions and an increased pore-water pressure at the toe of the slope due to infiltration of river water. Once the river level receded, the saturated slope would lose the stabilizing force of the water while maintaining the elevated pore-water pressure in the slope. A combination of these two effects could destabilize the river bank. The monitoring of slope inclinometer casings at the Carrot River landslide verified that the flood event did not trigger movement and the rapid drawdown mechanism was not observed (Pauls et al. 1999). It was determined that this was likely because the rise in river level did not saturate the slope.

Landslide movement at Highway No. 302 was associated with the rise and fall of the river level. In this case there was IPIs displacement data that supported movement following a spring flood event. Given the activity of the landslide the soils would be highly disturbed. It is likely that the lower slope would saturate easily due to the disturbed nature of the soils with the rise of the river level and fall of the river.

During this monitoring period there is strong evidence from the data that movement of the unstable slope was triggered by river level fluctuation. For example, a 1.75 m increase in river level and 1.5 m decrease in river level was observed between March 27, 2006 and April 26, 2006. The river level fluctuation corresponded with spring melt. As the river level dropped movement began to take place at the toe of the slope (Figure 5.5). This river level fluctuation could have caused further erosion removing material at the toe resisting movement or a rapid drawdown type scenario that triggered movement at the toe of the slope in May 2006. This movement continued through to July 2006 when the instrumentation was destroyed.

Movement at the Highway No. 302 landslide was approximately 360 mm per year following the drawdown of the river level at the toe of the slope. By June 20, 2006 a rate of movement of nearly 4000 mm per year was observed.

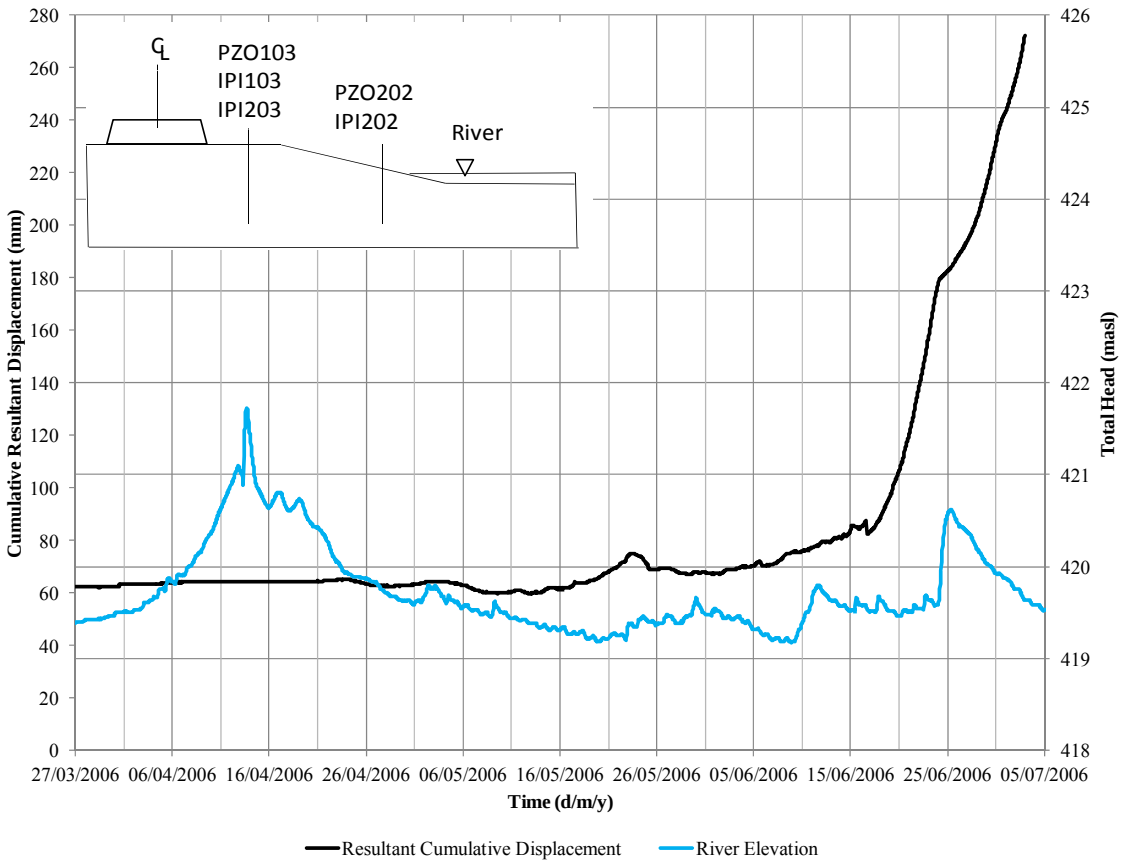

Figure 5.5: Resultant cumulative displacement at IPI202 and river level during spring and early summer 2006 to highlight a potential rapid drawdown mechanism.

Without monitoring pre-failure conditions it is difficult to verify the role of pore-water pressure on instability. Based on literature, site geology and data observations the trigger for movement of this multiple retrogressive landslide would be associated with the river. Either active erosion such as that described by Haug et al. (1997) or a rapid drawdown mechanism were observed as investigated by Pauls et al. (1999) could have caused the movement. Given the location of the landslide on the outside bend of a river meander, higher flows and higher velocity likely caused erosion, although either scenario is possible.

5.2 In-Place Inclinometer Data

This use of IPIs at Highway No. 302 appears to be the first case in which three connected IPIs were left in place until the sensors were destroyed. This provides an opportunity to evaluate the

IPIs data. Evaluation of the IPIs data will include a discussion of installation of the slope inclinometer casing, installation of the IPIs and a geometric analysis of casing curvature. Finally, the Highway No. 302 IPIs data will be compared with IPIs data from another landslide site in Saskatchewan.

5.2.1 Casing and IPIs Installation

5.2.1.1 Slope Inclinometer Casing Installation

A number of potential sources of error in traversing slope inclinometer probe readings were presented in Table 2.1. Installation of the slope inclinometer casing required the most attention to ensure a long casing life and limiting systematic error (DGSI 2009).

Slope inclinometer casing must be installed so that it is fixed at its base (i.e., installed 3 m to 6 m into stable bearing strata below the shear zone). As illustrated in Figure 3.8 it is recommended that the orientation of one of the two mutually perpendicular diametrically opposite pairs of grooves inside the casing be aligned in the expected direction of movement of the landslide (DGSI 2009). Normally, the pair of grooves along the expected direction of movement is labelled A-axis and the other pair is labelled B-axis. Such installation of inclinometer casing ensures maximum sensitivity of the probe along the A-axis, thereby avoiding potential errors and complex data processing.

Since the proper functioning of IPIs rely on the wheels remaining in the groves to control the orientation of the probe, bending in the B-axis could force the probe wheels out of the grooves during deformation of the casing. Orientation of the casing in the expected direction of movement and bending in that direction will put less eccentric force on the wheels of the IPIs.

Unfortunately, this recommended method of casing installation was not followed at Highway No. 302 because it is not consistent with SMHI standard procedure for installation of slope inclinometer casing. Given that the predominant direction of slope movement at Highway No. 302 was along the northeast-southwest direction, both the A-axis and the B-axis data must be scrutinized.

The slope inclinometer casing at Highway No. 302 was installed by pushing it through the grout and holding the casing from the top with the drill rig until the grout had set. DGSI (2009) describes this method of installation as the easiest but the worst way to overcome casing buoyancy. The problem with this method is that the casing goes into compression. This compressive force induces a wavy profile in the casing because of the flexibility of the casing (Figure 5.6). A wavy casing profile can increase the potential for the casing to contact the probe and reduce the lifespan of the casing. For example, if the IPIs probe were placed through an S-shape curve in the casing, the deformation of the casing may cause the probe to be near the casing wall and reduce the installation lifespan. Additionally, installation of the IPIs probe through the curved portions could affect the ability of the IPIs wheels to stay on track in the casing.

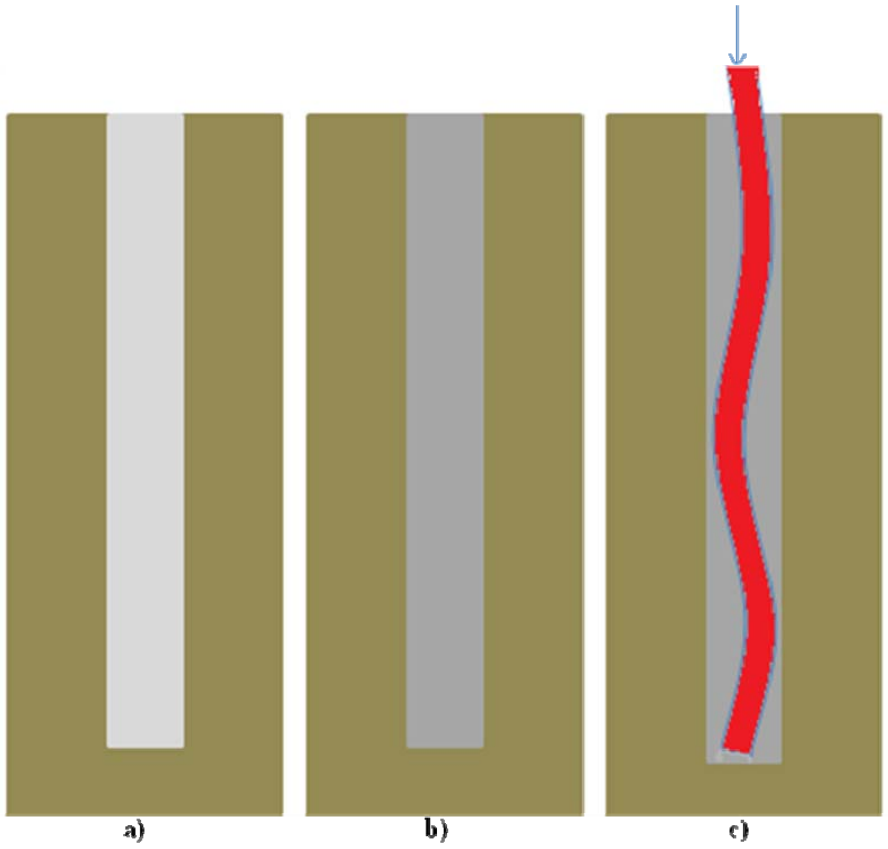

Figure 5.6: Sketch of the installation of slope inclinometer casing showing, a) drilled borehole with drilling fluid, b) replaced drilling fluid with cement-bentonite grout and c) install slope inclinometer casing by pushing and weighting from top until grout sets.

This problem increases with the increasing depth of installation. To avoid this situation a bottom anchor, bottom weight or pinning the casing from the bottom is recommended.

Finally, due to the depth of the borehole there was potential for the borehole to deviate from vertical. Figure 5.7 presents the profile of the SI202 at the toe of the slope which housed the IPIs that showed movement reversal. It is evident in this figure that there were problems with both curvature (wavy profile) and verticality since the casing was also found to deviate 1.9° to the south west. Both of these attributes can reduce the casing lifespan since by reducing the annular space and forcing the probe out from its grooves prematurely. A tilted installation can also reduce the lifespan since the probe is calibrated from vertical to ±10° and the initial tilt of the casing can reduce the amount of tilt available before the calibrated range is breached.

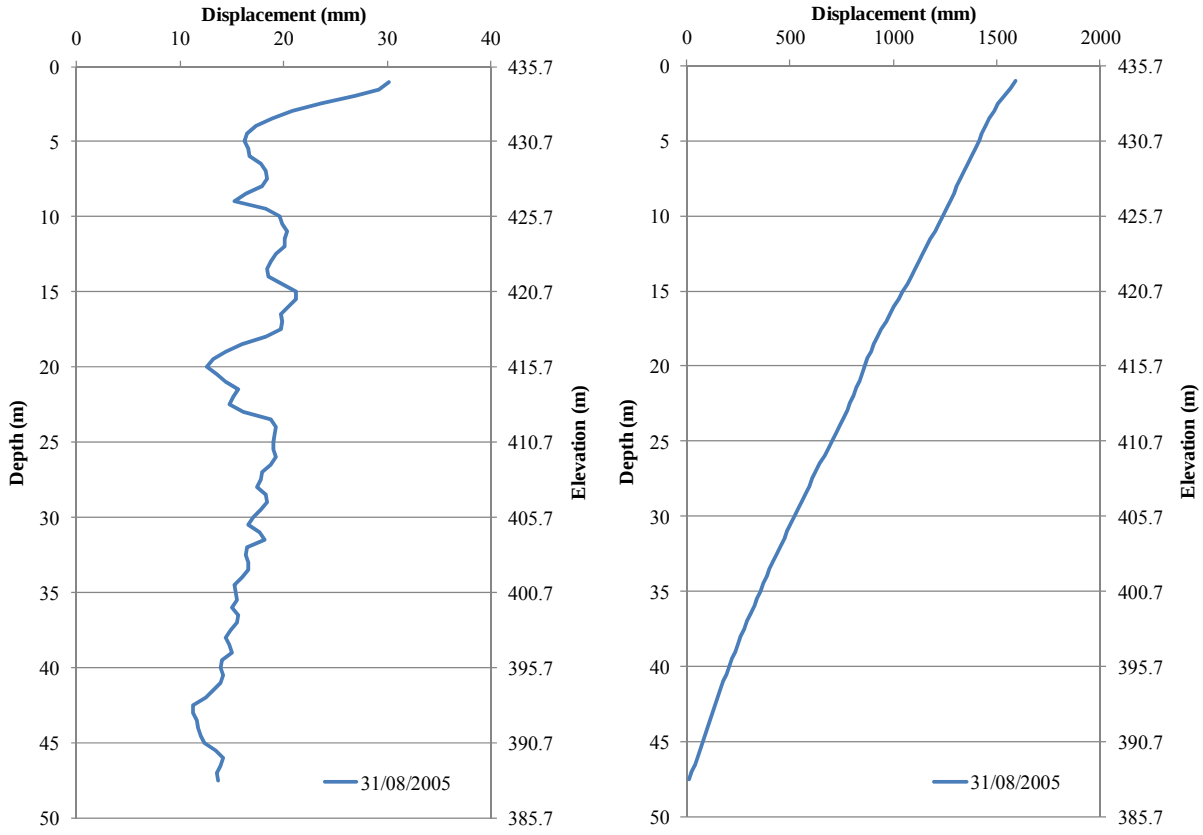

Figure 5.7: Initial casing survey highlighting resultant incremental displacement (casing straightness, left plot) and resultant cumulative displacement (casing profile, right plot).

5.2.1.2 In-Place Inclinometer Installation

As described in Chapter 3, the IPIs were suspended from the top of the slope inclinometer casing using a hook-and-cable assembly (Figure 3.10). Two situations may cause unexpected readings:

1. Slack in the cable after installation (ASCE 2000);

2. Settlement of the hook-and-cable assembly caused by the hook pushing on to flexible ABS casing; this could also result in depth position errors and may potentially affect probe readings.

ASCE (2000) indicates that during installation it is possible that the cable may have some slack in it. To remove slack from the cable it was suggested to add additional weight to the bottom IPIs sensor or to allow the probe to go lower than the desired depth of installation and pull the IPIs up into position.

Simeioni and Mongiovi (2007) described movements that were attributed to settlement of the top assembly after placement of the IPIs. It was stated that it could take one hour to two weeks for the settlement to stabilize with shifts up to ±100 mV. For IPIs with a 2 m gauge length this would equal ±14 mm.

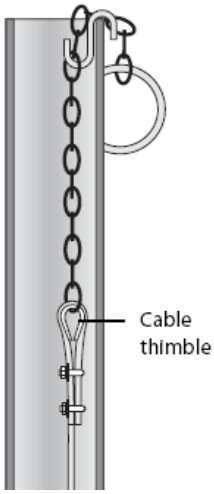

Figure 5.8: Top assembly termination of in-place inclinometers suspended in inclinometer casing (DGSI 2009).

Settlement of the top assembly at the Highway No. 302 landslide could be responsible for the large change in readings witnessed on October 13, 2005. Figure 5.9 (left) represents the change in the position of the sensors prior to and just after the disturbance on Oct. 13, 2005. Prior to October 13, 2005 the upper sensor in both IPI103 and IPI202 experienced the movement. The disturbance caused the sensors to move in a positive direction followed by movement in a negative direction. This type of down slope movement followed by upslope movement is unlikely and kinematically inadmissible. It is reasonable therefore to consider that settling of the head assembly could be brought about by landslide movement and cause a depth position change of the IPIs.

Figure 5.9 (center and right) shows the position of the IPI202 for 11 reading intervals. Since the lowest sensor was installed below the shear zone it should not have experienced displacement. A large disturbance affected all the IPIs on October 13, 2005. Since the lowest IPIs showed displacement either movement occurred at the lowest sensor or the IPIs installation came into contact with the casing. Also, observing the profile changes of the IPIs (positive and negative movement) it is reasonable to suspect that the IPIs came into contact with the casing.

The assumption with the IPIs is that the entire length remains rigid and should not bend. Dunnicliff (2002) indicated that narrow shear zones can cause the IPIs come in contact with the deformed casing and provide unexpected results. This was illustrated by Flentje et al. (2005).

Flentje et al. (2005) highlighted a scenario where IPIs provided unexpected (negative) upslope readings. Figure 5.10 shows the initial placement of IPIs 11567. The sensor is only 0.45 m long with a gauge tubing extending another 2.55 m for a total gauge length of 3 m. The sensor tip was placed at a depth of 7 m as the shear zone existed between 4 m to 5 m. The span of this instrument and the location of the shear zone caused the gauge tubing to experience flexing or bending with the result that an upslope displacement reading was reported by the IPIs. This displacement was actually what the IPIs sensor experienced well below the slip surface. Verification of this phenomenon was conducted using a traversing slope inclinometer probe survey.

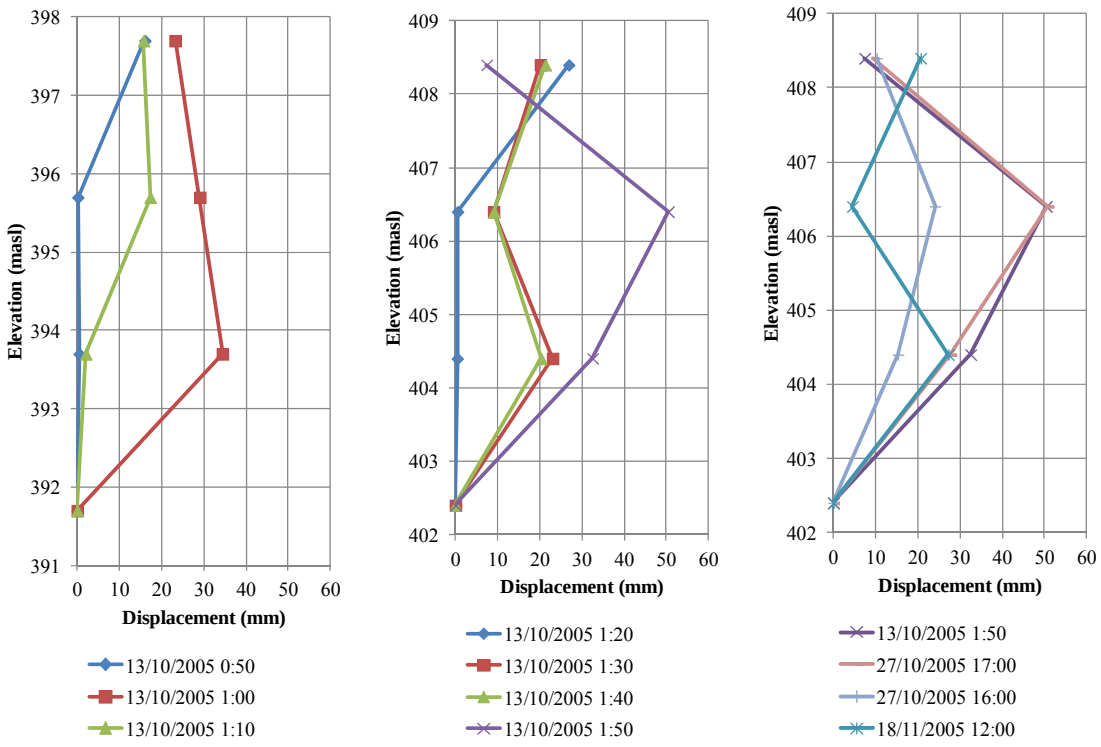

Figure 5.9: Displacement profiles during the movement on October 13, 2005 for IPI103 (left) and IPI202 (center), and further disturbances of IPI202 during fall (right).

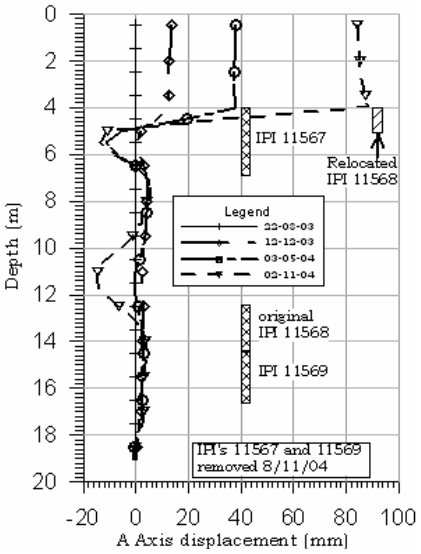

Figure 5.10: Negative displacement experienced by IPI 11567 (after Flentje et al. 2005).

IPI103 at the crest had multiple shear planes within an approximately 4 m thick zone (see Chapter 4 - Figure 4.10). At IPI103 the larger shear zone accommodates the 2.0 m gauge lengths and no additional disturbances were witnessed prior to the destruction of IPI103 in March 2005. IPI202 was installed at the toe of Highway No. 302 slope through a shear zone that was approximately 1.5 m thick (Figure 4.10b). The 2.0 m IPIs were longer than the shear zone thickness. Additionally, the lowest sensor of IPI202 extended 0.75 m into the shear zone.

It is possible that the initial disturbance of the IPIs was due to the movement of sensors in the casing from the settling of the IPIs assembly triggered by a global movement of the slope. This explanation is reasonable based on other literature and highly unlikely kinematics of upslope movement. The data from IPI202 indicates additional disturbances that may be attributed to the gauge lengths spanning a relatively narrow shear zone.

5.2.2 Geometric Analysis

5.2.2.1 Vertical Position of In-place inclinometers

Since the IPIs are suspended from the top of the casing, horizontal deformation would change the position of the sensor in the casing. Horizontal movement would tend to pull the IPIs up the casing and the depth position of the sensors would be affected.

Consider a single IPIs with a gauge length of 2 m sitting vertical at an origin, O, with coordinates (0,0,0) and the top of the sensor coordinates (0,0,2). In 3-dimensional space the resulting radius vector, *r*, from the origin is calculated as:

$$r = |r| = \sqrt{x^2 + y^2 + z^2} \quad \text{.....(5.1)}$$

When the position of the sensor sits vertically the radius is simply equal to the z-coordinate, 2 m. Since the IPIs has a fixed gauge length of 2 m, the radius value, *r*, can be considered fixed. When movement occurs in the x and y direction with a fixed radius, the vertical coordinate, z, at the origin must decrease (Figure 5.11). This value of decrease is calculated by rearranging equation 5.2.

$$z = |z| = \sqrt{r^2 - x^2 - y^2} \quad \text{.....(5.2)}$$

The value of decrease is then determined simply by subtracting the new z-coordinate from the radius. This is highlighted in Table 5.1. Although tilt values produce only small changes in depth position, this highlights that the position is not truly fixed. Secondly, the movement would tend to pull the IPIs up the casing since the suspension cable is of fixed length. Observing the values in Table 5.1 it is clear that vertical movement of the probe would require very large movements before significant depth position change occurs.

It has been shown that the IPIs can change vertical position due to movement. Since relatively small displacements were observed prior to the disturbances to the IPIs, an additional explanation is required.

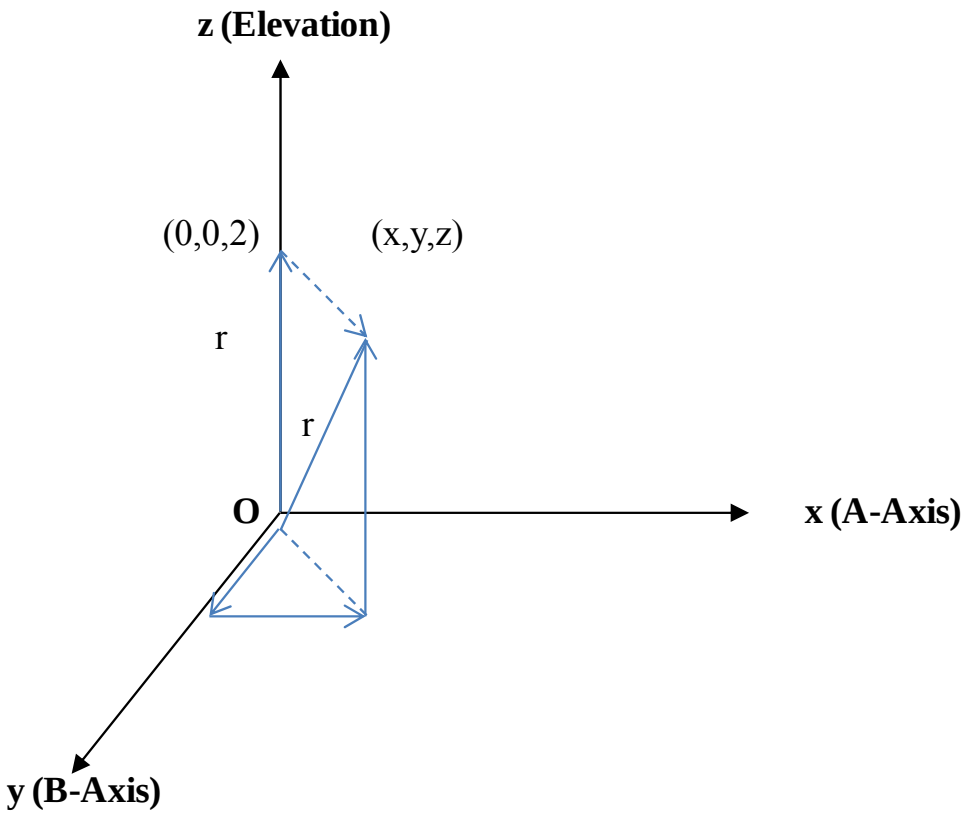

Figure 5.11: Decrease in the sensor origin due to lateral deflection.

Table 5.1: Estimates of change in vertical position, z (elevation) of a single sensor due to tilt.

x-displacement (mm)	y-displacement (mm)	Expected Increase in Elevation (mm)
0	0	0
50	50	1
100	100	5
150	150	11
200	200	20
250	250	31
300	300	46

5.2.2.2 Casing curvature and In-place inclinometers

A simple schematic in Figure 5.12 illustrates how limited the annular space is between the probe, gauge tubing and the inside casing wall. Once the annular space around the sensor closes, the probe will be subject to forces from the casing. When a traversing slope inclinometer probe is used this is the point at which the traversing slope inclinometer probe no longer passes through the casing. With the IPIs left down-hole, this would be the point where the curvature affects the instrument.

In order to determine the point at which the casing will come in contact with the IPIs two simplifying assumptions were required. They are that the deformed slope inclinometer casing was installed vertically and can be modeled with two circular arcs as indicated in Figure 5.13.

The schematic drawing provides the parameters to analyse the radius of curvature, r and the clearance of the IPIs from the casing wall, c_i. These values are determined form the shear

displacement, d, shear induced deformation profile thickness, t, to determine the radius of curvature, r. Additional inputs include the length of the probe, l_p, the diameter of the probe, w_p, the casing diameter, s, space between the probe and the outer casing wall, and the angle between the mid-point of the probe and top of the probe, θ_p.

First determining the radius of curvature can be accomplished by utilizing Pythagorean's theorem where:

$$r^2 = \left(\frac{t}{2}\right)^2 + \left(r - \frac{d}{2}\right)^2 \quad \text{.....(5.3)}$$

Rearranging equation 5.3 to solve for r:

$$r = \left(\frac{d^2 + t^2}{4d}\right) \quad \text{.....(5.4)}$$

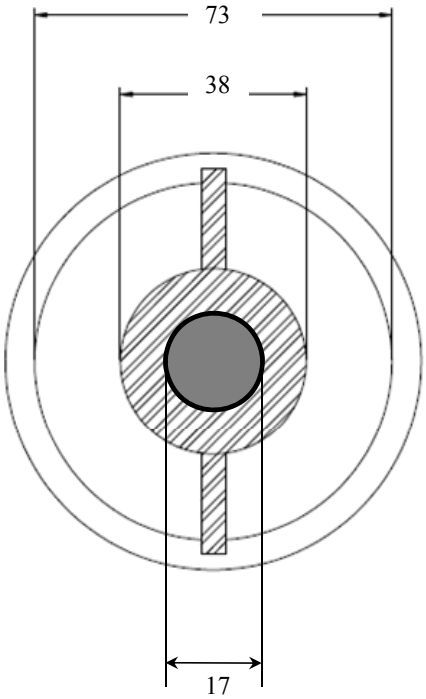

Figure 5.12: Cross section of casing highlighting the annular space in millimetres between the casing, tilt sensing probe and gauge length.

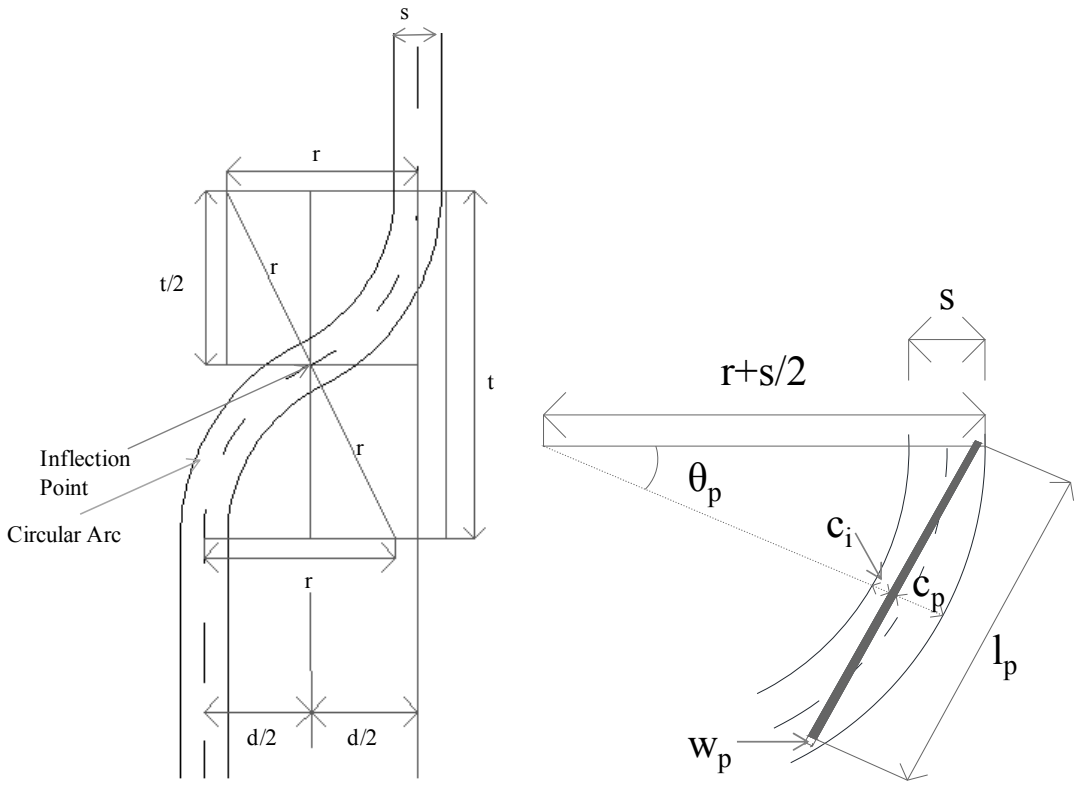

Figure 5.13: Schematic of radius of curvature, r and clearance of the sensors, c_i and c_p based on the selection of shear zone thickness, t, gauge length of probe, l_p and displacement, d.

As shear displacement increases the radius of curvature will decrease. As curvature decreases the annular space in the casing reduces. Once the radius of curvature is known for a particular displacement, the annular space remaining between the inner casing wall and probe, c_i can be determined:

$$c_i = s - \left(w_p + c_p\right) \quad \text{.....(5.5)}$$

where s, is the inside diameter if the casing, w_p is probe width and c_p is the clearance between the probe and outer casing wall.

In order to solve Equation 5.5, c_p must be determined. Using geometry, c_p can be determined from the angle θ_p which is:

$$\theta_p = \sin^{-1}\left(\frac{\frac{l_p}{2}}{r+\frac{s}{2}}\right) = \sin^{-1}\left(\frac{l_p}{2r+s}\right) \quad (5.6)$$

then;

$$c_p = \left(r+\frac{s}{2}\right) - \left(r+\frac{s}{2}\right)\cos\theta_p = \left(r+\frac{s}{2}\right)\left(1-\cos\theta_p\right) \quad (5.7)$$

finally,

$$c_p = \left(r+\frac{s}{2}\right)\left(1-\cos\left(\sin^{-1}\left(\frac{l_p}{2r+s}\right)\right)\right) \quad (5.8)$$

Substituting equation 5.8 into equation 5.5 to obtain:

$$c_i = s - \left[w_p + \left(r+\frac{s}{2}\right)\left(1-\cos\left(\sin^{-1}\left(\frac{l_p}{2r+s}\right)\right)\right)\right] \quad (5.9)$$

Using the previous calculations, the maximum allowable shear displacement, d can be determined. Using a spreadsheet, c_i can be calculated for a variety of shear displacements with the additional inputs of s, l_p, w_p, and t. The resulting values can be graphically represented by plotting c_i and d. Once c_i reaches zero and becomes negative the annular space has closed and the casing has contacted the instrument.

The following figures highlight the resulting analysis for IPI103 and IPI202. The results were considered using the probe diameter and gauge tube diameter since the curvature may have closed around the smaller diameter gauge tube. It should be noted this analysis considered only a single 2 m diameter probe and did not incorporate several interconnected probes.

Figure 5.14 and Figure 5.15 highlight the results from the analysis at IPI103. With a shear induced deformation profile thickness, t, of 4.0 m and a probe length, l_p, of 2.0 m the casing displaces 280 mm prior to casing contact with the probe. If the gauge length diameter of 17 mm

is used the IPIs sensor would exceed its calibrated range of 10° before the casing curvature affects the sensor. This analysis indicates that the disturbance to the sensor on October 13, 2005 was likely due to settlement of the top assembly; since it is unlikely that casing affected the sensors.

For IPI202 the shear induced deformation profile thickness, t, was 1.5 m and the gauge length, l_p was 2.0 m. Figure 5.16 and Figure 5.17 highlight the resulting maximum allowable shear deformation. In this case since the gauge length is longer than the shear zone and much less allowable deformation can occur before contact of the casing with the probe. For the case where the probe diameter is 38 mm, 40 mm is the maximum allowable shear displacement. The maximum allowable shear displacement increases to 63 mm when the 17 mm diameter gauge tubing is used. Since IPI202 deflected approximately 21 mm prior to installation of the IPIs and an additional 27 mm with the IPIs itself it is possible that the disturbance on Oct 13, 2005 was caused by contact of the probe with the casing. The analysis indicates that the IPIs could contact the casing between 40 mm and 63 mm of shear displacement.

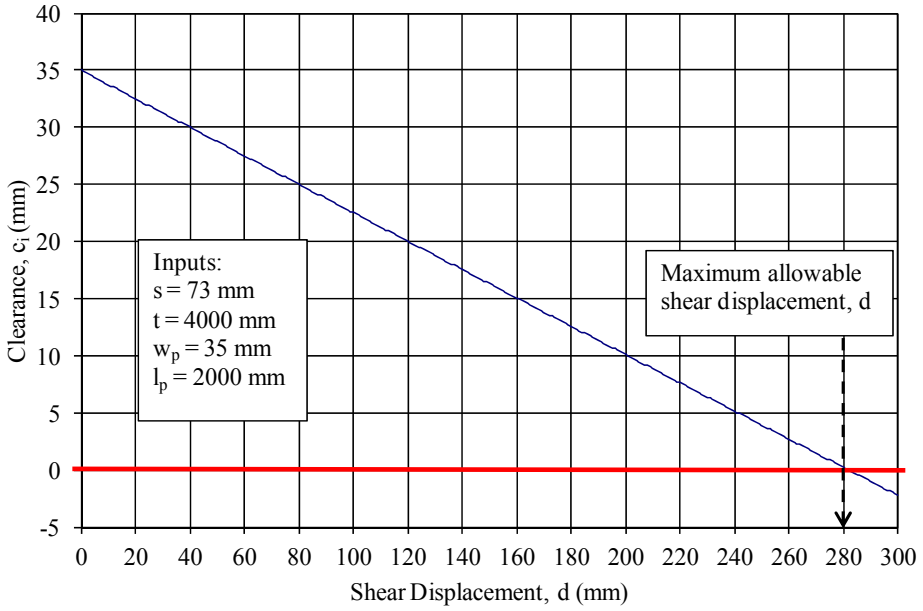

Figure 5.14: Clearance, c_i, versus shear displacement, d for IPI103 using the probe diameter of the sensor, w_p.

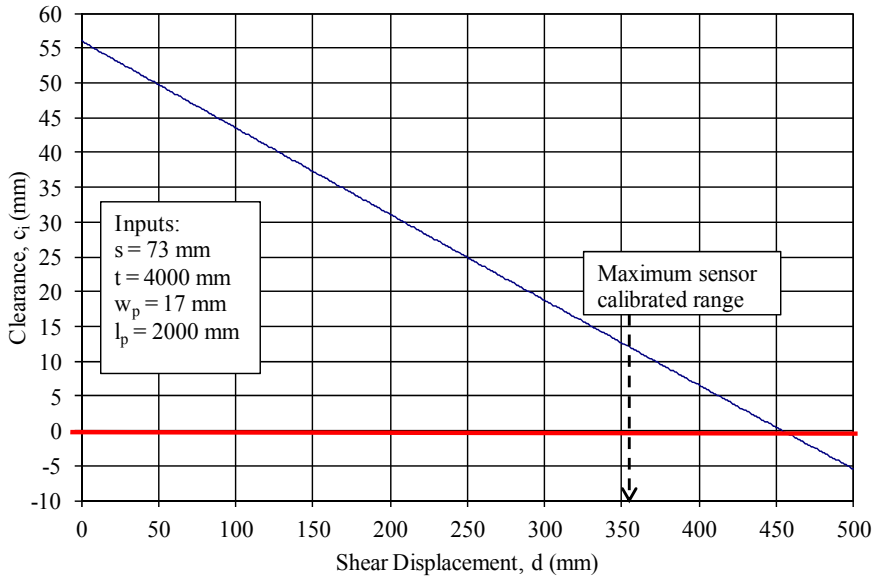

Figure 5.15: Clearance, c_i, versus shear displacement, d for IPI103 using the smaller gauge tubing diameter, w_p.

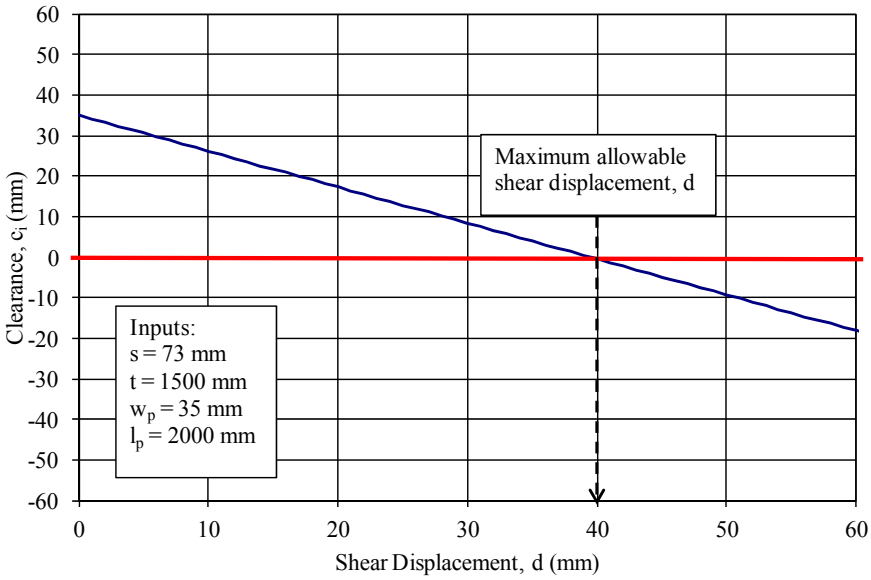

Figure 5.16: Clearance, c_i, versus shear displacement, d for IPI202 using the probe diameter of the sensor, w_p.

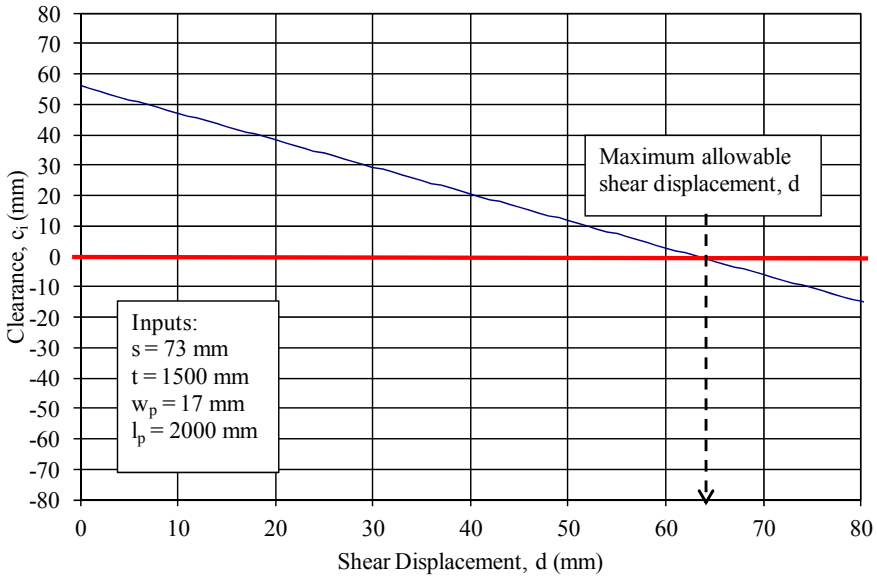

Figure 5.17: Clearance, c_i, versus shear displacement, d for IPI202 using the smaller gauge tubing diameter, w_p.

5.2.3 Application of In-Place Inclinometer Analysis to a Landslide Affecting Highway 11 near Aylesbury, Saskatchewan

Since IPI202 continued to provide readings that were difficult to interpret it is likely based on the analysis that casing was contacting the IPIs either on October 13, 2005 or shortly thereafter.

SMHI installed IPIs as part of an automated system at an active landslide near Aylesbury, Saskatchewan. A reversal was also witnessed at this landslide.

Highway 11 near Aylsebury, Saskatchewan was being affected by landslide movement. After the destruction of one slope inclinometer casing and approximately 3 mm of displacement in the next slope inclinometer casing, the IPIs were installed. The automated real-time monitoring was implemented since the landslide could negatively affect a portion of Highway 11. After months of consistent readings from the IPIs a shear key was constructed to stabilize the slope.

During excavation of the shear key the direction of slope movement was affected at the toe of the landslide. It was suggested that this anomaly was a disturbance brought about by the excavation and installation of a shear key upslope of the instrument (A. Kelly, Personal communication,

February 26, 2008). The excavation upslope of the instrument would allow movement of the slide mass upslope due to the removal of soil behind the instrument.

Installation of IPIs at Highway No. 302 connected each of the three IPIs with the universal joint so each sensor was connected. Installation of the IPIs at the Aylsebury slide was completed by independently hanging each IPIs and not connecting them. Table 5.2 highlights general comparisons for the Aylesbury site to the Prince Albert site. Some key highlights include the difference in depth and the difference in pre-installation deformation.

The first comparison of data from the Prince Albert and Aylesbury site was a plot of the A-Axis versus B-Axis movement. Correctly functioning IPIs should provide a consistent direction of movement. The plots of A-Axis versus B-Axis data are highlighted for IPI101 at Aylesbury and IPI202 at the Prince Albert landslide in Figure 5.18 and Figure 5.19, respectively.

A consistent direction was witnessed for movement at IPI101 at Aylesbury. The direction of movement during shear key construction was negative and positive again following the shear key construction.

Table 5.2: Comparison of installation of IPIs at Aylsebury and Highway No. 302.

Comparisons		**IPI101 Highway 11-04 Aylesbury**	**IPI202 Highway No. 302 Prince Albert**
Installation Depth	(m)	<10	>40
Gauge Length	(m)	2.0	2.0
Deformation Prior to Installation	(mm)	3.0	≈20

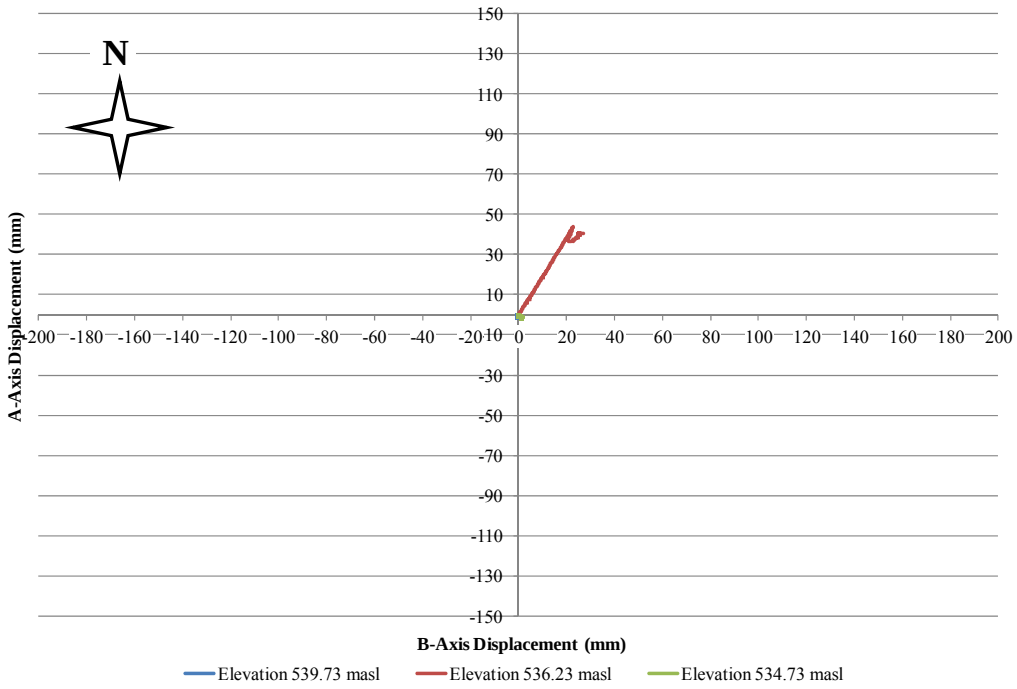

Figure 5.18: A-Axis versus B-Axis displacement for IPI101 at Highway 11-04 near Aylesbury landslide, near Aylesbury, Saskatchewan.

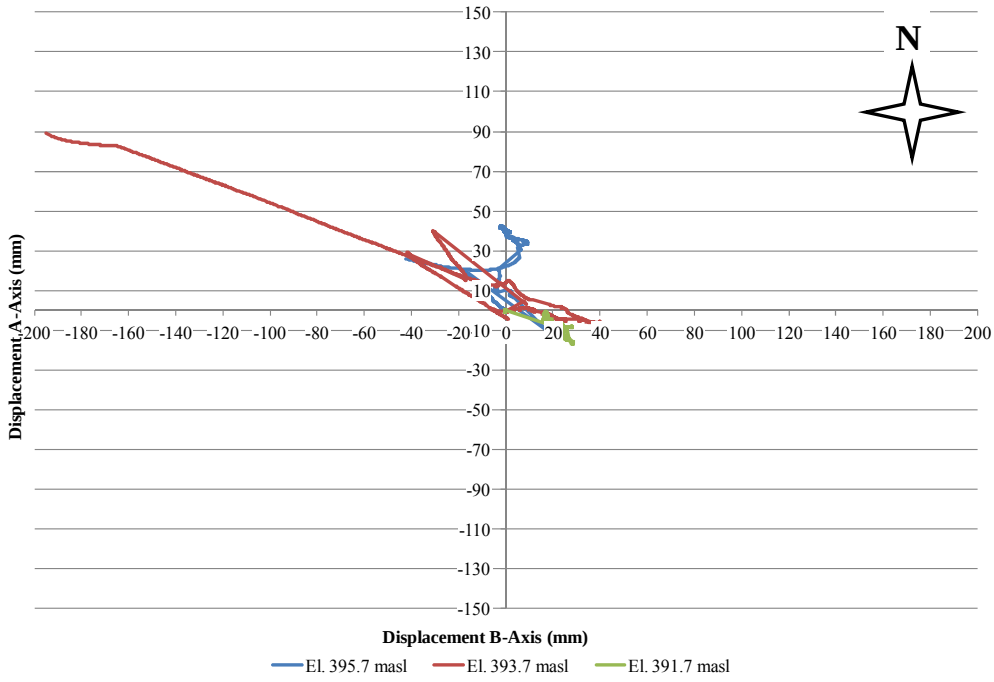

Figure 5.19: A-Axis versus B-Axis displacement for IPI202 at Highway No. 302 near Prince Albert, Saskatchewan.

The geometric analysis was applied to the Highway 11 data. Assuming a shear induced deformation profile thickness, t, of approximately 2.0 m and a probe length of 2.0 m the clearance, c_i was plotted against shear displacement, d. Approximately 45 mm of movement was indicated by the IPIs data prior to the reversal. Figure 5.20 and Figure 5.21 highlights that the casing may contact the probe for deformation of between 44 mm and 71 mm. This indicates that observed reversal may have been caused by either shear key construction or the casing contacting the IPIs. Since the direction was corrected after shear key construction and the slope stabilized, it is hypothesized that the upslope movement was caused by shear key construction.

Movement of all three sensors at IPI202 at the Highway No. 302 landslide indicated that the IPIs string was being affected by the casing. The IPIs are changing direction, while at IPI101 at Aylesbury the middle IPIs moves in a constant direction and the ones above and below the shear zone remain very near the origin. This single plot verifies that the IPIs at Highway No. 302 were likely caused by the casing contacting the IPIs.

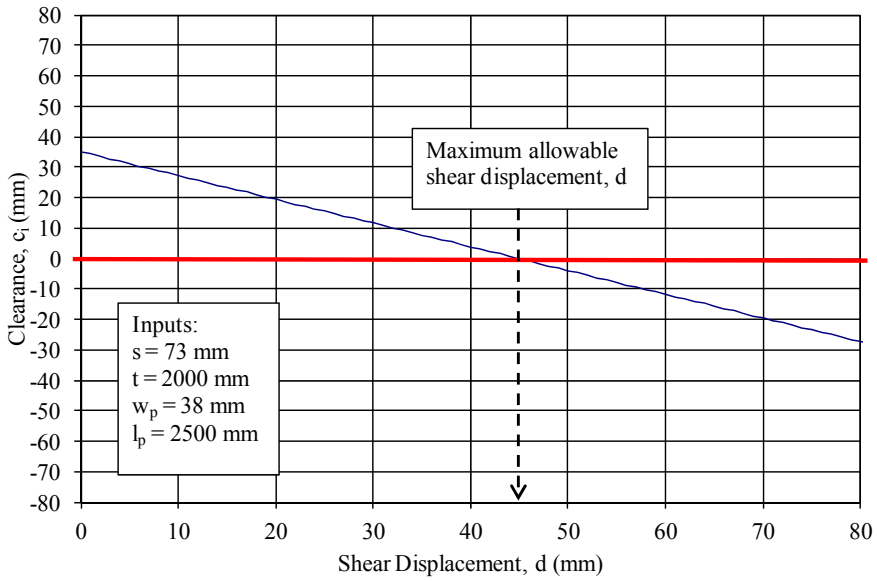

Figure 5.20: Clearance, c_i, versus shear displacement, d for IPI101 at the Aylesbury landslide using the probe diameter of the sensor, w_p.

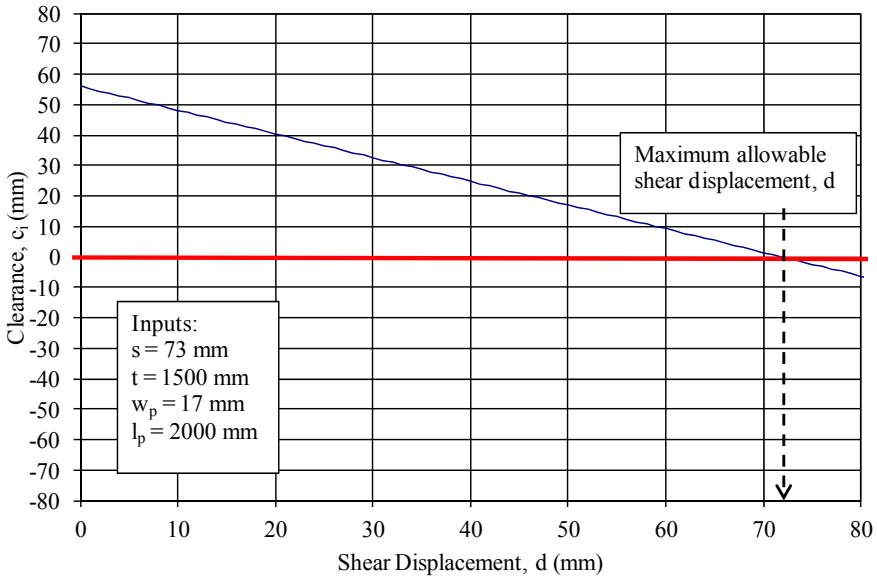

Figure 5.21: Clearance, c_i, versus shear displacement, d for IPI101 at the Aylesbury landslide using the smaller gauge tubing diameter, w_p.

5.3 Summary

The kinematics of the landslide was shown to have a retrogressive distribution based on all periodic monitoring and literature. Between February and May 2006 movement rates at the crest of the slope were greater than at the toe. It was therefore hypothesized based on this observation that the landslide may, for a period, move in a crest to toe fashion. This is a reasonable assumption provided that all the previous monitoring indicated greater toe movement thereby leaving slack in the multiple block system where the crest movement is catching up with the toe movement.

The trigger for movement at the toe was identified as a rise and fall in river level. High river flows could be responsible for erosion of toe material at the toe causing further movement. Alternatively, a rapid drawdown mechanism could have triggered movement. Regardless, the data was able to correlate movement at the toe when comparing the displacement data to the river level data. Since long term pore-water pressures could not be observed it is uncertain if increasing groundwater levels were responsible for initiating the slope movement.

Disturbance of the IPIs at Highway No. 302 occurred on October 13, 2005. This was likely due to the settlement of the IPIs sensors at the crest of the slope (IPI103). This would be instigated due to slack in the system and a subsequent tensioning of the head assembly due to landslide movement. Although this was also possible at IPI202, it was shown that the casing could have been contacting the IPIs early in the installation. Casing contact would explain additional unexpected readings where movement spikes and reversal in movement of the middle sensor was witnessed.

This analysis was also applied to a landslide near Aylesbury, Saskatchewan. Comparing the two data sets showed that the IPIs at the Highway No. 302 landslide were being affected by the casing. This resulted in unexpected and erratic data when compared to that of Aylesbury.

Chapter 6 Conclusions and Recommendations

6.1 Conclusions

Since the IPIs were successfully implemented to provide early warning of movement at the Highway No. 302 landslide it should be considered a useful tool for future use. It would be particularly useful to monitor landslides that present unacceptable risk to public safety, infrastructure, or sites that are difficult to access for routine monitoring.

The main benefit to using IPIs was the remote monitoring capability and the reduction in temporal gaps for displacement monitoring. For example, it was expected that toe movement would occur at greater rates compared to movement rates at the crest. In general this was true, however; the IPIs showed a period of movement in February 2006 where the crest moved at a greater rate than the toe of the slope. This movement was unexpected and may not have been captured with manual monitoring techniques.

When considering that this landslide was initiated after the last deglaciation and draining of Glacial Lake Saskatchewan, the monitoring period is very short. Based on results from the manual monitoring and supported by literature, the retrogressive nature of this landslide was confirmed. It was shown that the upper blocks of the landslide may move at greater than rates the toe since the toe has moved at much greater rates previously. This slack in the system may cause movement of the upper blocks without movement at the toe.

The IPIs were also used to identify a potential failure mechanism in relation to the river level fluctuation. This would occur due to erosion of the slope toe or alternately due to a rapid drawdown mechanism. Verification of the exact cause was beyond the scope of this work, but it was evident in the data that the IPIs at the toe of the slope experienced no movement until after

the river level rise and fall. Therefore, this system was successful for the observation of slope mechanism.

The success of the instrument related to risk management and identifying potential triggering mechanisms proves the validity of the IPIs as part of a real-time monitoring system. To use data from the IPIs to confidently assess kinematics of landslides would require additional quality assurance and quality control measures to ensure actual magnitude and direction of the movement is correct. This would require additional study to ensure the instrument is being used within its capacity and that the readings are verified by another means.

The IPIs at Highway No. 302 showed unexpected movement including upslope movement and movement in sensors that were installed below the expected zone of movement. It was shown that the IPIs may not be in a fixed position due to potential settlement that could occur in the top assembly and that the IPIs could be contacting the casing walls.

The probe may move slightly under the current top assembly installation. For example, the length of the cable is fixed, as tilt occurs small vertical movement can occur in the probe as the casing deforms. Although it takes large movements to have a significant impact on the sensor, the sensor was shown to be very sensitive to slight changes in position.

A geometric analysis was conducted to determine the approximate amount of movement IPIs can achieve based on the annular space between the casing and the probe. This was based on shear induced deformation profile thickness, casing diameter, and diameter and gauge length of the IPIs. The analysis used a simplifying assumption of symmetry of the radius of curvature about the bisecting axis of the shear zone. This analysis suggested that the IPI202 at the toe of the slope was affected by the probe contacting the deformed casing causing unexpected readings. Comparison of the Highway No. 302 IPIs data with that of the Aylesbury data concluded that the readings at IPI202 were affected by the casing contacting the probe. This was very evident when observing the plots showing the direction of movement.

Using the IPIs data in conjunction with the river level data it was concluded that the movement at the toe was affected by river level fluctuations. Pore-water pressure readings from the vibrating wire piezometers (VWP) appeared to be affected by the landslide movement and not

the cause of movement. Without long term pore-water pressure data the effect of groundwater levels on the stability of the landslide could not be explored as a triggering mechanism.

6.2 Recommendations

It is recommended that IPIs continue to be used for situations that may be of high risk or where regular access for monitoring is difficult. Movement and other data can be used to raise alarms and provide indication of the landslide mechanism. This identification of movement and triggers help provide warning and identifying the cause of the landslide allowing for an understanding of ways to improve stability.

To prolong the life of the IPIs the casing installation should be as vertical as possible and one set of grooves aligned with the expected direction of movement. A detailed review of traversing slope inclinometer probe surveys should be conducted so that the gauge length of the instrument is carefully selected and placed to the required depth. If a single, well defined shear zone exists, single IPIs should suffice to monitor the slope. If multiple shear zones exist, individual IPIs can be used for each shear zone. Gauge lengths that are much larger than the shear zone induced deformation profile should be avoided as they have been shown to become affected by the slope inclinometer casing.

All slope inclinometer casings should have a baseline reading with a traversing slope inclinometer probe. The installation of the IPIs should be adjusted based on these data. For additional trials using the IPIs it is recommended that regular site visits occur to check the top assembly or to take traversing slope inclinometer probe readings to verify the IPIs data. If possible it would be ideal to fix the IPIs from the bottom of the casing by either filling up the casing with something (such as silica sand) or providing a sacrificial gauge tube that extends up from the bottom of the sensor and contacts the base of the slope inclinometer casing. A site visit and manual reading should also be conducted if significant unexpected movement is recorded by the IPIs. Verifying IPIs data with a traversing slope inclinometer probe survey will help support the recommendation that the IPIs be used as both a risk management and landslide study tool.

6.3 Recommendations for Future Work

The passage of rigid instruments through casings installed in the ground is also applicable to other fields of study. Additional analysis on the geometry or curvature of casings of varying types would be beneficial. For example the analysis of curved casings could be applied to the passage of geophysical instruments down deep boreholes for the oil and gas industry. Deformation of well casings, the shape of the deformation zone and other potential issues could be explored. Essentially this could be done by developing a model to review the casings installed in the ground as a soil-structure interaction problem to evaluate the effect of movement on the casing profile and determine how much movmenet is allowable to still pass an instrument. It may be possible to evaluate the casing type and size to account for potential deformation. A three dimensional model would be required that can acount for the modeling of both the casing, soil and other material properties.

In order to better visualize the IPIs movement capabilities, a laboratory study is recommended. This study would consist of fixing a transparent casing (if it can be acquired) to a rigid object and simulating a shear zone movement. Displacements could then be measured using both an SI and IPIs for comparison. The IPIs and SI could be tested for a number of potential shear zones, positions, and associated instrument response. This would improve the ability to understand the capability of the IPIs and its use in landslide monitoring. Again, this review could also be transferable to other applications where casing curvature is an issue.

Applying information gathered in the laboratory could then be applied to the field. This would include implementing new (or improving existing) installation techniques or providing innovative ways to ensure the IPIs remain in a fixed location. This could be implemented in association with the SMHI who are actively using remote real-time monitoring at a number of sites.

Finally, to verify the kinematics and mechanisms of the Highway No. 302 multiple retrogressive landslide, more research is warranted. This could include a full-scale back analysis that would require numerical modeling characteristics using slope stability modeling and coupled stress / pore-water water pressure analysis. Initially a simple slope stability model could be used to verify the toe movement witnessed at site to determine if erosion or a rapid drawdown

mechanism would be more likely to trigger movement at the toe. Next the analysis could proceed to determine the more complex coupled stress / porewater pressure analysis to determine the relationship between the landslide blocks. This would involve modeling each landslide block including the shear zone. A linear elastic model should be sufficient to evaluate potential triggering mechanisms and to explore the stability of individual landslide blocks. This would verify that the upper landslide block can move with slack in the system as well as evaluate groundwater pressure changes or other potential triggers.

REFERENCES:

ASCE Task Committee on Guidelines for Instrumentation and Measurements for Monitoring Dam Performance. 2000. Guidelines for instrumentation and measurements for monitoring dam performance. American Society of Civil Engineers, Reston, Virginia.

Antunes, P.J., Kelly, A.J., Vu, H. Q. Clifton, A. W., Widger, A., and King, G.L. 2006. Application of a real-time monitoring system to a landslide on the Saskatchewan Highway Network. Proc. 59th Geotechnical Conference, Vancouver.

ASTM. 1998. Standard Test Method for Monitoring Ground Movement Using Probe-Type Inclinometers. ASTM International, West Conshohocken, Pa. American National Standard, Designation: D6230-98.

Boart Longyear Interfels. 2005. ARGUS Monitoring Software Instruction Manual.

Boutwell, Gordon P. and Schmidt, Paul D. 1998. Pre-instrumented riverbank slide. Geotechnical special publication in Stability of Natural Slopes in the Coastal Plain 77: 27-44.

Campbell Scientific, Inc. 2003. Campbell Scientific CR10X Instruction Manual.

Christiansen, E.A. 1968a. Pleistocene stratigraphy of the Saskatoon area, Saskatchewan, Canada. Canadian Journal of Earth Sciences, 5: 1167-1173.

Christiansen, E.A. 1968b. A thin till in west central Saskatchewan, Canada. Canadian Journal of Earth Sciences, 5: 329-336.

Christiansen, E.A. 1979. The Wisconsinan deglaciation of southern Saskatchewan and adjacent areas. Canadian Journal of Earth Sciences, 16: 913-938.

Christiansen, E.A. 1983. The Denholm landslide, Saskatchewan. Part 1: Geology. Canadian Geotechnical Journal, 20: 197-207.

Christiansen, E.A. 1992. Pleistocene stratigraphy of the Saskatoon area, Saskatchewan, Canada: an update. Canadian Journal of Earth Sciences, 29: 1767-1778.

Christiansen, E.A., and Sauer, E.K. 1984. Landslide Styles in the Saskatchewan Rivers Plain: Proceedings, 37th Canadian Geotechnical Conference, Toronto, Ont.: 35-48.

Christiansen, E.A., and Sauer, E.K. 1993. Red Deer Hill: a drumlinized, glaciotectonic feature near Prince Albert, Saskatchewan, Canada. Canadian Journal of Earth Sciences, 30: 1224-1235.

Christiansen, E.A., Sauer, E.K., and Schreiner, B.T. 1995. Glacial Lake Saskatchewan and Lake Agassiz deltas in east-central Saskatchewan with special emphasis on the Nipawin delta. Canadian Journal of Earth Sciences, 32: 334–348.

Christopher, J.E. 2003. Jura-Cretaceous Success Formation and Lower Cretaceous Mannville Group of Saskatchewan. Saskatchewan Industry Resources, Rep. 223, CD-ROM, 4-15.

Chursinoff, R.W. 1980. Measured ground movement by precise survey. M.Sc. Thesis, University of Saskatchewan, Saskatoon, Saskatchewan.

Clifton, A.W, Krahn, J. and Fredlund, D.G. 1981. Riverbank instability and development control in Saskatoon (Canada). Canadian Geotechnical Journal 18 (1): 95-105.

Clifton, A. W., Yoshida, Richard T., and Chursinoff, Roy W. 1986. Regina Beach - A Town on a Landslide. Canadian Geotechnical Journal 23 (1): 60-68.

Clifton Associates Ltd. 2005. Landslide Investigation of Slide Near Prince Albert Penitentiary, C.S. 302-02, West of Prince Albert.

Cruden, D. M., and Varnes, D. J. 1996. “Landslides types and processes.” Landslides: Investigation and mitigation, Transportation Research Board. National Academy of Sciences, Washington, D.C.: 36–75.

DGSI. 2006. Slope Inclinometer Manual. Slope Indicator a division of Durham Geo-Enterprises, Mukilteo, Washington, USA. URL <http://www.slopeindicator.com/>, [December 13, 2008].

DGSI. 2008a. Slope Inclinometer Technical Support. Tech Note. Slope Indicator a division of Durham Geo-Enterprises, Mukilteo, Washington, USA. URL <http://www.slopeindicator.com/support/inclinometers/technote-inclin-accuracy.html>, [December 13, 2008].

DGSI. 2008b. In-Place Inclinometer Manual. DGSI a division of Durham Geo-Enterprises, Mukilteo, Washington, USA. URL <http://www.slopeindicator.com/>, [December 13, 2008].

DGSI. 2008c. Vibrating Wire Piezometer Manual. DGSI a division of Durham Geo-Enterprises, Mukilteo, Washington, USA. URL <http://www.slopeindicator.com/>, [December 13, 2008].

DGSI. 2009. Casing Installation Guide. DGSI a division of Durham Geo-Enterprises, Mukilteo, Washington, USA. URL <http://www.slopeindicator.com/>, [February 13, 2011].

Dunnicliff, J. 1993. Geotechnical instrumentation for monitoring field performance, Wiley, New York.

Dunnicliff, J. 2002. Geotechnical Instrumentation News. Geotechnical News (2): 26-28.

Dunnicliff, John and Mikkelsen, P. Erik. 2000. Overcoming buoyancy during installation of inclinometer casing. Geotechnical News 18 (3): 19-19.

Eckel, B.F., Sauer E. Karl, and Christiansen, E.A. 1987. Petrofka Landslide, Saskatchewan. Canadian Geotechnical Journal 24 (1): 81-99.

Fenton, M.M., Schreiner, B.T., Nielsen, E., and Pawlowicz, J.G. 1994. Quaternary Geology of the Western Plains. In G.D. Mossop and I. Shetson (comp.) *Geological Atlas of the Western Canada Sedimentary Basin*, , Canadian Society of Petroleum Geologists and Alberta Research Council, URL <http://www.ags.gov.ab.ca/publications/wcsb_atlas/atlas.html>, [December 13, 2008].

Flentje, P., Chowdhury, R.N., Tobin, P. and Brizga, V. 2005. Towards Real-Time Landslide Risk Management in an Urban Area. Landslide Risk Management, Proceedings of the

International Conference on Landslide Risk Management 18th Annual Vancouver Geotechnical Society Symposium, 31 May - 4 June 2005: 741-751.

Fung, K., Barry, B., and Wilson, M. (Editors). 1999. Atlas of Saskatchewan. University of Saskatchewan: Saskatoon.

Geokon Inc. 2008a. IPI6300 Vibrating Wire In-Place Inclinometer Information Sheet. Geokon Inc, Lebanon, New Hampshire, USA. URL <http://www.geokon.com/>, [December 13, 2008].

Geokon Inc. 2008b. IPI6150 MEMS In-Place Inclinometer Information Sheet. Geokon Inc, Lebanon, New Hampshire, USA. URL <http://www.geokon.com/>, [December 13, 2008].

Haug M.D., Sauer, E.K., and Fredlund. , D.G. 1977. Retrogressive slope failures at Beaver Creek, south of Saskatoon, Saskatchewan, Canada. Canadian Geotechnical Journal, 14: 288-301.

Hayes, B.J.R., Christopher, J.E., Rosenthal, L., Los, G., McKercher, B., Minken, D., Tremblay, Y.M., and Fennel, J. 1994. Chapter 19: Cretaceous Mannville Group. In G.D. Mossop and I. Shetson (comp.) *Geological Atlas of the Western Canada Sedimentary Basin*, , Canadian Society of Petroleum Geologists and Alberta Research Council, URL <http://www.ags.gov.ab.ca/publications/wcsb_atlas/atlas.html>, [December 13, 2008].

Hodge, Robert A. and Freeze, Allan R. 1977. Groundwater flow systems and slope stability. Canadian Geotechnical Journal, 14: 466-476.

ISRM. 1981. ISRM, Rock Characterization Testing and Monitoring, ISRM Suggested Methods. , International Society for Rock Mechanics (1981).

Johnson, Brian K. 2002. An application for a single-sensor in-place inclinometer. Geotechnical News (2): 27-29.

Kelly, A.J., Sauer, E.K., Christiansen, E.A., Barbour, S.L., and Widger, R.A. 1995. Deformation of the Deer Creek bridge by an active landslide in clay shale. Canadian Geotechnical Journal, 32: 701–724.

Kelly, A.J., Clifton, A.W., Antunes, P.J., Widger, R.A. 2004. Application of a Landslide Risk Management System to the Saskatchewan Highway Network. Proc. 57th Geotechnical Conference, Quebec City.

Kelly, A.J., Antunes, P.J., Vu, H.Q., Clifton, A.W., Widger, R.A., King, G.L. 2005a. Retrogressive Landslide Near Prince Albert, Saskatchewan: A Case History. Proc. 58th Geotechnical Conference, Saskatoon.

Kelly, A.J., Antunes, P.J., Vu, H.Q., Clifton, A.W., Widger, R.A., King, G.L. 2005b. Analysis of Multiple Landslide Blocks on a Highway Crossing of the Frenchman River Valley, Saskatchewan. Proc. 58th Geotechnical Conference, Saskatoon.

Krahn, J., Johnson, R.F., Fredlund, D.G., and Clifton, A.W. 1979. A highway cut failure in Cretaceous sediments at Maymont, Saskatchewan. Canadian Geotechnical Journal, 16: 703-715.

MacDonald, A.B. and Sauer, E.K. 1970. The engineering significance of Pleistocene stratigraphy in the Saskatoon area, Saskatchewan, Canada. Canadian Geotechnical Journal, 7: 116-126.

Millard, M.J. 1990. Geology and Groundwater Resources of the Prince Albert Area (73H), Saskatchewan. Resources Division, Limited Report, SRC Publication No. R-1210-8-E-90.

Mikkelsen, P.E. 1996. Chapter 11, Field Instrumentation. In A.K. Turner and R.L. Schuster (eds.), *Landslides, Investigation and Mitigation, Special Report 247*: 278-316. Washington, D.C.: Transportation Research Board, National Research Council.

Mikkelsen, P. E. 2003. Advances in inclinometer data analysis. Proc., 6th Int. Symp. on Field Measurements in Geomechanics, Oslo, Norway, 555–567.

Mikkelsen, P.E. and Wilson S.D. 1983. Field Instrumentation: Accuracy, Performance, Automation and Procurement. In K. Kovari (ed), *Proceedings of the International Symposium on Field Measurements in Geomechanics,* Vol. 1, Zurich: 251-272. Rotterdam: Balkema.

Mikkelsen, P. E. and Green, G.E. 2003. Piezometers in fully grouted boreholes. Proc., 6th Int. Symp. on Field Measurements in Geomechanics, Oslo, Norway, 545–554.

Misfeldt, G.A., Sauer, E.K., and Christiansen, E.A. 1991. The Hepburn Landslide: an Interactive Slope-Stability and Seepage Analysis. Canadian Geotechnical Journal, 28: 556–73.

Pauls, G.J, Sauer, E.K., Christiansen, E.A., and Widger, R.A. 1999. A Transient Analysis of Slope Stability Following Drawdown After Flooding of a Highly Plastic Clay. Canadian Geotechnical Journal 36 (6): 1151-1171.

Picarelli, L., Urciuoli, G., and Russo, C. 2004. Effect of groundwater regime on the behaviour of clayey slopes. Canadian Geotechnical Journal, 41: 467-484

RocTest Ltd. 2008. Little Dipper In-place inclinometer Information Sheet. RocTest Ltd. St. Lambert, Quebec, Canada. URL <http://www.roctest.com/>, [December 13, 2008].

RST Instruments Ltd. 2008. Digital MEMS Inclinometer Information Sheet. RST Instruments Ltd. URL <http://www.rstinstruments.com/>, [December 13, 2008].

Sauer, E.K. 1974. Geotechnical Implications of Pleistocene Deposits in Southern Saskatchewan. Canadian Geotechnical Journal, 11: 359-373.

Sauer, E.K. 1978. The engineering significance of glacier ice-thrusting. Canadian Geotechnical Journal, 15: 457-472.

Sauer, E.K. 1983. The Denholm landslide, Saskatchewan, Part II: analysis. Canadian Geotechnical Journal, 20: 208-220.

Sauer, E.K., and Christiansen, E.A. 1991. Preconsolidation pressures in the Battleford Formation, southern Saskatchewan, Canada. Canadian Journal of Earth Sciences, 28: 1613-1623.

Simeioni, L. and Mongiovi, L. 2007. Inclinometer Monitoring of the Castelrotto Landslide in Italy. Journal of Geotechnical and Geoenvironmental Engineering ASCE 133 (6): 653-666.

Stauffer, M.R., Gendzwill, D.J., and Sauer, E.K. 1990. Ice-thrust features and the Maymont landslide in the North Saskatchewan River valley. Canadian Journal of Earth Sciences, (27): 229-242.

Thomson, S., and Hayley, D.W. 1975. The Little Smokey landslide. Canadian Geotechnical Journal, 12: 379-392.

Thomson, S. and Tweedie, R.W. 1978. Edgerton Landslide. Canadian Geotechnical Journal 15 (4): 510-521.

Whitaker, S.H. and Christiansen, E.A. 1972. The Empress Group in Southern Saskatchewan. Canadian Journal of Earth Sciences, 9: 353-360.

Wieczorek, G.F. 1996. "Landslides Triggering Mechanisms." Landslides: Investigation and mitigation, Transportation Research Board. National Academy of Sciences, Washington, D.C.: 36–75.

Wilson, S.D. and Mikkelsen, P.E. 1978. Chapter 5, Field Instrumentation. In R.L. Schuster and R.J. Krizek (eds.), *Landslides: Analysis and Control, Special Report176*: 112-138. Washington, D.C.: Transportation Research Board, National Research Council.

Yoshida, R.T., and Krahn, J. 1985. Movement and stability analysis of the Beaver Creek landslide, Saskatchewan, Canada. Canadian Geotechnical Journal, 22: 277-285.

APPENDIX A – PROGRESSION OF FAILURE

Figure A. 1: Highway No. 302 looking west, August 2005, landslide intersecting the highway near the red sign (Photograph courtesy of Saskatchewan Ministry of Highways and Infrastructure.

Figure A. 2: Blocks indicative of a multiple retrogressive landslide, notice Highway No. 302 in the background, Fall 2005 (from Antunes et al. 2006).

Figure A. 3: Highway No. 302 looking west Spring 2006, highway converted to gravel for maintenance purposes (Photograph courtesy of the Saskatchewan Ministry of Highways and Infrastructure).

Figure A. 4: Development of main scarp June 2006 (Photograph courtesy of the Saskatchewan Ministry of Highways and Infrastructure).

Figure A. 5: Grading of scarp and continued maintenance of roadway to protect public as highway was still in use (Photograph courtesy of the Saskatchewan Ministry of Highways and Infrastructure).

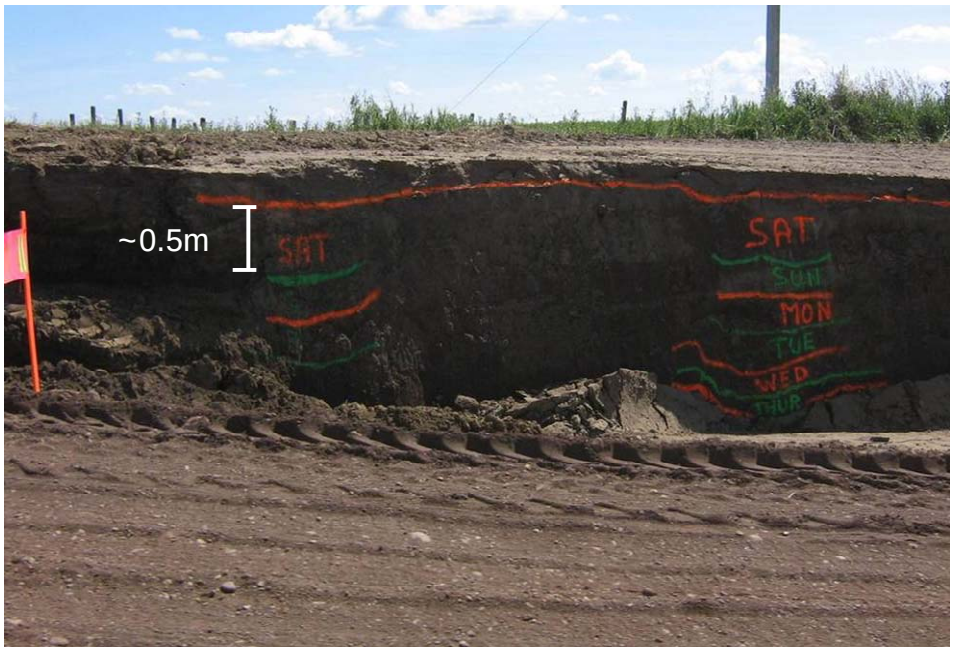

Figure A. 6: Movement at head scarp measured per day in mid-July 2006 (Photograph courtesy of the Saskatchewan Ministry of Highways and Infrastructure).

Figure A. 7: Slope at the end of June 2007 (Photograph by Chad Salewich).

Figure A. 8: Slope in mid-October 2007 (Photograph by Chad Salewich).

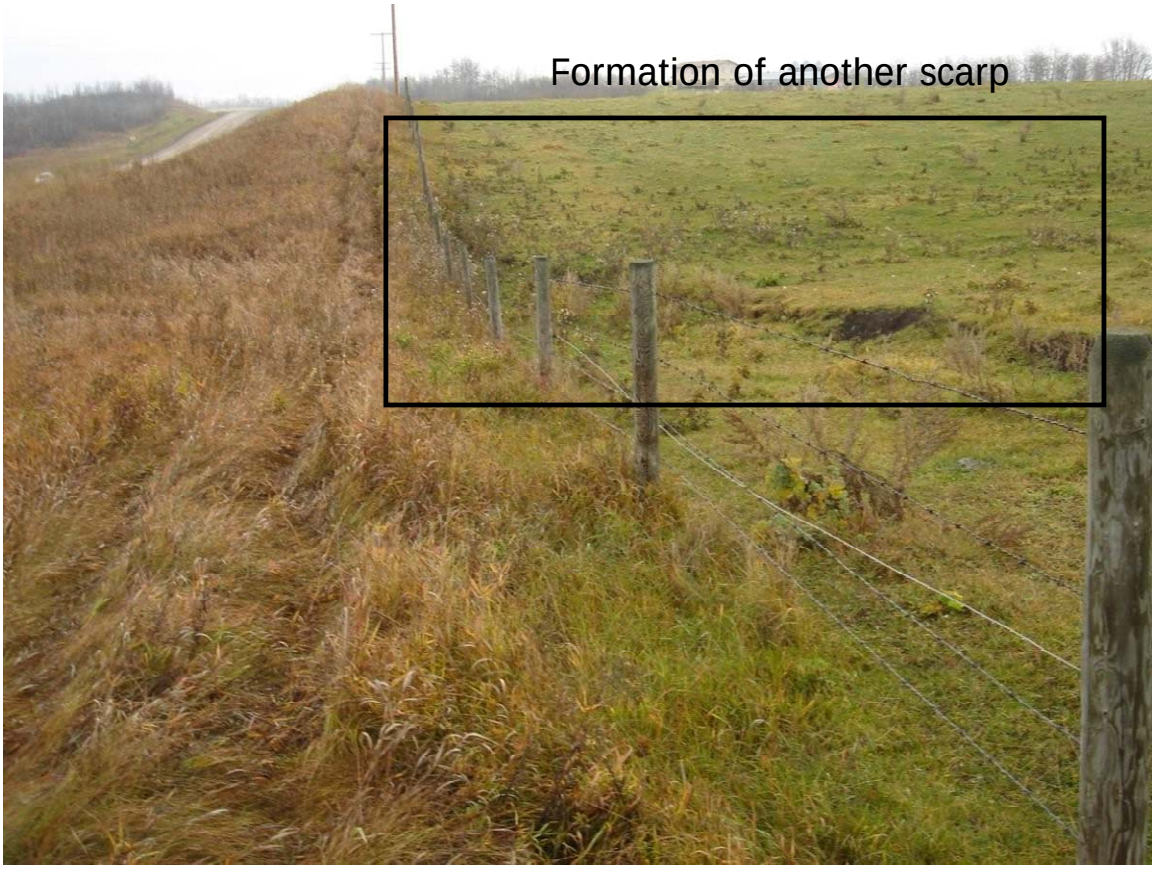

Figure A. 9: Formation of a new scarp now entering a rancher's field mid-October 2007 (Photograph by Chad Salewich).

APPENDIX B - BOREHOLE LOGS

SHT 73-H/4 2002

101

LANDSLIDE 302-02

13: 5891917.493N/441815.879E (NAD83)

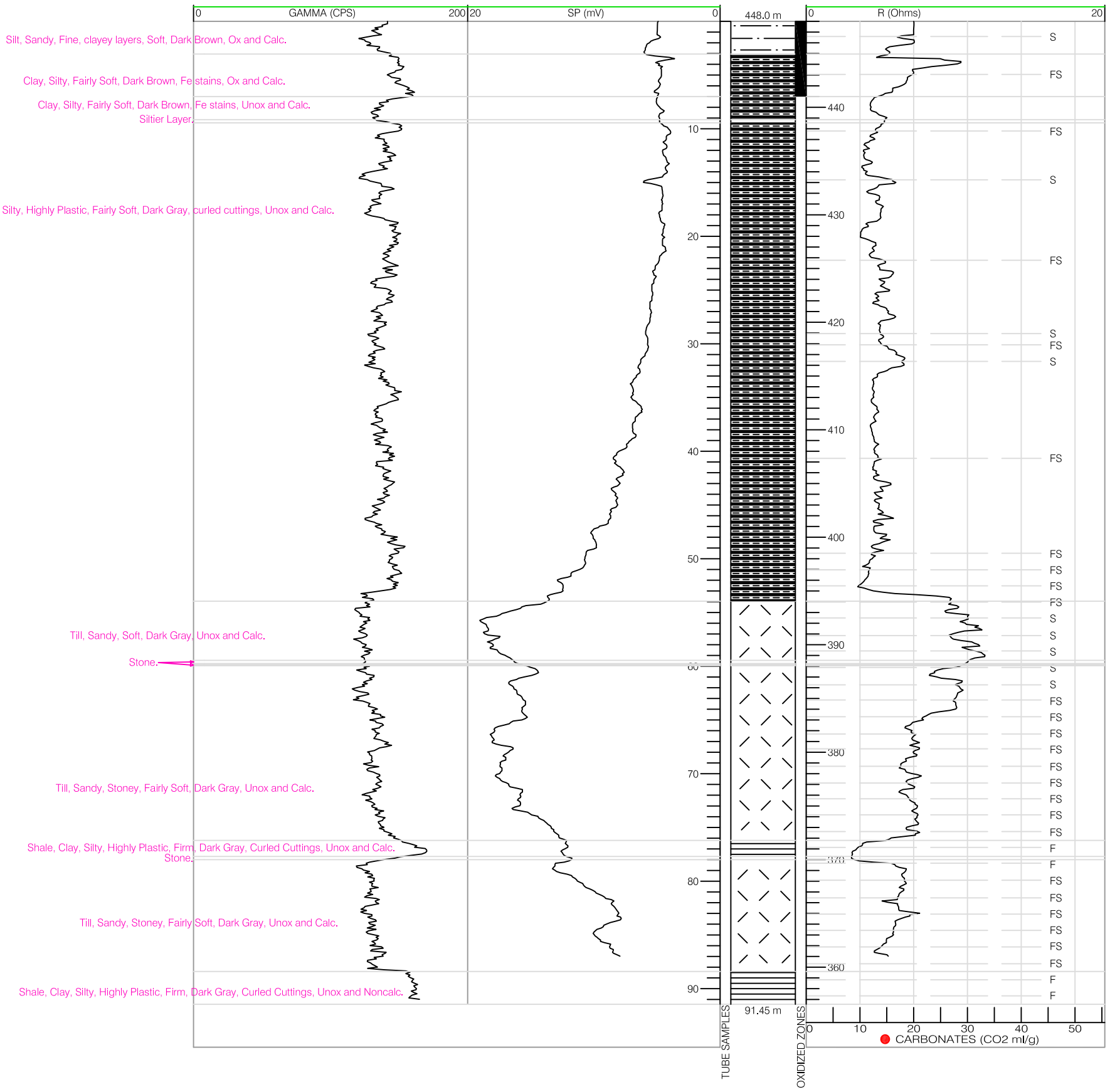

Highways and Transportation	DRILLED BY: M. MINCHUK	LOGGED BY: L. SINCLAIR	GAMMA SCALE (CPS): 0-200	**SHT LANDSLIDE 302-02 BOREHOLE 101**				
	DRILL START: 2002/10/21	DRILL END: 2002/10/22	SP SCALE (mV): 0-20					
	COND. WATER: 1100 µsiemens/cm	S.G. MUD: ----	R SCALE (Ohms): 0-20	ABANDONMENT: GROUTED		2002	UTM: 13: 5891917.493N/441815.879E (NAD83)	
GEOLOGY BY:	COND. MUD: 1600	C.S. 302-02	CALIPER SCALE (In): N/A	DRAWN BY: WEISGERBER	DATE: 2002/11/08	NTS 73-H/4		SCALE 1:500

ACAD DWG: \\SASKATOON\GROUP\ESD\GEOTECH\PROJECTS\LANDSLIDE_302-02\LOGS\LOG101.DWG LAST REV DATE: 2007/04/18

SHT 73-H/4 2002

SI1

LANDSLIDE 302-02

13: 5891940.700N/441775.402E (NAD83)

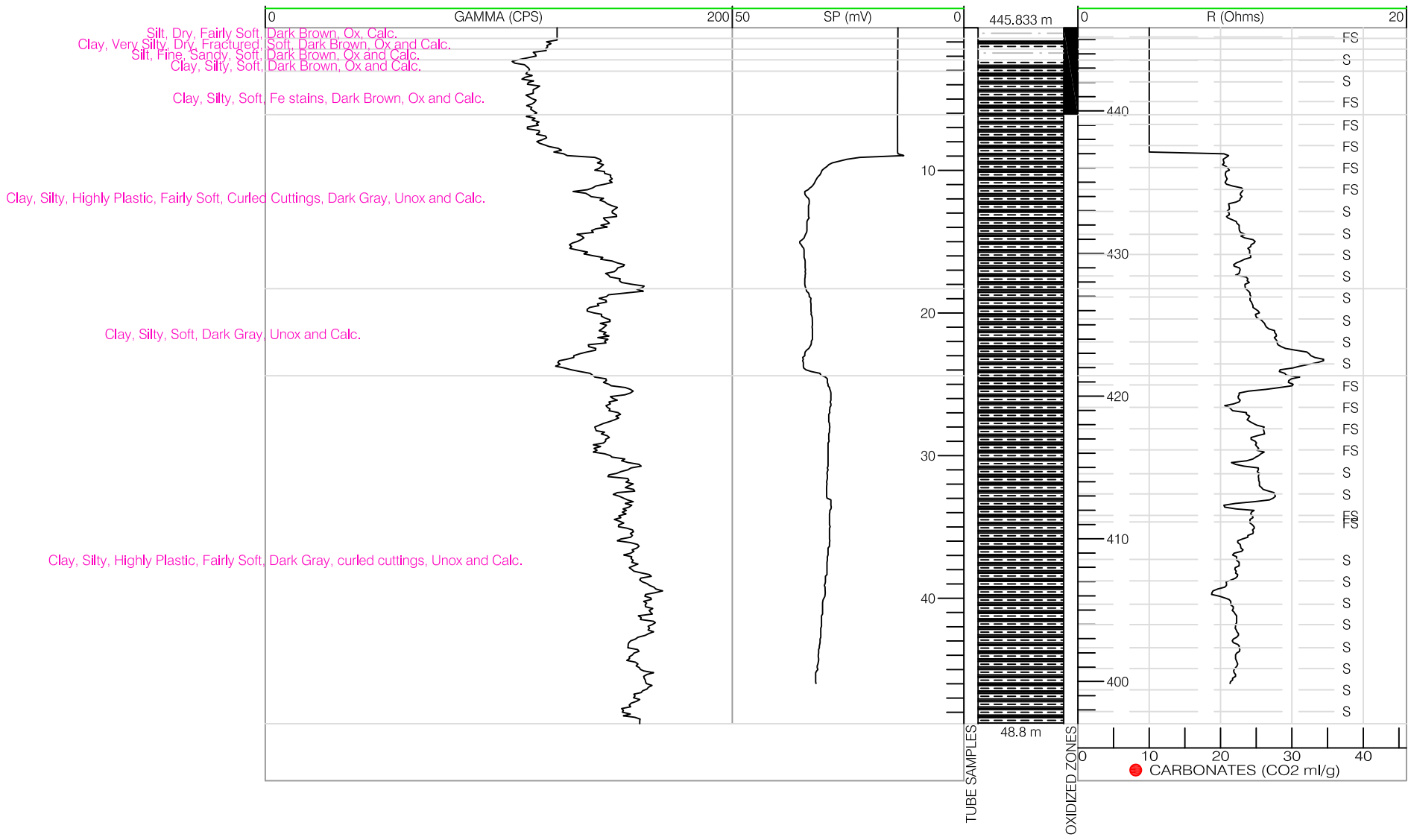

Highways and Transportation	DRILLED BY: M. MINCHUK	LOGGED BY: L. SINCLAIR	GAMMA SCALE (CPS): 0-200	SHT LANDSLIDE 302-02 BOREHOLE SI1				
	DRILL START: 2002/10/15	DRILL END: 2002/10/16	SP SCALE (mV): 0-50					
	COND. WATER: 1100 µsiemens/cm	S.G. MUD: ----	R SCALE (Ohms): 0-20	ABANDONMENT: S.I. INSTALLED	2002	UTM: 13: 5891940.700N/441775.402E (NAD83)		
GEOLOGY BY:	COND. MUD: 1500	C.S. 302-02	CALIPER SCALE (In): N/A	DRAWN BY: WEISGERBER	DATE: 2002/11/08	NTS 73-H/4		SCALE 1:500

130

ACAD DWG: \\SASKATOON\GROUP\ESD\GEOTECH\PROJECTS\LANDSLIDE_302-02\LOGS\LOGSI1.DWG LAST REV DATE: 2007/04/18

SHT 73-H/4 2004

SI2

PA PEN LANDSLIDE

13: 5891919.311N/441577.937E (NAD83)

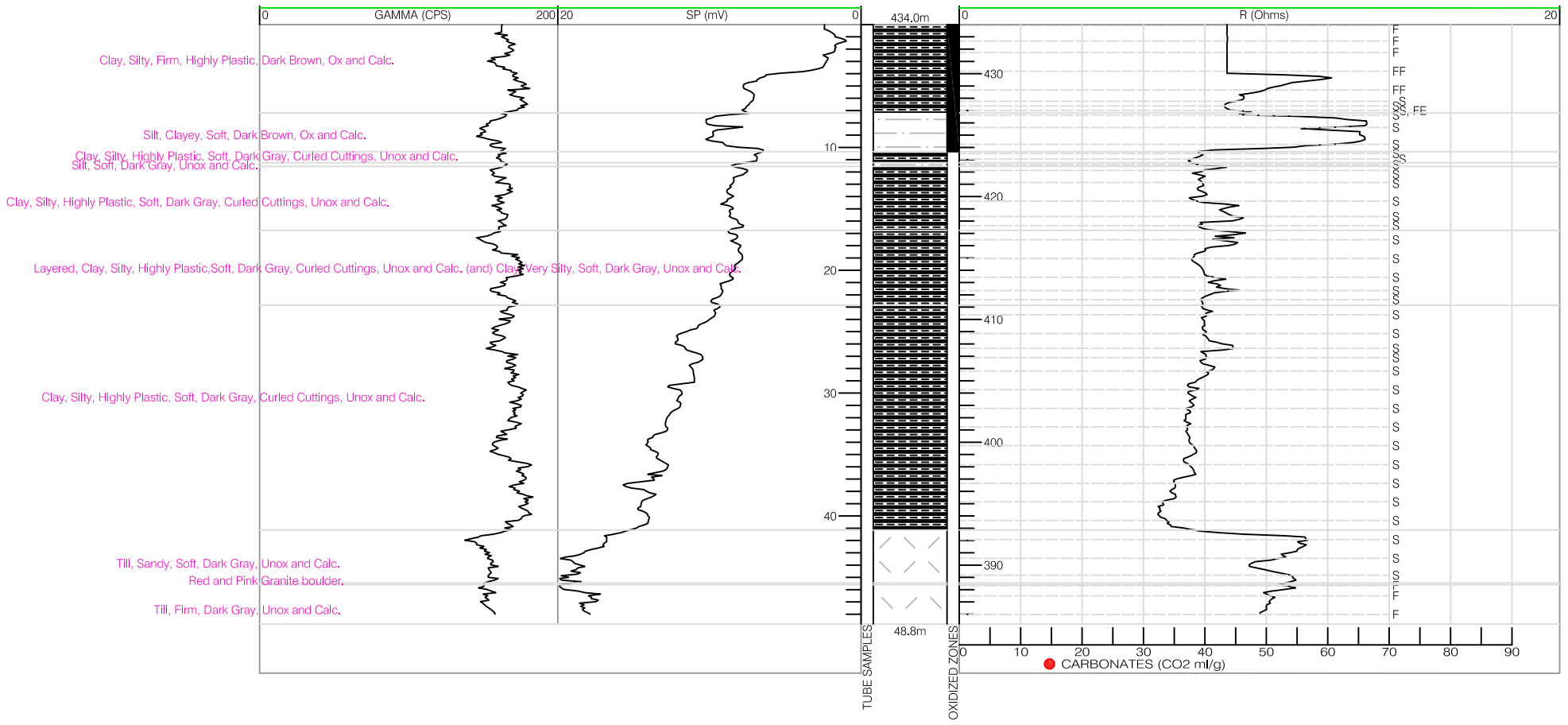

Highways and Transportation	DRILLED BY: M. MINCHUK	LOGGED BY: L. SINCLAIR	GAMMA SCALE (CPS): 0-200	SHT PA PEN LANDSLIDE BOREHOLE S.I.2				
	DRILL START: 2004/05/25	DRILL END: 2004/05/26	SP SCALE (mV): 0-20					
	COND. WATER: 500 µsiemens/cm	S.G. MUD: ----	R SCALE (Ohms): 0-20	ABANDONMENT: S.I. INSTALLED	2004	UTM: 13: 5891919.311N/441577.937E (NAD 83)		
GEOLOGY BY:	COND. MUD: 800	C.S. 302-02	CALIPER SCALE (In): 131	DRAWN BY: B. THOMPSON	DATE: 2004/06/22	NTS 73-H/4		SCALE 1:500

ACAD DWG: \\SASKATOON\GROUP\ESD\GEOTECH\PROJECTS\PA_PEN_LANDSLIDE_302-02\LOGS\LOGSI2.DWG LAST REV DATE: 2007/04/18

SHT 2005

SI #3

PA Penitentiary Landslide

13: N/E (NAD83)

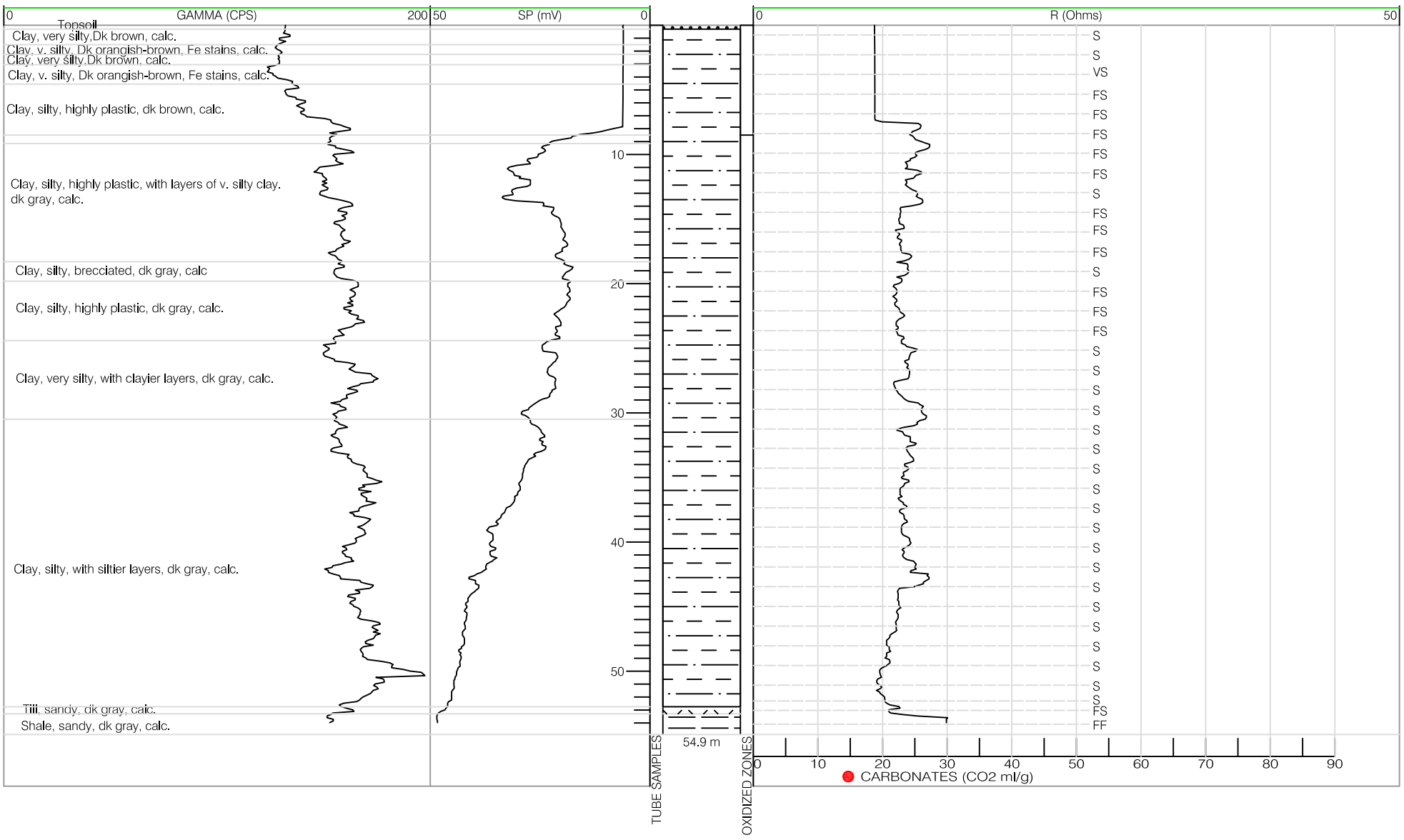

Highways and Transportation	DRILLED BY: M. MINCHUK	LOGGED BY: L. SINCLAIR	GAMMA SCALE (CPS): 0-200	PA Penitentiary landslide SI #3				
	DRILL START: 2005/07/25	DRILL END: 2005/07/26	SP SCALE (mV): 0-50					
	COND. WATER: n/a µsiemens/cm	S.G. GROUT: 1.36	R SCALE (Ohms): 0-50	ABANDONMENT: S.I. Installed		2005	UTM: 13: N/E (NAD83)	
GEOLOGY BY: n/a	COND. MUD: n/a	C.S. 302-02	CALIPER SCALE (In): n/a	DRAWN BY: J. BALL	DATE: 2005/11/01	NTS n/a	n/a	SCALE 1:500

ACAD DWG: \\SASKATOON\GROUP\ESD\GEOTECH\PROJECTS\project-name-here\LOGS\LOG#.DWG

LAST REV DATE: 2005/11/01

SHT 2006

401

PA_PEN_LANDSLIDE

13: N/E (NAD83)

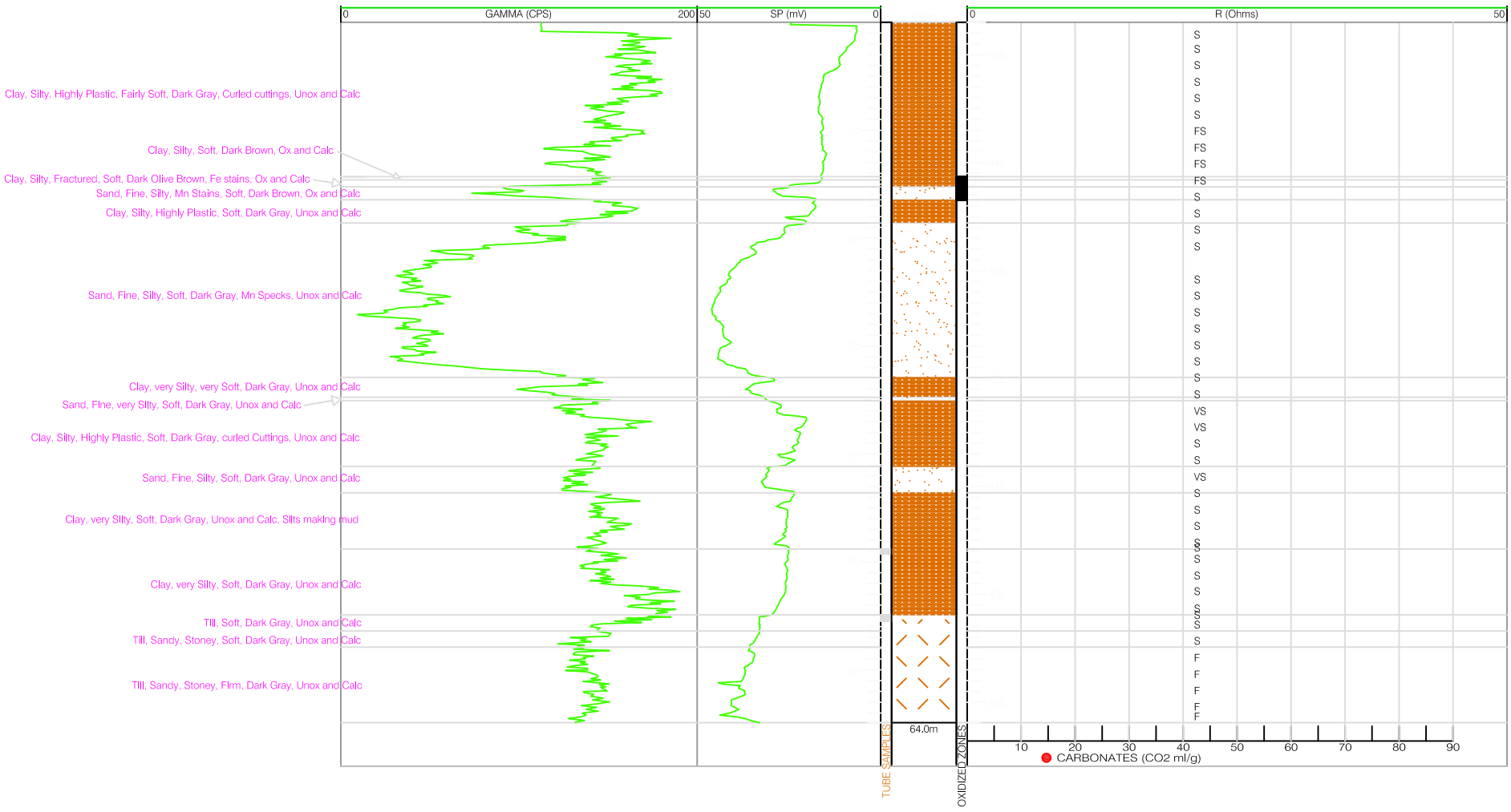

Highways and Transportation	DRILLED BY: M. MINCHUK	LOGGED BY: L. SINCLAIR	GAMMA SCALE (CPS): 0-200	**SHT PA PEN LANDSLIDE BOREHOLE 401**				
	DRILL START: 2006/08/21	DRILL END: 2006/08/23	SP SCALE (mV): 0-50					
	COND. WATER: 1000 µsiemens/cm	S.G. GROUT:	R SCALE (Ohms): 0-50	ABANDONMENT: Vibrating Wire Piezometer Installed	2006	UTM: 13: 5892071.0N/441904.0E (NAD83)		
GEOLOGY BY:	COND. MUD: 1400	C.S. 302-02	CALIPER SCALE (In):	DRAWN BY: J.OSBACK	DATE: 2006/09/08	NTS		SCALE 1:500

ACAD DWG: \\SASKATOON\GROUP\ESD\GEOTECH\PROJECTS\project-name-here\LOGS\LOG#.DWG LAST REV DATE: 2005/

SHT 2007

BH 402

PA PEN LANDSLIDE

13: 5891348.0N/441863.0E (NAD83)

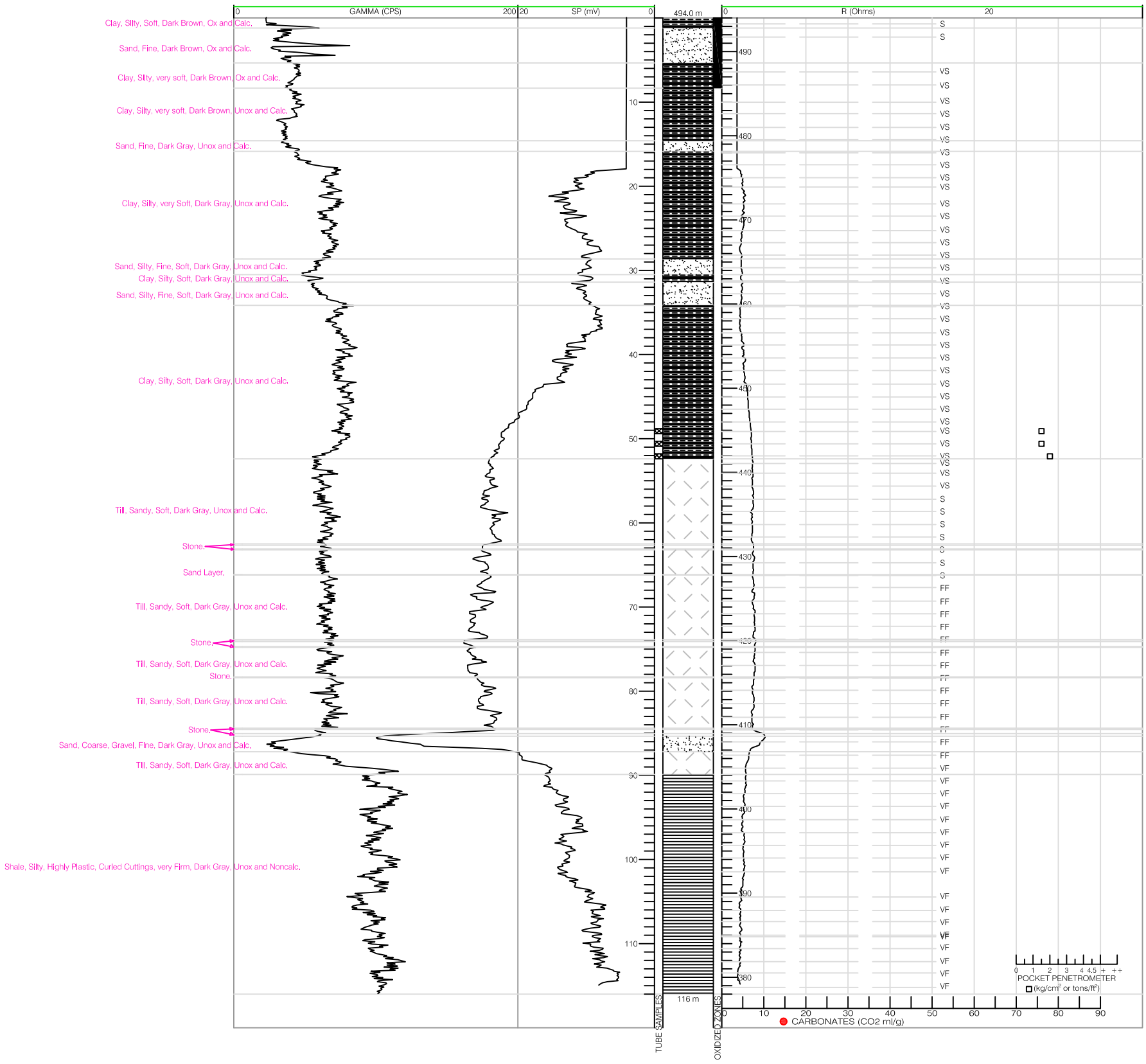

Highways and Transportation	DRILLED BY: M. MINCHUK	LOGGED BY: L. SINCLAIR	GAMMA SCALE (CPS): 0-200	SHT PA PEN LANDSLIDE BOREHOLE 402			
	DRILL START: 2007/03/22	DRILL END: 2007/03/19	SP SCALE (mV): 0-20				
	COND. WATER: 600 µsiemens/cm	S.G. GROUT:	R SCALE (Ohms): 0-20	ABANDONMENT: GROUTED	2007	UTM: 13: 5891348.0N/441863.0E (NAD83)	
GEOLOGY BY:	COND. MUD: 1225	C.S. 302-02	CALIPER SCALE (In): 1.25-18	DRAWN BY: J. OSBACK	DATE: 2007/04/17	NTS	SCALE 1:500

ACAD DWG: \\SASKATOON\GROUP\ESD\GEOTECH\PROJECTS\PA PEN LANDSLIDE\LOGS\BH 402.DWG

LAST REV DATE: 2007/04/18

APPENDIX C - SLOPE INCLINOMETER PLOTS

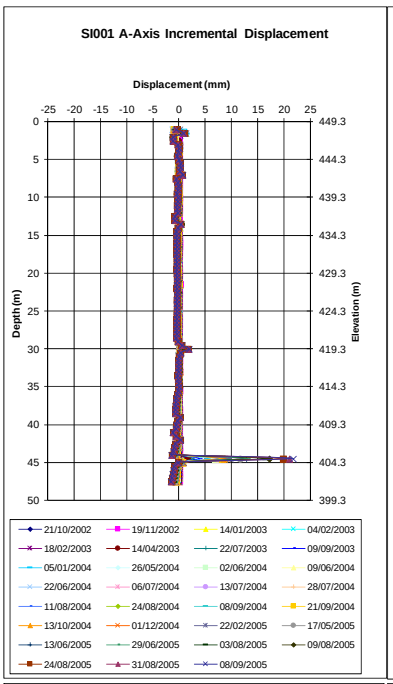
SI001 A-Axis Incremental Displacement
Displacement (mm)
Depth (m)
Elevation (m)
21/10/2002 19/11/2002 14/01/2003 04/02/2003
18/02/2003 14/04/2003 22/07/2003 09/09/2003
05/01/2004 26/05/2004 02/06/2004 09/06/2004
22/06/2004 06/07/2004 13/07/2004 28/07/2004
11/08/2004 24/08/2004 08/09/2004 21/09/2004
13/10/2004 01/12/2004 22/02/2005 17/05/2005
13/06/2005 29/06/2005 03/08/2005 09/08/2005
24/08/2005 31/08/2005 08/09/2005

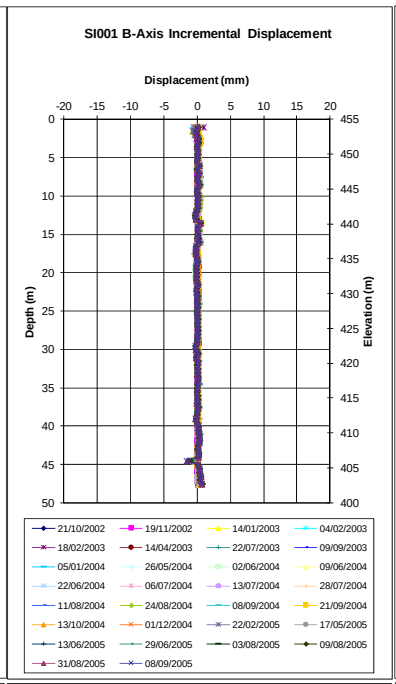
SI001 B-Axis Incremental Displacement
Displacement (mm)
Depth (m)
Elevation (m)
21/10/2002 19/11/2002 14/01/2003 04/02/2003
18/02/2003 14/04/2003 22/07/2003 09/09/2003
05/01/2004 26/05/2004 02/06/2004 09/06/2004
22/06/2004 06/07/2004 13/07/2004 28/07/2004
11/08/2004 24/08/2004 08/09/2004 21/09/2004
13/10/2004 01/12/2004 22/02/2005 17/05/2005
13/06/2005 29/06/2005 03/08/2005 09/08/2005
31/08/2005 08/09/2005

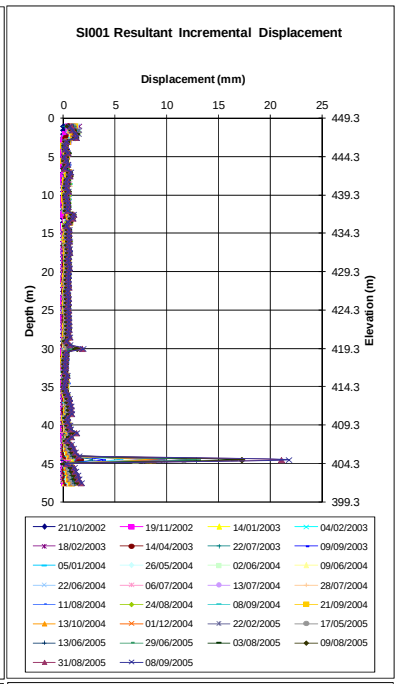
SI001 Resultant Incremental Displacement
Displacement (mm)
Depth (m)
Elevation (m)
21/10/2002 19/11/2002 14/01/2003 04/02/2003
18/02/2003 14/04/2003 22/07/2003 09/09/2003
05/01/2004 26/05/2004 02/06/2004 09/06/2004
22/06/2004 06/07/2004 13/07/2004 28/07/2004
11/08/2004 24/08/2004 08/09/2004 21/09/2004
13/10/2004 01/12/2004 22/02/2005 17/05/2005
13/06/2005 29/06/2005 03/08/2005 09/08/2005
31/08/2005 08/09/2005

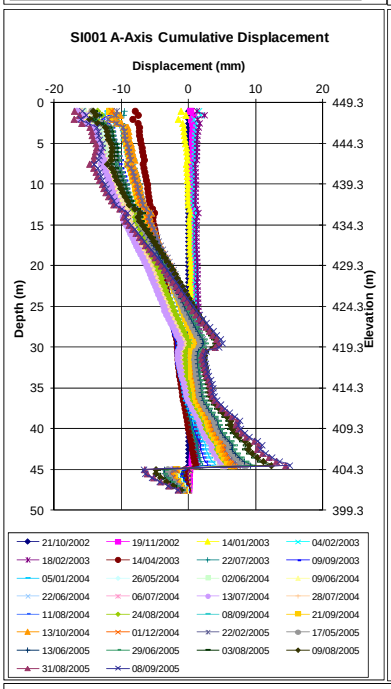
SI001 A-Axis Cumulative Displacement
Displacement (mm)
Depth (m)
Elevation (m)
21/10/2002 19/11/2002 14/01/2003 04/02/2003
18/02/2003 14/04/2003 22/07/2003 09/09/2003
05/01/2004 26/05/2004 02/06/2004 09/06/2004
22/06/2004 06/07/2004 13/07/2004 28/07/2004
11/08/2004 24/08/2004 08/09/2004 21/09/2004
13/10/2004 01/12/2004 22/02/2005 17/05/2005
13/06/2005 29/06/2005 03/08/2005 09/08/2005
31/08/2005 08/09/2005

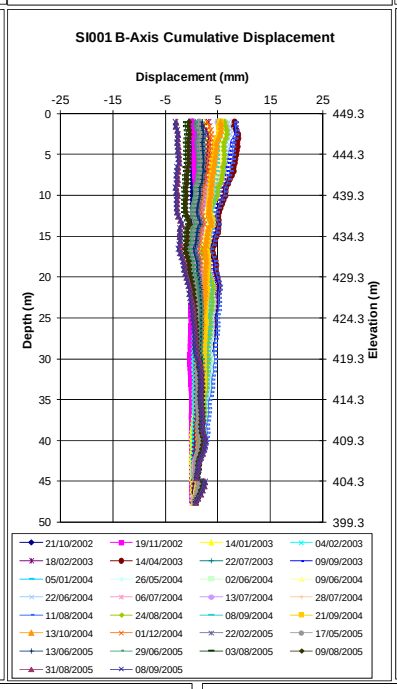
SI001 B-Axis Cumulative Displacement
Displacement (mm)
Depth (m)
Elevation (m)
21/10/2002 19/11/2002 14/01/2003 04/02/2003
18/02/2003 14/04/2003 22/07/2003 09/09/2003
05/01/2004 26/05/2004 02/06/2004 09/06/2004
22/06/2004 06/07/2004 13/07/2004 28/07/2004
11/08/2004 24/08/2004 08/09/2004 21/09/2004
13/10/2004 01/12/2004 22/02/2005 17/05/2005
13/06/2005 29/06/2005 03/08/2005 09/08/2005
31/08/2005 08/09/2005

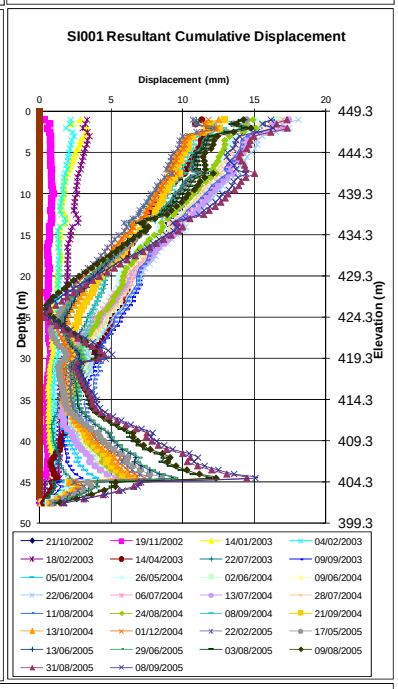
SI001 Resultant Cumulative Displacement
Displacement (mm)
Depth (m)
Elevation (m)
21/10/2002 19/11/2002 14/01/2003 04/02/2003
18/02/2003 14/04/2003 22/07/2003 09/09/2003
05/01/2004 26/05/2004 02/06/2004 09/06/2004
22/06/2004 06/07/2004 13/07/2004 28/07/2004
11/08/2004 24/08/2004 08/09/2004 21/09/2004
13/10/2004 01/12/2004 22/02/2005 17/05/2005
13/06/2005 29/06/2005 03/08/2005 09/08/2005
31/08/2005 08/09/2005

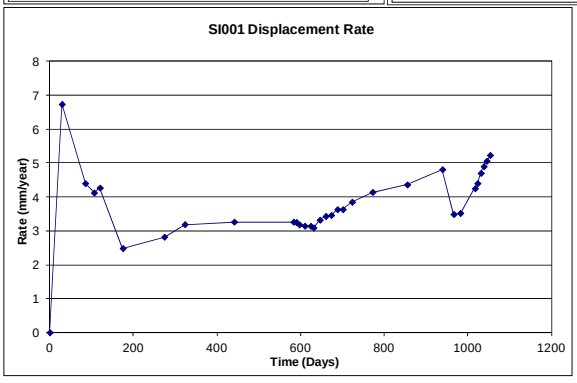
SI001 Displacement Rate
Rate (mm/year)
Time (Days)

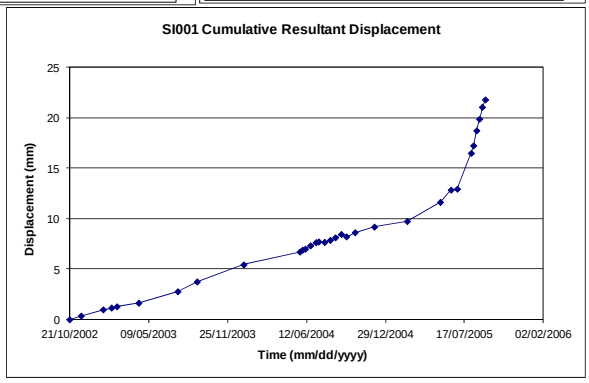
SI001 Cumulative Resultant Displacement
Displacement (mm)
Time (mm/dd/yyyy)
21/10/2002
09/05/2003
25/11/2003
12/06/2004
29/12/2004
17/07/2005
02/02/2006

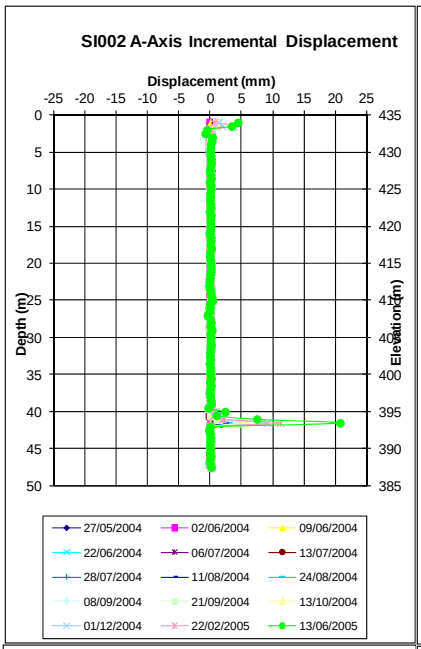
SI002 A-Axis Incremental Displacement
Displacement (mm)
Depth (m)
Elevation (m)
27/05/2004
02/06/2004
09/06/2004
22/06/2004
06/07/2004
13/07/2004
28/07/2004
11/08/2004
24/08/2004
08/09/2004
21/09/2004
13/10/2004
01/12/2004
22/02/2005
13/06/2005

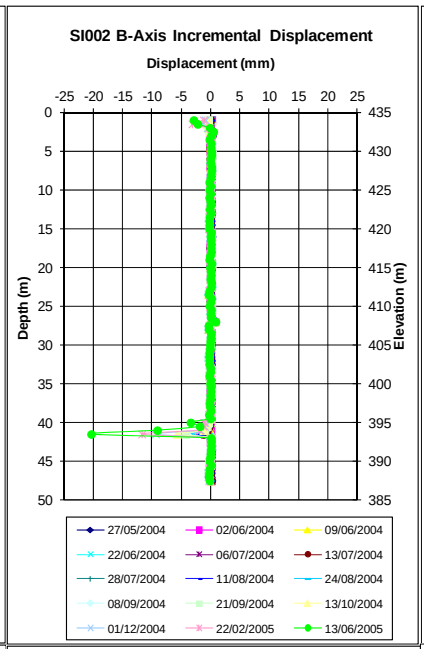
SI002 B-Axis Incremental Displacement
Displacement (mm)
Depth (m)
Elevation (m)
27/05/2004
02/06/2004
09/06/2004
22/06/2004
06/07/2004
13/07/2004
28/07/2004
11/08/2004
24/08/2004
08/09/2004
21/09/2004
13/10/2004
01/12/2004
22/02/2005
13/06/2005

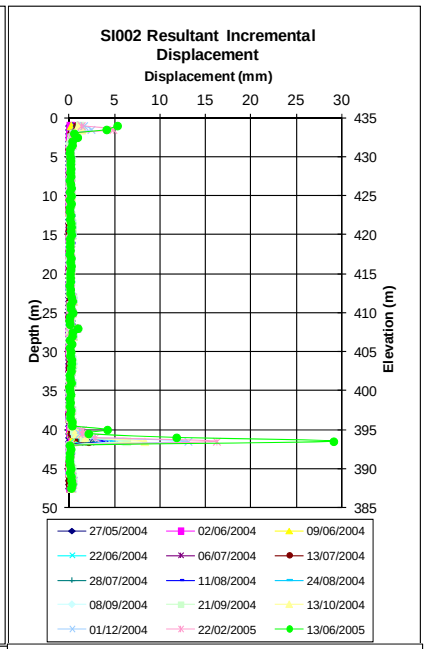
SI002 Resultant Incremental Displacement
Displacement (mm)
Depth (m)
Elevation (m)
27/05/2004
02/06/2004
09/06/2004
22/06/2004
06/07/2004
13/07/2004
28/07/2004
11/08/2004
24/08/2004
08/09/2004
21/09/2004
13/10/2004
01/12/2004
22/02/2005
13/06/2005

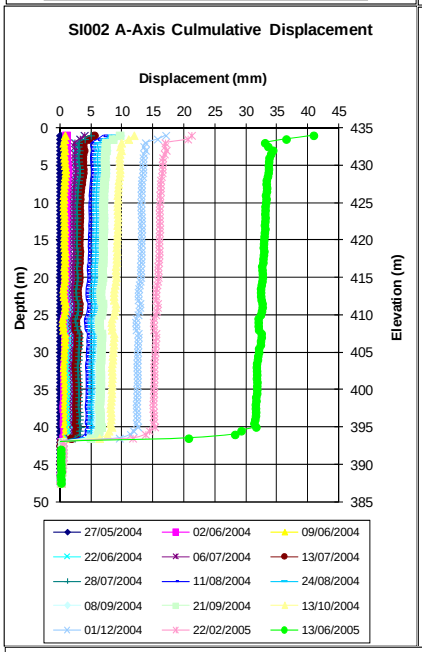
SI002 A-Axis Culmulative Displacement
Displacement (mm)
Depth (m)
Elevation (m)
27/05/2004
02/06/2004
09/06/2004
22/06/2004
06/07/2004
13/07/2004
28/07/2004
11/08/2004
24/08/2004
08/09/2004
21/09/2004
13/10/2004
01/12/2004
22/02/2005
13/06/2005

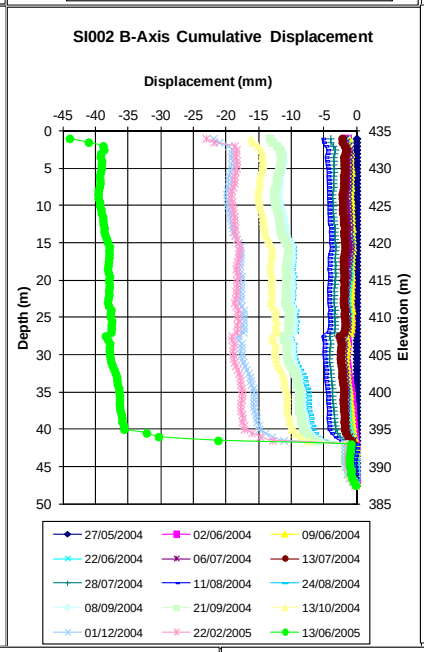
SI002 B-Axis Cumulative Displacement
Displacement (mm)
Depth (m)
Elevation (m)
27/05/2004
02/06/2004
09/06/2004
22/06/2004
06/07/2004
13/07/2004
28/07/2004
11/08/2004
24/08/2004
08/09/2004
21/09/2004
13/10/2004
01/12/2004
22/02/2005
13/06/2005

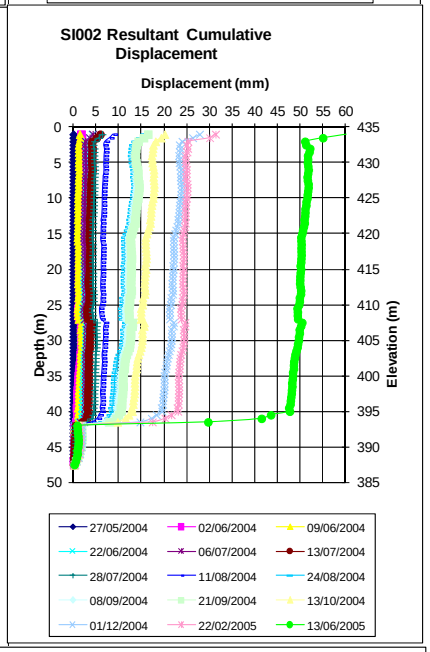
SI002 Resultant Cumulative Displacement
Displacement (mm)
Depth (m)
Elevation (m)
27/05/2004
02/06/2004
09/06/2004
22/06/2004
06/07/2004
13/07/2004
28/07/2004
11/08/2004
24/08/2004
08/09/2004
21/09/2004
13/10/2004
01/12/2004
22/02/2005
13/06/2005

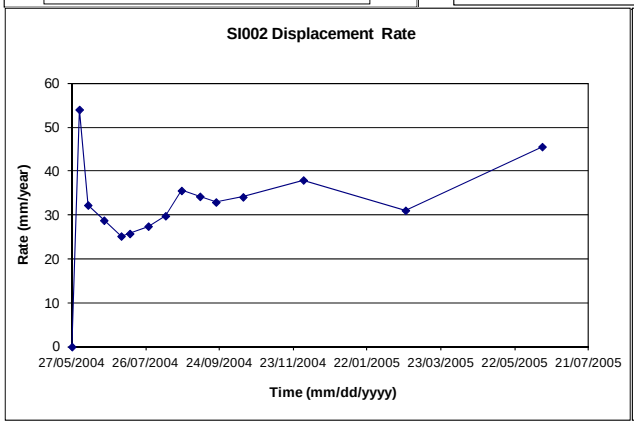
SI002 Displacement Rate
Rate (mm/year)
27/05/2004
26/07/2004
24/09/2004
23/11/2004
22/01/2005
23/03/2005
22/05/2005
21/07/2005
Time (mm/dd/yyyy)

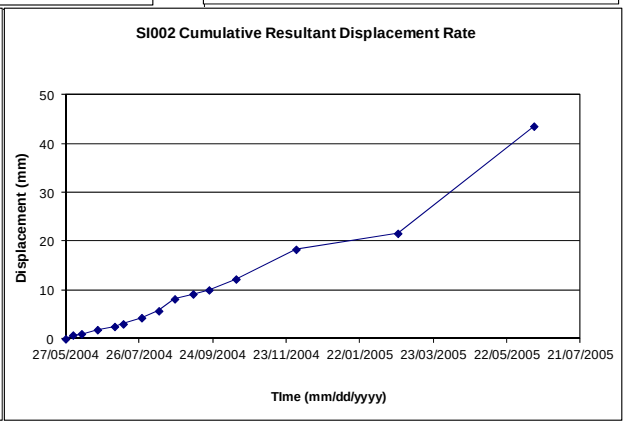
SI002 Cumulative Resultant Displacement Rate
Displacement (mm)
27/05/2004
26/07/2004
24/09/2004
23/11/2004
22/01/2005
23/03/2005
22/05/2005
21/07/2005
Time (mm/dd/yyyy)

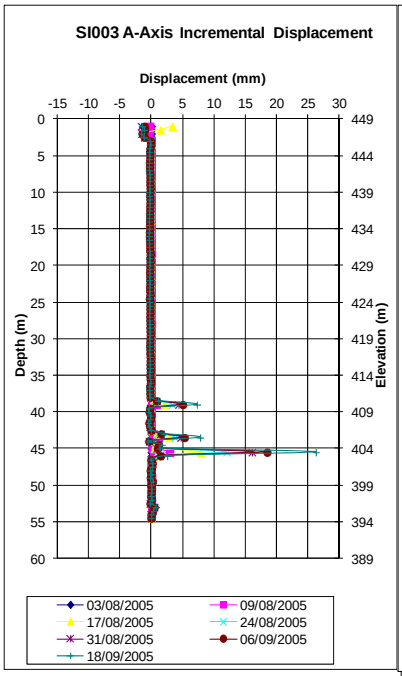
SI003 A-Axis Incremental Displacement
Displacement (mm)
Depth (m)
Elevation (m)
03/08/2005
09/08/2005
17/08/2005
24/08/2005
31/08/2005
06/09/2005
18/09/2005

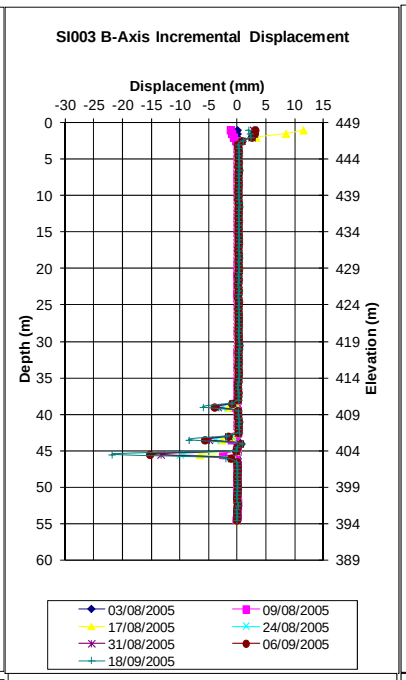
SI003 B-Axis Incremental Displacement
Displacement (mm)
Depth (m)
Elevation (m)
03/08/2005
09/08/2005
17/08/2005
24/08/2005
31/08/2005
06/09/2005
18/09/2005

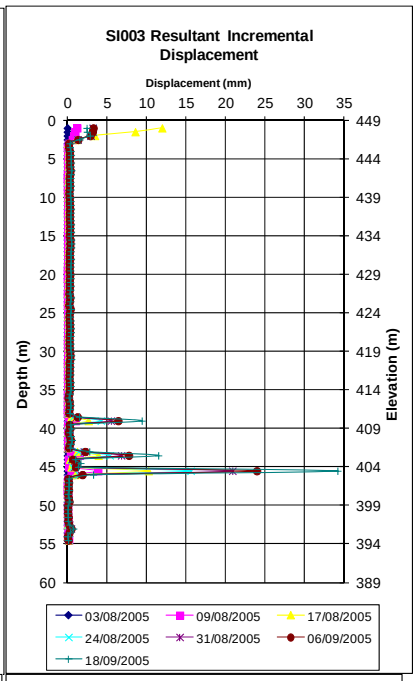
SI003 Resultant Incremental Displacement
Displacement (mm)
Depth (m)
Elevation (m)
03/08/2005
09/08/2005
17/08/2005
24/08/2005
31/08/2005
06/09/2005
18/09/2005

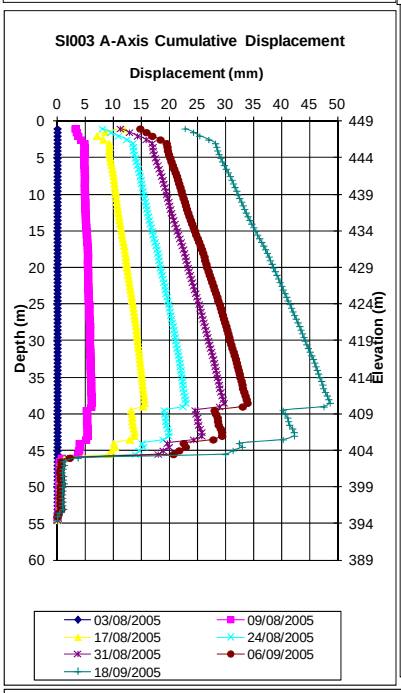
SI003 A-Axis Cumulative Displacement
Displacement (mm)
Depth (m)
Elevation (m)
03/08/2005
09/08/2005
17/08/2005
24/08/2005
31/08/2005
06/09/2005
18/09/2005

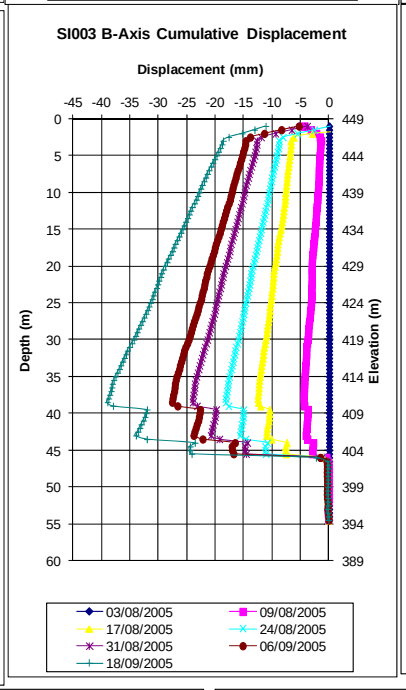
SI003 B-Axis Cumulative Displacement
Displacement (mm)
Depth (m)
Elevation (m)
03/08/2005
09/08/2005
17/08/2005
24/08/2005
31/08/2005
06/09/2005
18/09/2005

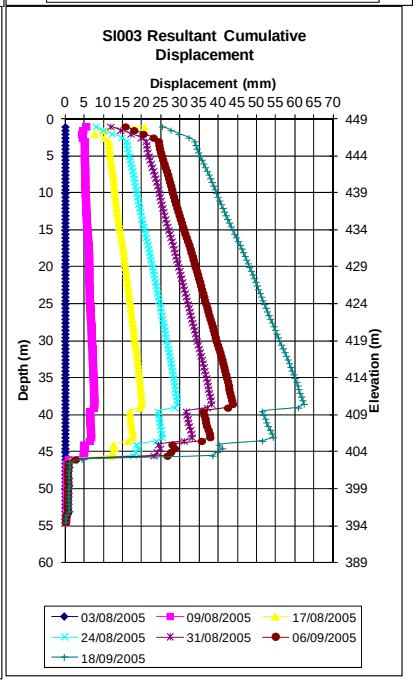
SI003 Resultant Cumulative Displacement
Displacement (mm)
Depth (m)
Elevation (m)
03/08/2005
09/08/2005
17/08/2005
24/08/2005
31/08/2005
06/09/2005
18/09/2005

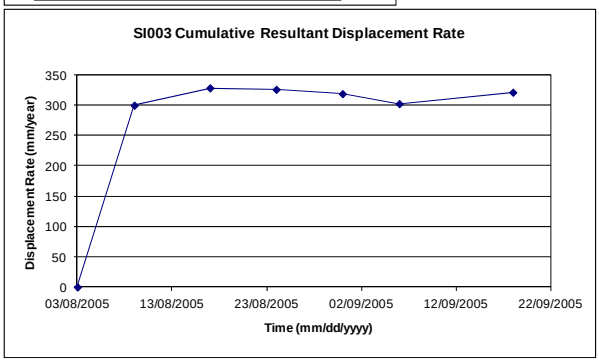
SI003 Cumulative Resultant Displacement Rate
Displacement Rate (mm/year)
Time (mm/dd/yyyy)
03/08/2005
13/08/2005
23/08/2005
02/09/2005
12/09/2005
22/09/2005

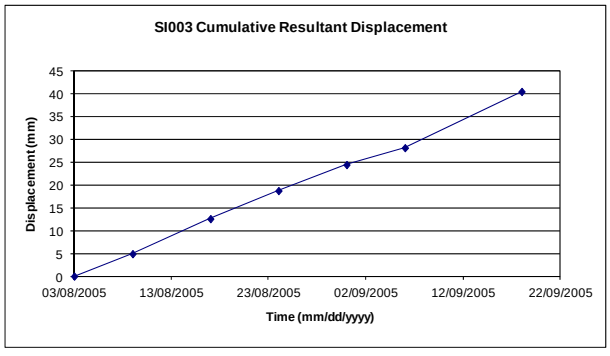
SI003 Cumulative Resultant Displacement
Displacement (mm)
Time (mm/dd/yyyy)
03/08/2005
13/08/2005
23/08/2005
02/09/2005
12/09/2005
22/09/2005

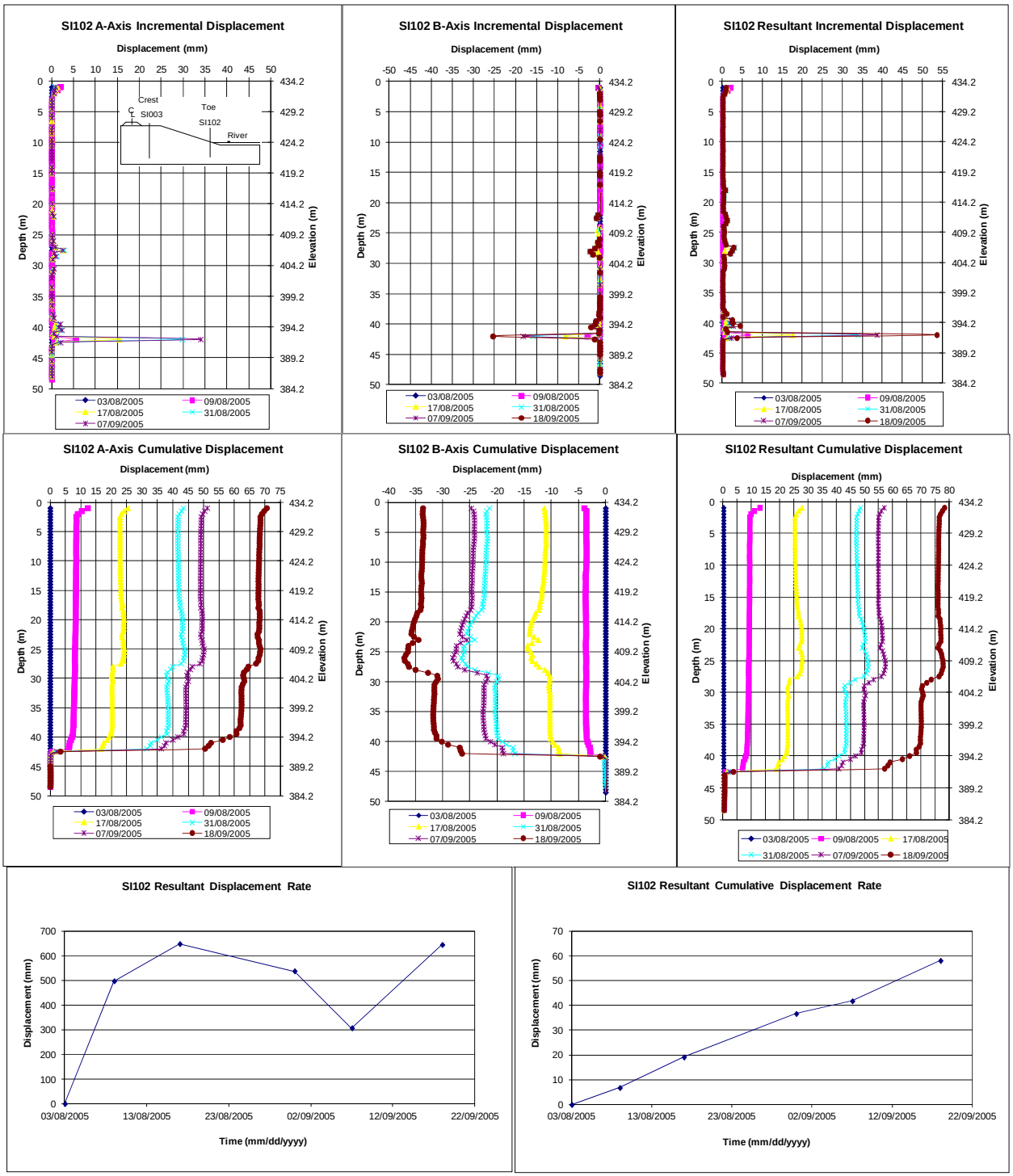
SI102 A-Axis Incremental Displacement
Displacement (mm)
Depth (m)
Elevation (m)
Crest
Toe
SI003
SI102
River
03/08/2005
09/08/2005
17/08/2005
31/08/2005
07/09/2005
SI102 B-Axis Incremental Displacement
Displacement (mm)
Depth (m)
Elevation (m)
03/08/2005
09/08/2005
17/08/2005
31/08/2005
07/09/2005
18/09/2005
SI102 Resultant Incremental Displacement
Displacement (mm)
Depth (m)
Elevation (m)
03/08/2005
09/08/2005
17/08/2005
31/08/2005
07/09/2005
18/09/2005
SI102 A-Axis Cumulative Displacement
Displacement (mm)
Depth (m)
Elevation (m)
03/08/2005
09/08/2005
17/08/2005
31/08/2005
07/09/2005
18/09/2005
SI102 B-Axis Cumulative Displacement
Displacement (mm)
Depth (m)
Elevation (m)
03/08/2005
09/08/2005
17/08/2005
31/08/2005
07/09/2005
18/09/2005
SI102 Resultant Cumulative Displacement
Displacement (mm)
Depth (m)
Elevation (m)
03/08/2005
09/08/2005
17/08/2005
31/08/2005
07/09/2005
18/09/2005
SI102 Resultant Displacement Rate
Displacement (mm)
03/08/2005
13/08/2005
23/08/2005
02/09/2005
12/09/2005
22/09/2005
Time (mm/dd/yyyy)
SI102 Resultant Cumulative Displacement Rate
Displacement (mm)
03/08/2005
13/08/2005
23/08/2005
02/09/2005
12/09/2005
22/09/2005
Time (mm/dd/yyyy)

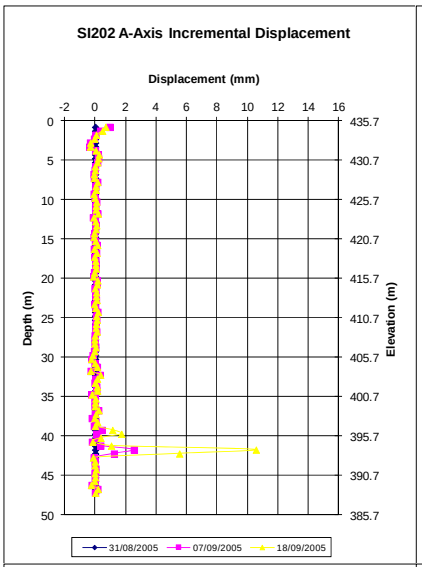
SI202 A-Axis Incremental Displacement
Displacement (mm)
Depth (m)
Elevation (m)
31/08/2005
07/09/2005
18/09/2005

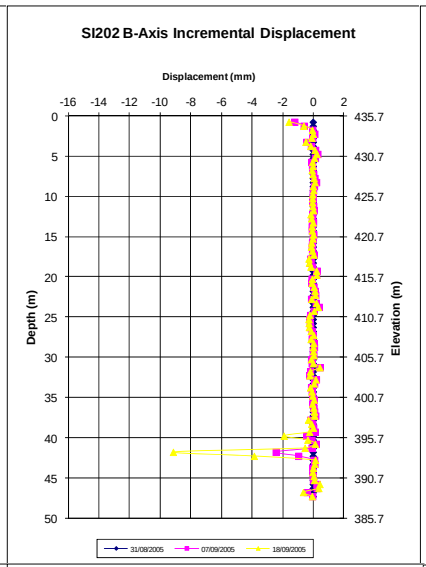
SI202 B-Axis Incremental Displacement
Displacement (mm)
Depth (m)
Elevation (m)
31/08/2005
07/09/2005
18/09/2005

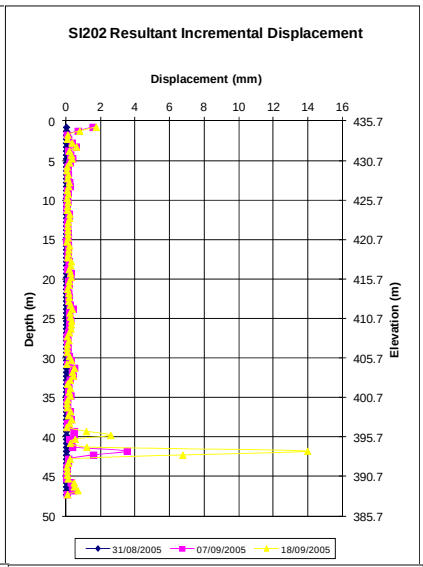
SI202 Resultant Incremental Displacement
Displacement (mm)
Depth (m)
Elevation (m)
31/08/2005
07/09/2005
18/09/2005

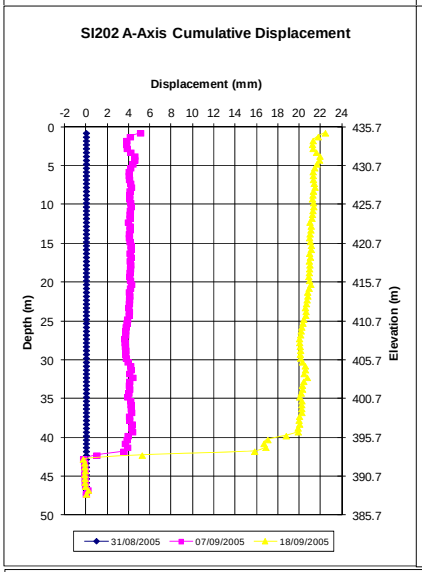
SI202 A-Axis Cumulative Displacement
Displacement (mm)
Depth (m)
Elevation (m)
31/08/2005
07/09/2005
18/09/2005

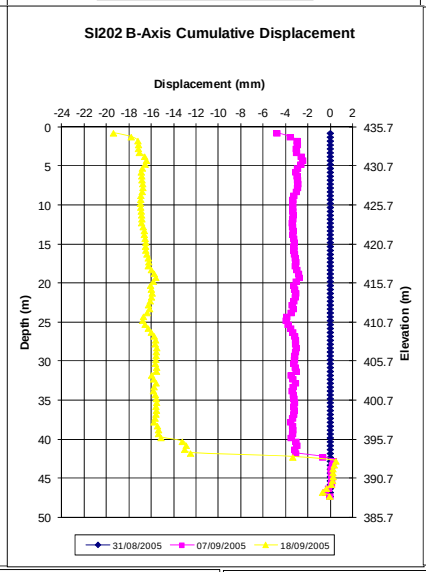
SI202 B-Axis Cumulative Displacement
Displacement (mm)
Depth (m)
Elevation (m)
31/08/2005
07/09/2005
18/09/2005

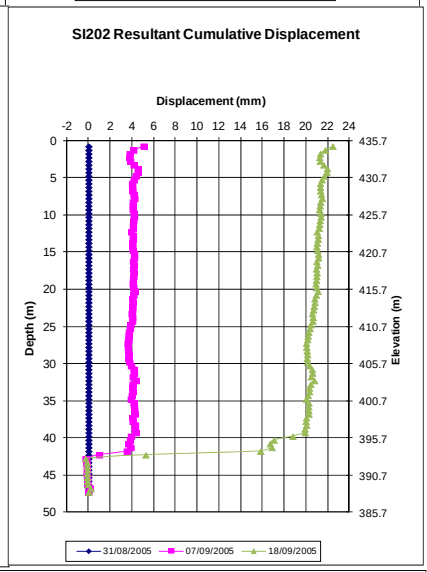
SI202 Resultant Cumulative Displacement
Displacement (mm)
Depth (m)
Elevation (m)
31/08/2005
07/09/2005
18/09/2005

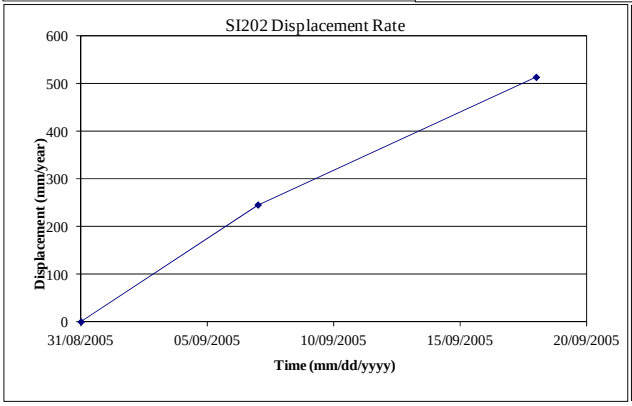
SI202 Displacement Rate
Displacement (mm/year)
31/08/2005
05/09/2005
10/09/2005
15/09/2005
20/09/2005
Time (mm/dd/yyyy)

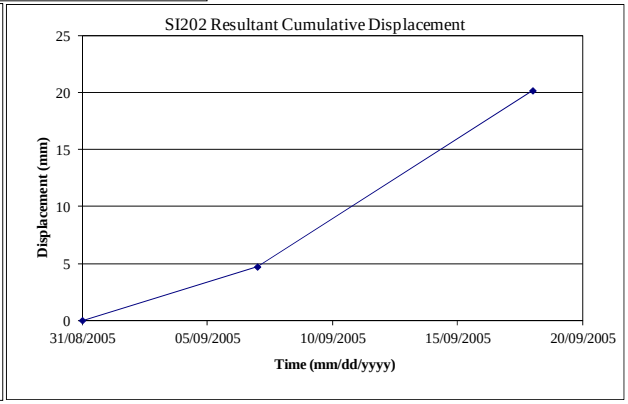
SI202 Resultant Cumulative Displacement
Displacement (mm)
31/08/2005
05/09/2005
10/09/2005
15/09/2005
20/09/2005
Time (mm/dd/yyyy)

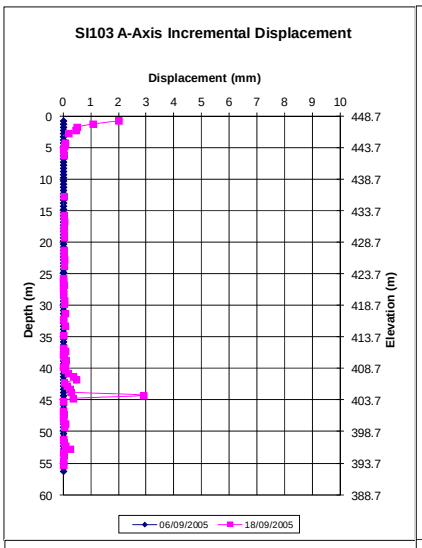
SI103 A-Axis Incremental Displacement
Displacement (mm)
Depth (m)
Elevation (m)
06/09/2005
18/09/2005

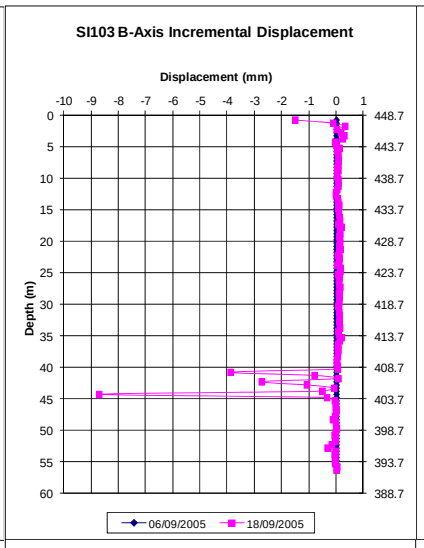
SI103 B-Axis Incremental Displacement
Displacement (mm)
Depth (m)
Elevation (m)
06/09/2005
18/09/2005

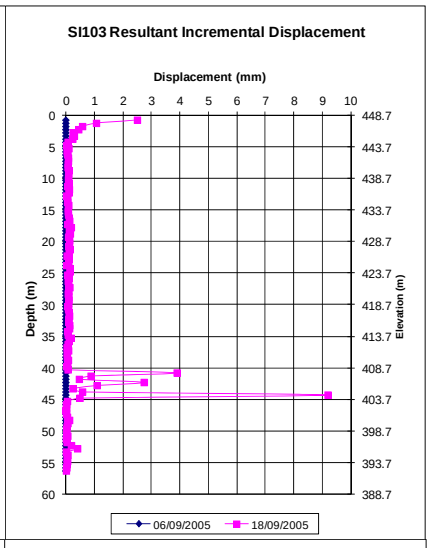
SI103 Resultant Incremental Displacement
Displacement (mm)
Depth (m)
Elevation (m)
06/09/2005
18/09/2005

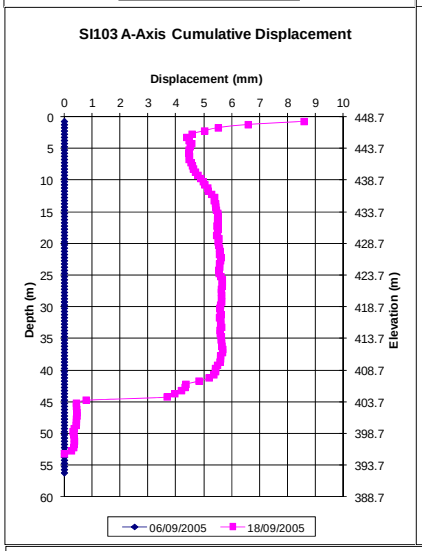
SI103 A-Axis Cumulative Displacement
Displacement (mm)
Depth (m)
Elevation (m)
06/09/2005
18/09/2005

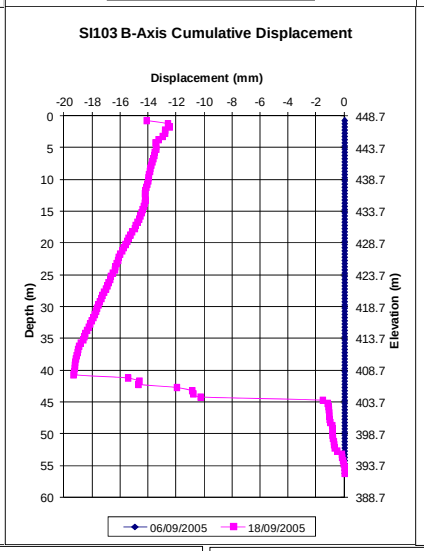
SI103 B-Axis Cumulative Displacement
Displacement (mm)
Depth (m)
Elevation (m)
06/09/2005
18/09/2005

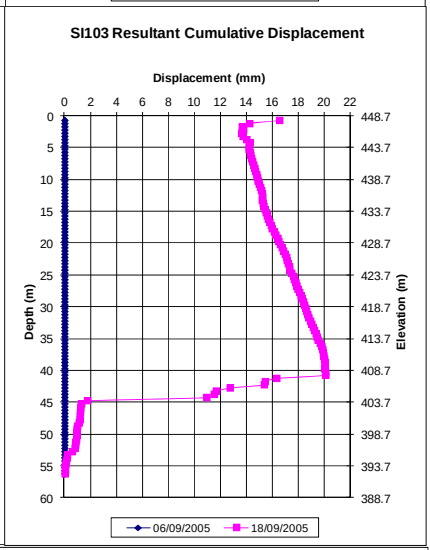
SI103 Resultant Cumulative Displacement
Displacement (mm)
Depth (m)
Elevation (m)
06/09/2005
18/09/2005

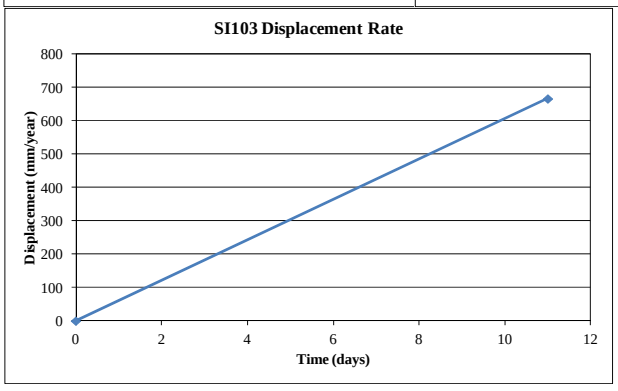
SI103 Displacement Rate
Displacement (mm/year)
Time (days)

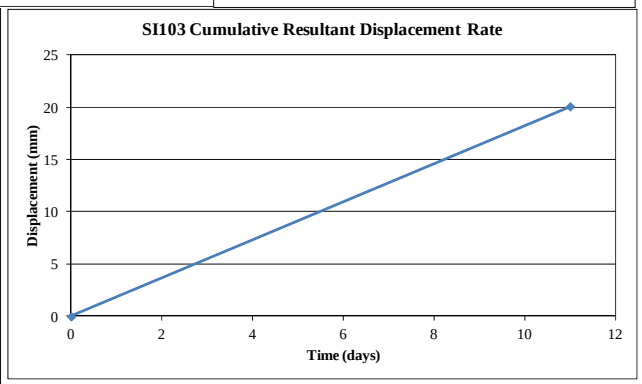
SI103 Cumulative Resultant Displacement Rate
Displacement (mm)
Time (days)